Revision 1

Biosilica as a Source for Inspiration in Biological Materials Science

MARCIN WYSOKOWSKI[1], TEOFIL JESIONOWSKI[1] and HERMANN EHRLICH[2*]

[1] Poznan University of Technology, Institute of Chemical Technology and Engineering, Berdychowo 4, 61-131 Poznan, Poland

[2] TU Bergakademie Freiberg, Institute of Experimental Physics, Leipziger str. 23, 09596 Freiberg, Germany, email: Hermann.Ehrlich@physik.tu-freiberg.de

ABSTRACT

Biomineralization is an evolutionarily ancient phenomenon and one of the fundamental biological processes by which living organisms produce minerals with multifunctional properties. Among the more general biomineralization processes, those involving silica (biosilicification), calcium-based biominerals (calcification) and iron-based biominerals (biomagnetism) have been described in a wide pattern of living organisms, from single cells to higher plants, animals and even humans. After 25 years of extensive studies of biosilicification, diverse biomacromolucules have been proposed and confirmed as active players in this special field of biomineralization. Despite these discoveries, biosilicification is still a paradigm and a cause of scientific controversy. This review has the ambitious goal of providing thorough and comprehensive coverage of biosilicification as a multifaceted topic with intriguing hypotheses and numerous challenging open questions. The structural diversity, chemistry and biochemistry of biosilica in viruses, bacteria, plants, diatoms and sponges are analyzed and discussed here. Special attention is paid to prospects and trends in applications of biosilica for technology, materials science and biomedicine.

INTRODUCTION

Biomineralogy is an interdisciplinary research field dealing with the phenomena of biomineralization, demineralization, and remineralization, which have occurred naturally since life began. Nowadays, biomineralization is defined as the fundamental biological process by which living organisms produce minerals with multifunctional properties. These include hardening existing subcellular organic matrices and tissues, producing protective armors and shells against external damage of diverse origins (predators, UV irradiation, toxic metals, etc.), as well as performing magnetic navigation. The knowledge that can be extracted from biomineralization is the driving force for recent progress in biomimetics. This concept is on track to become a powerful approach in modern materials science, nanotechnologies and biomaterial-inspired chemistry. The best way to enable understanding of the basic principles of biomineralization on a molecular level is a coherent synergetic approach using explicit reasoning and well-tested explanatory principles of multidisciplinary experience, knowledge and new technologies.

Biominerals are minerals produced by living organisms. According to the modern point of view, at the most basic level, biomineralization is initiated by organic scaffolds capable of exerting precise control over the spatial localization of nucleation and growth of mineral phases, amorphous or crystalline. Observations of biominerals have looked at typical crystals, and led to the introduction of such terms as "biocrystal" and "bio-crystallization" (Cho et al. 1996; Mastropietro et al. 2017) because of their origin. Initially it was thought that their crystallographic appearance was determined by the rules of mineralogy (Bonucci 2014). On the other hand, there has been increasing awareness that the biomineralization process occurs in the context of an organic matrix; and that this plays a conditioning role in mineralization by

promoting or by inhibiting the deposition of the inorganic substance. A number of theories based on predominantly mineralogical or on predominantly biological concepts have consequently been put forward, but in neither case has any definitive explanation of the mechanism of biomineralization emerged. As a result, the whole topic is still widely debated (Pokroy et al. 2004; Gower 2008; Checa et al. 2013; Zolotoyabko et al. 2017). According to previous studies, "biocrystals" which can also possess polycrystalline and mesocrystalline behavior diffract X-rays and electrons in a similar way to single crystals on the meso-scale. However, other studies, such as that of Pokroy et al. (2004), have revealed that in biological calcite and aragonite the crystal lattices are anisotropically distorted, and attribute this to the action of intracrystalline biomolecules. This diverse set of proposed pathways results from the complexity of both the free-energy landscapes and the reaction dynamics that govern particle formation and interaction within diverse biomineralizing systems (De Yoreo et al. 2015).

The main challenge in a search for a definitive solution to the problem of the mechanism of biomineralization is the need to revisit certain widespread beliefs. There is a deeply rooted conviction that the inorganic substance has from the outset a crystalline organization, which then persists unchanged until the tissue is eventually reabsorbed; however, the actual evidence is that the first mineral particles are non-crystalline. Moreover, some biominerals (e.g. bone) are considered stable, permanent structures, whereas they in fact undergo deep, although poorly known, changes during their lifespan (Bonucci 2014).

Furthermore, in recent years there has been a shift in attention from prior studies that focused on specific organic–inorganic interactions that modulate the crystal morphology via the conventional crystallization pathway (Gower 2008) to recent studies showing that many biominerals are formed via an amorphous precursor pathway (Pouget et al. 2009; Weiner and Addadi 2011; De Yoreo et al. 2015). In modern biomineralization, crystallization from transient

amorphous precursor particles is believed to be a widespread strategy that enables the efficient transport of mineral constituents with low solubility to the crystallization site (De Yoreo et al. 2015).

Oriented attachment is one of the key mechanisms of biomineralization processes that form the structure and account for the unique physicochemical properties of biological materials (Li et al. 2012; Ivanov et al. 2014). Of particular interest in this regard are those biomineralizing organisms (biomineralizers) which are able to produce structures where the organic component of the biomineral possesses properties of crystals while the inorganic part remains amorphous. Typical examples of such biomineralizers include a broad variety of unicellular and multicellular organisms which produce biosilica (see Table 1).

Silicon is found in nature as silicic acid ($Si(OH)_4$). The concentrations of silicic acid in modern oceans and freshwaters range between 10 and 180 μM (Marron et al. 2013); however, silicic acid autopolymerizes to silica at concentrations above 2 mM (Preari et al. 2014; Spinthaki et al. 2016) and with a strong dependence on pH (Belton et al. 2012; Iler 1978; Goto 1956; Wilhelm and Kind 2015). Consequently, silicon uptake and the formation of biosilica within living cells need highly specialized biochemical mechanisms, which are responsible for the synthesis of diverse siliceous structures. Such structures have been described in bacteria, algae, plants, yeast, fungi, protists, sponges, mollusks, ascidians, crustaceans and brachiopods (Ehrlich 2010). Also fish and mammals, including humans, can produce biosilica as a result of pathological biomineralization (Ehrlich et al. 2010c; Skinner and Ehrlich 2013). Biogenic silica exhibits diversity in structure, density and composition, and can exist in several structural forms, including sheet-like, globular, fibrillar, helical, tubular, and folded sheets. Different levels of structural organization of biosilica are encountered in nature (Figure 1). These range from

nanogranules in bacteria or mitochondria (Figure 2) to hierarchically structured three-dimensional siliceous skeletons of marine glass sponges that reach heights of up to two meters (Ehrlich et al. 2010b) (Figure 3).

Glass sponges, which are psychrophilic organisms, can produce huge biosilica-based skeletons at temperatures between –2 C and 4 C (Tabachnick et al. 2017). For example, some of the largest dimensions reported for any sponge were those of a colony of *Aphrocallistes vastus* found in cold, shallow waters off western Canada. The hexactinellid colony measured 3.4 m in length, 1.1 m in height and 0.5 m in width (Austin and Conway 2007). More recently, one glass sponge species belonging to the hexactinellid family Rossellidae and subfamily Lanuginellinae has been reported to be over 3.5 m in length, 2.0 m in height and 1.5 m in width.

There is a great deal of speculation as to the possible pathways followed by the silicic acid after it enters the living cell until it polymerizes around the corresponding organic template to form one of the structures reported in the literature (see Table 1). Consequently, the long-term objective of biosilicification research is to elucidate the molecular recognition mechanisms used by organic macromolecules to control this biomineralization process. The following statement is found in a paper by Swift and Wheeler (1992): *"Most biominerals appear to be composites of organic material and mineral. Whether biosilica is such a composite is unresolved because of a lack of evidence for such organic components."* Today, after 25 years, we have made great progress in the identification of diverse biomacromolucules that are both proposed and confirmed as active players in biosilicification.

In this review we focus on the structural diversity of biosilica in selected prokaryotes, unicellular and multicellular eukaryotes, with special attention paid to biosilica of poriferan

(sponge) origin. This article also illustrates how the structures and functions of biosilicifiers can inspire new forms of artificial biomineralization and technology for biomimetics. This review has the ambitious goal of providing thorough and comprehensive coverage of biosilicification as a multifaceted topic with controversial hypotheses and numerous open questions. We begin with a brief description of biosilicas of viral, bacterial and plant origin and their practical applications. Next, we examine biosilicification in diatoms as a source for materials science. Finally, we discuss the current state of work related to the unique siliceous structures in sponges, taking inspiration from recently obtained experimental results. Attention is also directed at silicofossils. We are optimistic that both the efforts related to the implications of biosilica and the numerous open questions raised in this review will inspire the mineralogical community to research biosilicification as an ancient and intriguing natural phenomenon.

DIVERSITY OF BIOSILICA MORPHOLOGIES

Keeping in mind that silicon is the second most common element in the Earth's crust (Kuhlman 1963), we should not be surprised that biosilica is the second most abundant biomineral, after $CaCO_3$. The process by which inorganic silicon is incorporated into living organisms as silica is called biosilicification. Globally, it occurs on a scale of gigatons. Silicon, in the form of silicic acid, is a fundamental nutrient for numerous phyla. Siliceous structures have been described in both pro- and eukaryotes (Ehrlich et al. 2010c).

Different levels of hierarchically structured three-dimensional organization are seen in nature, from biosilica nanogranules in bacteria and mitochondria, to the up to 2 m high and 70 cm wide siliceous skeletons of marine glass sponges (Figure 1) (Uriz et al. 2003; Ehrlich et al. 2007b, 2010c; Wagner and Kelley 2017). Based on thorough analysis of the literature, numerous examples of siliceous structures described in diverse phyla are summarized in Table 1.

VIRUS SILICIFICATION

Silicified phages have been identified in extreme thermal environments, and the silicification has been suggested to be critical for their preservation and dispersal. External mineralization of a viral cage-like structure was first reported by Steinmetz et al. (2009). However, this experiment was performed in ambient conditions. Laider and Stedman (2010) described successful silicification of the bacteriophage T4 under laboratory conditions that closely simulated those found in silica-depositing hot springs. Silicification of viruses at 71 °C and pH ~9.2 has been reported by Peng et al. (2013). This unique feature has recently been exploited in a bioinspired approach to generate a thermostable virus by introducing an artificial hydrated silica exterior on individual virions. Similarly, to thermophiles, silicified viruses can survive longer at high temperature than their wild type relatives (Wang et al. 2015).

Interestingly, artificial silicification of viruses has become an inspiration for the development of organic–inorganic hybrid nanostructures (Altintoprak et al. 2015) and vaccines (Wang et al. 2012; Wang et al. 2015, 2016). Naik et al. (2002) demonstrated that some of the silica-binding peptides isolated from a combinatorial phage display peptide library can be used in precipitating silica from a solution of silicic acid *in vitro*. On the other hand, viruses combine several advantages, namely high availability, robustness, and an exact replication of the particle shape and dimension. These are genetically determined, and result in a narrow size distribution that makes them interesting biotemplates for the development of silica-based materials. It is noteworthy that their multivalent protein coating can be modified by high-surface-density conjugation of peptides, inducing and governing silica deposition from precursor solutions *in vitro*. The tobacco mosaic virus (TMV) is the best-characterized virus (Alonso et al. 2013); its structure and physical and chemical properties are well known, and it is now the most extensively

8

used template for various hybrid inorganic–organic materials for medicine, biotechnology, and energy (Wen and Steinmetz 2016; Schenk et al. 2017).

Moreover, it has been proven that a silica shell protects viruses against desiccation (Laidler et al. 2013) and thermal shock (Laidler et al. 2013). Therefore, inorganic protective coats significantly modify the chemical, physical and biological properties of the virus and are beneficial for virus reprocessing and protection (Mateu 2011). Thus, an artificial silicification technique paves the way to overcome the limitations of the native virus and opens up multiple applications of viruses with therapeutic potential. Furthermore, such a material-based incorporation of viruses provides an efficient strategy to develop viral materials with the characteristics of functional shells. Although the filamentous virus or virion particle acts as a biotemplate for the silicification process, biomedical applications, such as drug delivery, have not been explored, probably owing to biosafety concerns (Albert et al. 2017).

BACTERIA

Cell membranes of microorganisms might function as seed crystals for Si precipitation, which is well known from biogeosystems with Si supersaturation, for example, geothermal springs (Sommer et al. 2006) (Figure 2c). Due to their small size, bacteria as a group have the highest surface area-to-volume ratio of any group of living organisms, and this, together with the presence of charged chemical groups on their cell surface, is responsible for the potent mineral-nucleating ability of these cells (Douglas 2005).

The microbial communities in hot springs are closely associated with the siliceous sinter ($SiO_2 \cdot xH_2O$) that precipitates from near-boiling fluids (> 80 °C) along the bottoms and edges of these springs and geysers. Commonly these specific environments are dominated by bacteria belonging to the orders Aquificales (Blank et al. 2002; Lalonde et al. 2005) and Cyanobacteria

9

(Konhauser et al. 2001; Hugo et al. 2011). Inagaki et al. (1998, 2003) and Doi et al. (2009) identified the bio-deposition of amorphous silica by an extremely thermophilic bacterium, *Thermus thermophilus*, isolated from a siliceous deposit formed from geothermal water at a geothermal power plant in Japan. Orange et al. (2011) reported silicification of the hyperthermophilic archaean *Methanocaldococcus jannaschii*.

Biosilicification under such harsh environmental conditions is mostly studied as a mechanism of fossilization. However, Amores and Warren (2009) reported that cyanobacteria of *Synechococcus* sp. are metabolically active after five days of silicification. The directed biosilicification of live cell surfaces is likely a bacterial strategy to protect the cell functionality against the potentially inhibitory effects of mineral encrustation. Cyanobacteria can manage their surface biomineralization burden to preserve the functions of the cell core, which is consistent with known bacterial strategies to avoid or delay cell entombment (Amores and Warren 2009).

It has been suggested that most microbes found in hot springs and geothermal plants play a rather passive role in the silicification process, by providing organic surfaces that facilitate the binding of silica polymers and colloids from solution. It should be noted that the colloidal silica surface has a residual negative charge, and that the bacterial surface is also negatively charged (except at extremely low pH) (Amores and Warren 2007). Thus, sorption reactions can occur by either (i) hydrogen bonding between dissolved silica and cell hydroxyl functional groups; (ii) a metal cation, such as Fe (Ferris et al. 1986; Orange et al. 2011) or Al (Bai et al. 2012), creating a bridge between anionic cell functional groups and the silica; or (iii) direct electrostatic interaction of silica with cell surface tertiary amine groups (Demadis et al. 2015; Pohnert 2002; Knecht and Wright 2004; Reitner and Thiel 2011; Spinde et al. 2011; Spinthaki et al. 2017) or the use of hybrid NH_3^+/COO^--terminated surfaces as surrogates for charged and ionizable groups (Wallace et al. 2009). Therefore, the microbial surface ligands might also be considered as favorable

nucleation sites for silica precipitation (Konhauser et al. 2004). After silica precipitation is initiated on the bacterial surface, continued growth presumably occurs autocatalytically due to the increased surface area generated by the small silica phases (Konhauser et al. 2004).

The growing realization that such sinters co-occur with microbial cells that themselves undergo biomineralization has generated interest from astrobiologists seeking to understand the fossilization of biosignatures for early life on Earth and possibly other planets (Lau et al. 2008). Interest has also arisen in bioengineering, due to the phenomenon whereby bacteria encapsulated in silica retain their bioactivity and remain accessible to external reagents by diffusion through the porous silica (Alvarez et al. 2009). Also extreme biosilicification (Ehrlich 2017) can inspire the creation of advanced materials and technologies. For example, Xiong et al. (2013) performed a biomimetic silicification that confers an artificial shell on cyanobacteria to alleviate photoinhibition. Thus, the photosynthesis of the resulting silicified cyanobacteria becomes more efficient under strong light conditions. Such a material-based improvement shows the potential of the photosynthetic efficiency of cyanobacteria under strong light, which enhances the photosynthetic biomass.

PLANT BIOSILICA

Plants take up silicon in the form of soluble $Si(OH)_4$ or $[Si(OH)_3O]^-$ (Currie and Perry 2007), which are released into the soil by the weathering of silicates. Silicic acid can be taken up by plant roots passively or actively, and later it is polymerized as amorphous $SiO_2 \cdot H_2O$ and deposited in root endodermis, leaf epidermis, and abaxial epidermis of inflorescence bracts (Kumar et al. 2017b). It is often proposed that silica crosslinks the cell wall polymers, adding to their compressive strength. Some plants accumulate a large amount of amorphous silica (20–30 wt%), which occurs in various morphological forms including plates, fans, prickle hairs and

dumbbells (Sato et al. 2017). As reviewed by Neethirajan et al. (2009) some silica bodies in plants such as phytoliths serve a variety of functions, including lending the plant structural rigidity by supporting the shoot, providing resistance to lodging (falling over), and giving mechanical strength and rigidity to the leaves. The hardness of these structures deters obvious predators.

The biosilica related mineral tabasheer (or tabashir) occurs as a siliceous deposit in the lacuna of the bamboo culm, especially in sympodial taxa from tropical climates such as *Melocanna baccifera* and *Bambusa arimdinacea* (for review see Judd 1887). In addition, some species of bamboo contain extracellular silica in the hollow stems as a gelatinous mass about one inch thick and containing about 1% organic matter. This substance, known as 'tabasheer' or 'bambusa' depending on its origin, can be easily isolated from the plant tissues and appears to be the residue of the watery liquid also found in the hollow internodes of the plant. Jones et al. (1960) examined it by optical and X-ray diffraction and electron microscopy, comparing its structure with that of opal phytoliths, silica gel and opal of inorganic origin. Small fragments of tabasheer have been shown to be composed, like opal, of roughly spherical particles about 100 Å in diameter, linked together into chains or clumps (Figure 4) (Thomson 1836; Klinowski et al. 1998).

Sato et al. (2017) hypothesized that the microstructure of plant biosilica is closely related to its functions. Insights into the mechanisms responsible for plant biosilicification may be an important step for the design of functional and environmentally friendly silica glass in the future (Sahebi et al. 2015; Sato et al. 2017). The passive (Exley 2015) and active (Kumar et al. 2017a,b) theories of silica deposition are a topic of scientific discussion and controversy. According to the passive mode of silicification, silica deposition is a result of silicic acid condensation due to

dehydration, such as during transpirational loss of water from the aboveground organs (Kumar et al. 2017b). This hypothesis infers that silica deposition in plants is a spontaneous process resulting from auto-condensation of Si molecules as the sap undergoes dehydration. The active hypothesis proposes the involvement of certain specific cells and biomolecules, including proteins, peptides or polysaccharides, capable of condensing soluble silicic acid to solid silica. In 2017, Kumar et al. (2017a) reported strong evidence that the controlled mineral deposition in silica cells is independent of water evapotranspiration.

Both theories are excellently reviewed by Kumar et al. (2017b), and the reader is referred to that article for details. In fact, silica deposition cannot be explained solely by either one of the two hypotheses, and both of the proposed mechanisms may be involved simultaneously.

BIOSILICA OF DIATOMACEOUS ORIGIN

The modern aquatic silica cycle is dominated by silica-secreting phytoplankton, principally diatoms. Consequently, they are the most extensively studied of all of the biosilicifiers that are used as geobiological indicators (Skinner and Ehrlich 2013). Diatoms are a major group of phytoplankton involved in the global biogeochemical cycling of silica, and are inherent in virtually every environment, ranging from water and ice to soil (Medlin 2016; Mishra et al. 2017; Krajina et al. 2018). Also, terrestrial diatoms now hold promise for use in catchment hydrology— for tracing runoff flow sources and pathways across a wide range of spatial scales (Pfister et al. 2017). These unicellular microalgae are able to produce their siliceous cell walls using organic templates even at natural extremes like acidic hot spring waters (pH 1.5, 88 °C) (Denicola 2000) and at –20 °C within the ice-based foams in Antarctic seas (see for review Ehrlich 2017). Diatoms are among the most productive organisms on Earth, responsible for an estimated 20% of global primary production, and a corresponding 240 ± 40 teramoles of biogenic silica

13

precipitation annually (Treguer et al. 1995; Tréguer and De La Rocha 2013; Durkin et al. 2016).

Diatoms produce sophisticated biosilica-based cell walls (frustules) (Desikachary and Dweltz 1961) which are hierarchically organized structures from nano- to microscale and with a high degree of hybridization. According to morphological and structural variations of the biosilica frustules, over 100,000 different species of diatoms are classified (Sprynskyy et al. 2017). Their shapes vary from circular/triangular to bipolar, and their sizes from two up to a few hundred micrometers (Figure 5). Some even grow to an exceptional 5500 μm. They are broadly categorized into radial forms with nanostructured pore patterns (centrics) and forms with bilateral symmetries (pennates) (Ehrlich and Witkowski 2015; Hildebrand and Lerch 2015).

Different views on the principles of biosilicification can also be found in the literature with respect to diatoms (see for review Ehrlich and Witkowski 2015). Diatom cell walls are regarded as a paradigm for the controlled production of nanostructured silica with intricate structures, but the mechanisms allowing biosilicification to proceed at high rates remain enigmatic. According to the established point of view (Tesson and Hildebrand 2010; Hildebrand and Lerch 2015) both organic compounds and organelles in the diatom cell are involved in the formation of mineralized nanostructures of the frustules. For example, the Silica Deposition Vesicles (SDV) are examples of specialized compartments where silica structures are synthesized. After this process is completed, the entire formation undergoes exocytosis and forms a new frustule. Soluble silicic acid is the form for silicon transport into the cell; however, it is thought that solid silica structures are condensed inside the SDV.

Determination of the locations of biosilica-associated organic molecules with high precision is therefore expected to provide clues to their roles in biosilica morphogenesis (Gröger et al. 2016). Among organic substances associated with diatom silica, the following five classes

of biomolecules on nanoscale have been identified by the Kröger Group as the key players in biosilicification: specifically modified (poly)peptides silaffins, silacidins, unique long chain polyamines (LCPAs), cingulins from the diatom's microrings, as well as the recently discovered membrane-associated proteins termed silicanins (Kotzsch et al. 2016, 2017). Combinations of these biomolecules can be formed via electrostatic interactions. It is unclear whether these molecular classes can resemble some kind of structural framework for mechanical support and near-perfect micro-architectural design in diatoms. The best candidate in this case is nanofibrillar β-chitin, recently discovered within siliceous cell walls of the well-investigated diatoms *Thalassiosira pseudonana* (Figure 6) (Brunner et al. 2009) and *T. rotula* (Figure 7) (Ehrlich & Witkowski, 2015). *T. pseudonana* is the first diatom for which the genome has been successfully sequenced and the presence of chitin synthase genes confirmed (Armbrust et al. 2004). *Thalassiosira* diatoms produce not only highly crystalline β-chitin fibers within siliceous frustules, but also long thin chitin nanofibers that extend from the theca through specialized pores within the biosilica (Durkin et al. 2009). Therefore chitin, as a biological material with a highly ordered crystalline structure, together with the low-molecular-weight biomolecules listed above, may be responsible for biosilicification in diatoms which appeared on the Earth more than 140 million years ago (Durkin et al. 2016).

Siliceous structures of diatoms as a source for materials science

The highly specialized nanostructure of diatom cell walls determines photonic properties on the nanoscale, being involved in photosynthesis, staving off predators due to the unique mechanical resilience of frustules (Hamm et al. 2003), and acting as a counterbalance to turgor pressure (Ehrlich and Witkowski 2015). Diatom nanotechnology (Kröger and Poulsen 2008; Townley et al. 2008; Gordon et al. 2009; Losic et al. 2009; Medarevic et al. 2016; Losic 2018), a new research field, has recently emerged to explore and apply these biomaterials and their

properties in modern technologies. Their structure and composition continue to inspire a variety of biomimetic synthesis approaches (Sumper and Brunner 2006) with respect to the creation and design of lightweight structures (Hamm 2015), photonic nanomaterials (Yoneda et al. 2016), sensors (Yang et al. 2011; Leonardo et al. 2016; Kamińska et al. 2017), lab-on-chip (Merola et al. 2015), biofuels (Mishra et al. 2017) and materials for energy storage (Nowak et al. 2017; Sun et al. 2017), drug delivery (Aw et al. 2011; Albert et al., 2017; Papathansiou et al. 2017), fertilizers (Grzesik et al. 2015) and adsorption (Qi et al. 2017; Wysokowski et al. 2017). Therefore, untangling the mechanism of diatom biomineralization processes will provide new insights relating to advanced combinations of nanostructured composite ceramic materials and lightweight architecture for technological applications (Hamm 2005; Nassif and Livage 2011; Ehrlich and Witkowski 2015; Hildebrand and Lerch 2015).

Due to the high potential of diatoms for nanobiotechnology, and for effective use in engineering applications, it is necessary to evaluate the nanostructure and micro-mechanical properties of the siliceous frustules. Mechanical analysis and characterization of diatom structures have been pursued mainly using atomic force microscopy (AFM), nanoindentation, and scanning electron microscopy (SEM). Hamm et al. (2003) used needle loading tests to measure the forces necessary to break single, living diatom cells. Applying finite element method (FEM) simulations, the researchers calculated the tensile and compressive stress values within the diatom cell before failure. They proved that these mechanical parameters depend on whether pressure is applied on the valve face or at the girdle region, and take values ranging from 155 to 680 N mm^{-2}. This suggests that the siliceous frustules in diatoms have both high ultimate tensile and high ultimate compressive strength, and confirms that they are an effective armor against many potential predators (Hamm et al. 2003; Hamm 2005). Recently, Aitken et al. (2016) used *in*

16

situ three-point bending and nanoindentation experiments to investigate the mechanical properties and fracture behavior of frustules of the diatom *Coscinodiscus* sp. These experiments revealed similarities in the elastic properties of the biosilica found in the frustule and in the girdle band, with an average modulus from three-point bending tests of 36.4 ± 8.3 GPa. The researchers hypothesize that the unprecedentedly high specific strength of the frustule, exceeding that of all other reported natural biomaterials, is due to the combination of the honeycomb sandwich plate architecture and extremely low flaw density in the constituent biosilica (Aitken et al. 2016). Moreno et al. (2015) performed simulations on the aforementioned diatom frustules, as well as another diatom structure (pennate *F. kerguelensis*), to correlate the mechanical response with specific morphology variables. Successful application of 3D CAD models to simulate the experimental diatom frustules can be exploited to design advanced diatom-inspired artificial materials of low density and high strength.

Optical nanotechnology requires materials with periodical structures with nanoscale features. These are very challenging to produce by standard manufacturing techniques, but diatoms make such structures all the time (Bradbury 2004). Therefore, it is crucial to analyze the diatom siliceous ultrastructures as a strategy for their survival under light, while at the same time searching for new applications of these biological materials in optical nanotechnology.

Diatom frustules are regarded as living photonic crystals composed of periodic refractive index materials (Fuhrmann et al. 2004; Yamanaka et al. 2008). The theoretical analyses of optical properties support the experimental results and suggest a strong interaction especially between blue light and the inner silica material of the frustules. Such interactions between blue light and biosiliceous inner nanostructures may serve for reducing excess blue light and enhancing the diatom's photosynthesis (Yamanaka et al. 2008). It is suggested that the photonic crystalline

17

characteristics of the frustule can support an efficient light-harvesting antenna (Yoneda et al. 2016). Versatile morphologies of nanophotonic structures found in diatoms contribute to their ecological success (Romann et al. 2015; Goessling 2017), and the practice of biomimetics through cell culture (Parker and Townley 2007; Su et al. 2015) may be beneficial in advanced optical applications (Ferrara et al. 2014), including solar cells, photoluminescence-based biosensors and electroluminescent or photoluminescent devices (Ren et al. 2013; LeDuff et al. 2016).

In the past decade, mesoporous silica nanoparticles with large surface area and pore volume have attracted considerable attention for applications in drug delivery (Cicco et al. 2015, Papathansiou et al. 2017) and biomedicine (Walsh et al. 2017). Recently, biosilica from diatoms has been proposed as an alternative source of mesoporous materials in the field of multifunctional supports for cell growth (Cicco et al. 2016).

BIOSILICA OF PORIFERAN ORIGIN: CHEMISTRY, STRUCTURE AND FUNCTION

Sponges (Porifera) are the most simple and ancient multicellular animals on Earth, and live attached to the seabed or another substratum (Ehrlich 2011, 2013). Sponges are suggested to have been the first animals to inhabit the Earth (Gold et al. 2016), their earliest record having been found in 1.8 billion-year-old sediments (Nichols and Wörheide 2005). The phylum Porifera is divided into four classes: Hexactinellida, Demospongiae and Homoscleromorpha, which have siliceous skeletons (Figure 8), and Calcarea with a calcareous skeletal network (van Soest et al. 2012). Sponges contain only a few different cell types, of which the special cells known as silicoblasts produce the spicules—siliceous structures, of any type and size (Florkin 1968) but often needle-shaped. These spicules often form a distinct skeleton, but occasionally they are loosely distributed throughout the sponge body without identifiable order, or are lacking entirely.

18

Traditionally, the size, type, shape and combination of spicules and their skeletal arrangements served as the basis for sponge systematics (Boury-Esnault and Rutzler 1997); recently, however, these structures have attracted a great deal of attention from experts in materials science, biophotonics (Sarikaya et al. 2001), tissue engineering (Guo et al. 2017), bioengineering and biomimetics (Andre et al. 2012; Natalio et al. 2013; Schoeppler et al. 2017).

Modern views on the chemistry of silica-based skeletal structures in sponges

Scientific controversy is the driving force of scientific advance—and this applies in particular in the case of silicification in sponges. It is established that the siliceous sponge spicules of both the Hexactinellida and Demospongiae consist of hydrated amorphous silica (Ehrlich 2011; Masse et al. 2016). Chemically, they differ only slightly in their SiO_2-to-H_2O ratio, which is 5:1 for desma-bearing demosponges (Lithistida) and 4:1 for Hexactinellida (Ehrlich 2011). The major trace elements found in the spicules and siliceous sponge skeletons (S, Ca, K, Na, and Cl) are also the most common in seawater (Sandford 2003). Recent findings show that heavy metal (Cd, Pb and Cu) incrustations are also commonly found in siliceous tissues of marine sponges (Illuminati et al. 2016). Aizenberg et al. (2004) suggested that sodium may play an important role in determining the physicochemical properties of glass sponge spicular formations.

According to the modern view, four different organic templates which may be involved in biosilicification in demosponges and glass sponges have been isolated and proposed: silicateins in demosponges and hexactinellids (Shimizu et al. 1998; Müller et al. 2007, 2013), glassin in hexactinellids (Shimizu et al. 2015), collagen (Ehrlich et al. 2010b) and chitin (Ehrlich et al. 2008b, 2016), the latter two in hexactinellids. In the section below the various theories of silicification in demosponges as well as glass sponges will be compared and discussed.

19

Demosponges (Demospongiae)

The demosponges (Demospongiae Sollas 1885) form by far the largest group, with 95% of all extant sponges. They are also the most diverse group (van Soest et al. 2012). Some are freshwater sponges, but predominantly they are marine species occurring from the intertidal zones to the deepest seas, with nearly 7,000 species worldwide (Morrow and Cardenas 2015). The skeleton is composed of monaxonic or tetraxonic (never triaxonic) siliceous spicules bound together with the collagen-like protein spongin in discrete fibers or loosely aggregated and ubiquitous collagenous filaments, forming the ground substance of the intercellular matrix.

The following parts are identified in siliceous spicules, from the inside outwards:

(a) the axial filament, a definite organic structure (Figures 9–12) located within the axial channel (Figure 9);

(b) the siliceous tube, stratified or homogeneous;

(c) the spicule sheath.

The organic nature of the axial filaments in the spicules of Demosponges have been known since experiments carried out by Kölliker (1864). The matter of this filament was termed spiculine in the 19th century (for review see Ehrlich 2011); the exact chemical nature of this construct is still unknown, although there is now no doubt that it is proteinaceous, there being several proteins as candidates (for details see below). Intriguing initial results concerning the structural properties of axial filaments in demosponges were obtained using TEM in the course of studies on spiculogenesis in the demosponge *Mycale contarinii* (Levi 1963). It was shown that the spicule is initially formed in the silicoblast in the form of a proteic rodlet (Figure 10) which is produced in two great vacuoles. This axial rodlet was electron-dense and of fibrillary nature, with spiral fibers 70–100 Å in diameter (Levi 1963).

In 1998, Morse's team (Shimitzu et al. 1998) studied spicules and isolated axial filaments from the marine demosponge *Tethya aurantia* using small-angle X-ray diffraction. The studies revealed a regular, repeating structure, which has been identified as silicatein, within the filament with a periodicity of 17.2 nm, as would be expected if a simple repeating subunit structure underlies the macroscopic filament. This finding was also consistent with the electron micrographic evidence for paracrystallinity of the protein filaments from silica spicules of another sponge observed earlier (Garrone 1978). However, the interpretation of the X-ray diffraction diagrams of the extracted filaments given by Shimizu et al. (1998) was strongly disputed by Croce et al. (2004). The use of synchrotron radiation for fiber diffraction study of demosponge spicules has enabled analysis of the axial filaments inside their natural siliceous case. The results (Croce et al. 2003, 2004) show that silica contributes to the formation of the highly ordered arrangement of protein units in the axial filament by embodying the units in regular mesoporous scaffolding. The next breakthrough was made during investigations of the initial stages of *Suberites domuncula* demosponge spicule formation, carried out using nano-electron diffraction (NED) coupled with automated diffraction tomography (ADT) (Mugnaioli et al. 2009). Primordial crystalline structures were observed in the form of intracellular nanorods within the axial filament. The nanorods had a layered structure that is similar to smectitic phyllosilicates. Intriguingly, these intracellular nanorods have been considered as precursors of mature spicules. These data have recently been re-examined in a comparative study, using TEM and HRTEM, on crystalline structures in spicules of *T. aurantia* and *S. domuncula* (Werner et al. 2017). However, no kind of mineral nanostructures has been identified to date. Moreover, investigations of the group of spicules located within one fragment of the *S. domuncula* demosponge body (see for details Eckert et al. 2006) using SEM (Figure 11) have provided strong evidence for the simultaneous existence of axial filaments with diverse morphologies and

density. For example, in some locations the axial filament has a characteristic nanofibrillar

organization (Figure 11c). These nanofibrils are not tightly bound to each other and remain

unmineralized. At the same time, axial filaments with mineralized surface (Figure 12 a,b), or

even with a hard triangular morphology (Figure 12 c–f) and without more visible nanofibrillar

architecture have been observed within the same group of spicules (see Figure 11). These

different physical states of the axial filaments may be responsible for the contradictory

explanations of the nature and origin of these structures put forward by different researchers. For

example, in the Werner and Zlotnikov Groups, attention has been paid only to the crystalline

phases in axial filaments like that represented in Figure 12, and the nanofibrillarly structured

axial filaments in the same sponge have been overlooked.

Consequently, in the literature the following explanations are to be found: in the

Demospongiae species the axial filament (AF) consists of a mesh-like organic lattice filled with

silica. Such organic crystal lattices, assembled in a six-fold symmetry along the AF axis, show a

striking similarity to those of inorganic crystals (Werner et al. 2017). This assumes: (i) a growth

process by the incorporation of molecules at lattice steps; and (ii) the development of a hexagonal

AF morphology ({110}-facets) as the result of an overall energetic equilibrium state. According

to Werner's team, AF-related biosilicification is thermodynamically a maturation-driven process,

where straight interfaces are generated with equal angles but alternating facet lengths according

to a hexagonal lattice (*S. domuncula*). During the growth process, steps of lattice units are formed

predominantly at the interfaces of the small facets to generate energetically equilibrated faces

(*T. aurantium*). This hypothesis is supported by the analogy of inorganic crystal growth, where

atoms are incorporated at surface steps (Werner et al. 2017). Recent experimental results have

shown that the organic axial filament defining the scaffold of demosponge spicules is in fact a

perfect single crystal made of proteins (Werner et al. 2015; Schoeppler et al. 2017). Using data from three different methods at the ESRF beamlines—nanotomography (ID16A), microtomography (ID19) and SAXS (ID13)—crystallographic branching of this protein crystal was shown to be responsible for the highly regular morphology of these naturally occurring glass structures. Using spicules with varying levels of structural complexity from three different organisms, it was demonstrated that the branching of the spicule follows specific crystallographic directions defined by the crystalline properties of the axial filament (Schoeppler et al. 2017). However, a thorough analysis of the SEM images shown in Figure 12 has called into question the correctness of this interpretation.

Today, the silicatein pathway for the formation of axial filaments in diverse demosponges is most established (Shimizu et al. 1998; Weaver and Morse 2003; Müller et al. 2007). Silicateins share high sequence similarity with cathepsin L and other members of the papain-like family of cysteine proteases and the larger superfamily of catalytic triad-containing hydrolases (Shimizu et al. 1998). Silicateins are assembled into a linear fiber that is found within the core of demosponge spicules, and it has been proved that this enzyme catalyzes silica formation via a hydrolysis pathway from organically functionalized silicic acid precursors at neutral pH (Cha et al. 1999) and room temperature (Tabatabaei Dakhili et al. 2017). However, the catalytic activity of silicateins at the alkalinity of sea water (pH 8.8) or at temperatures around 0 °C or lower has been never reported. Furthermore, Kozhemyako et al. (2009) identified silicatein genes (AcSilA and AcSilB) in the non-spicule-forming marine sponge *Acanthodendrilla* spp.

How demosponges can produce spicules

Recently, researchers have succeeded in finding unique cells while investigating the spicules of the *S. domuncula* demosponge (Eckert et al. 2006; Ehrlich 2010). Initially these cells

line up on the surface of the spicules, as can be well seen on the SEM image (Figure 13a). The characteristic structural feature of the cells is that they produce collagenous nanofibrils (Figure 13b). Interestingly, the cells once aligned move from left to right (Figure 13 c,d) leaving behind a collagenous nanofibrillar layer. Thus, the initially smooth surface of the spicule becomes rough due to the presence of the new collagenous nanolayer (Figure 13 e,f). The diameter of these unique cells is about 1 μm. However, the axial channel of the *S. domuncula* spicule has the same diameter (Figures 11c and 12). Moreover, the diameter of the nanofibrils of the axial filament is identical with that of the collagenous nanofibrils produced by the cells. Based on these observations, the following hypothetical mechanism of spicule formation in the case of *S. domuncula* has been proposed (Figure 14). The collagen-producing cells find a space where they can line up and start to form the "embryonal" axial filament. Initially it can exist in the form of a bundle of collagenous fibrils, with strong axial orientation between two cells (Figure 14). Each of the cells undergoes fission, and the embryonal axial filament can grow divergently in this way. Around this time the silicification must begin, and the first silica-based layer must be established around the "embryonal" axial filament (Figure 14). The cells which at this step are located within the initial siliceous microtube take the opportunity to fission and, correspondingly, move out from the tube and land on the siliceous surface (Figure 14). After that, a new generation of the collagen-producing cells arises. They line up on the surface of the prototype spicule in a way similar to that shown in Figure 13. After that the cycle repeats again and again. Because of this phenomenon, layer-by-layer structures, which are characteristic of siliceous sponge spicules, can be and have been observed using SEM (Uriz et al. 2003; Uriz 2006).

According to this suggestion, the axial filament is nothing but collagen nanofibrils made by the initial collagen-producing cells. However, as reported above, axial filaments of demosponges usually appear as very dense filaments, sometimes triangular or quadrangular in cross-section. This is not surprising, because axial filaments are located within axial channels, which in turn may be used for ion transport. Thus, it is not the organic but the inorganic components of the axial filaments that determine the formation of the triangular or quadrangular structures, which seem so unusual to biologists. The mineralogical events within axial channels of the sponge spicules, as examples of closed spaces saturated with respect to calcium ions, are still uninvestigated.

Glass sponges (Hexactinellida)

Hexactinellida Schmidt (Porifera) is a class of more than 700 species, all marine sponges, defined by their production of siliceous spicules of hexactinic, triaxonic (cubic) symmetry, or shapes clearly derived from such forms by either reduction of primary rays or addition of terminal branches to the ends of primary rays. In addition, unique siliceous network structures, including some with honeycomb microarchitecture, are found in some hexactinellids (Figure 15).

Silicatein-like proteins were first identified in the hexactinellid sponges by Müller's group (Müller et al. 2008a, 2008b). In studying the nanoscale structure of the axial filament in the giant anchor spicule of the silica sponge *Monorhaphis chuni* (Figure 16), around which the body of the sponge is assembled, Zlotnikov's team (Zlotnikov et al. 2014, 2015; Werner et al. 2015) found that the filament reveals a 3D mesoporous silica structure templated by a perfect protein lattice. The silicatein-containing structure (nearly 2 μm in diameter) provides the vertical axis of the spicule, which is composed of a silica cylinder (~150 μm in diameter) and surrounding silica lamellae (2–10 μm wide), separated by a filament of ultrathin organic layers. According to these

25

authors, the silicatein enzymatic proteins are self-assembled into a perfectly ordered body-centered tetragonal lattice, while retaining their ability to biomineralize silica.

Hexactinellids contain structures similar to the axial channels and axial filaments reported in the spicules of demosponges as described above (Figure 17 and 18). However, in some species the diameters of the axial channels are larger than 1 μm and may range between 5 and 20 μm (see Figure 18).

In 2016, another silica-occluded protein, named "glassin," as the main constituent in the extracted water-soluble fraction, was isolated from glass sponge spicules (Shimizu et al. 2015). Glassin is different from silicateins and is the main constituent in the water-soluble fraction of the demineralized skeletal elements of *Euplectella* glass sponges. This protein consists of two similar histidine-rich domains and a connecting domain. Each of the histidine-rich domains is composed of three segments: an amino-terminal histidine- and aspartic acid-rich sequence, a proline-rich sequence in the middle, and a histidine- and threonine-rich sequence at the carboxyl terminus (Shimizu et al. 2015).

The discovery of paracrystalline proteins within amorphous biosilica-based structures in sponges is ground-breaking in the understanding of biomineralization. It is now known that in some cases, the biological organism which regulates mineral formation does not control its shape evolution beyond setting the thermodynamic boundary conditions necessary for a specific architecture to form. More importantly, it has been demonstrated (Schoeppler et al. 2017) that in these cases, microstructure formation is analytically defined and can be quantitatively described in both time and space. Consequently, the next aim is to address the fundamental question of how nature takes advantage of thermodynamic principles to generate complex morphologies, and to study the interplay between the physics of materials and cellular control in this process.

Moreover, spiculogenesis as an example of biosilicification in sponges takes place in psychrophilic species occurring in habitats with temperatures between –1.9 °C (Antarctic seas) and 10 °C. There is still a lack of knowledge on the mechanisms of biosilicification at such low temperatures, from both the biochemical and thermodynamic points of view. Also, the chemical composition of sponges where spiculogenesis occurs is unknown. Undoubtedly, such parameters and factors as pH, ionic strength and Si concentrations which are involved in the control of *in situ* biomineralization should be investigated in the future.

The silicatein- and glassin-based theories are in conflict with the proposed role of collagen and chitin as alternative templates in spicule formation in glass sponges (Ehrlich 2010; Ehrlich et al. 2010; Ehrlich et al. 2016). The structural protein collagen and the structural aminopolysaccharide chitin are suggested to be responsible for the unique mechanical flexibility of the anchoring spicules in, respectively, the *Hyalonema sieboldi* and *Sericolophus hawaiicus* glass sponges.

Chitin is well-known as a primary component of cell walls in various invertebrates (Wysokowski et al. 2015). Recently, fungus-like mycelial fossils have been discovered in 2.4 billion-year-old vesicular basalt of submarine volcanics (Bengston et al. 2017). This discovery suggests that organisms with chitin-containing skeletons have inhabited submarine volcanics for more than 2.4 billion years. The oldest chitin in multicellular organisms, with a record of 505 MYR, has been reported in the demosponge *Vauxia gracilenta* (Ehrlich et al. 2013). Evidence confirming the presence of chitin in skeletal structures of diverse freshwater and marine sponges has been reported by the Ehrlich Group since 2007 (Figure 19).

Nanofibers containing α-chitin crystallites of 2 nm diameter have been identified within the amorphous silica matrix of the demosponge *Verongula gigantea* (Ehrlich et al. 2011)

27

(Figure 20). Also, five species of glass sponges contain chitin in their siliceous frameworks and spicules (Ehrlich et al. 2007b, 2016). The presence of chitin in biosilicifiers like sponges is a fact; however, the mechanism of the possible templating activity of this polysaccharide in biosilicification remains unknown.

On the other hand, there is currently special interest in the newly discovered highly hydroxylated fibrillar collagen isolated from *H. sieboldi* in up to one-meter-long spicules (Figure 21). It contains an unusual [Gly–3Hyp–4Hyp] motif that is predisposed for silica precipitation, and provides a novel template for biosilicification in nature (Ehrlich et al. 2010b). This collagen will present a layer of hydroxyl groups that can undergo condensation reactions with silicic acid molecules with a consequent loss of water. As a result, the initial layer of condensed silicic acid will be held fixed to the collagenous template in a geometric arrangement that will favor the further polymerization of silicic acid.

It therefore appears that collagen was a novel template for biosilicification that emerged at an early stage during metazoan evolution, and that the occurrence of additional trans-3-Hyp plays a key role in stabilizing silicic acid molecules and initiating the precipitation of silica. The similarity of action between silicateins and hydroxylated collagen with respect to possible mechanisms of silicification is intriguing. As reported by Croce et al. (2004), simulation of the interactions between the silicatein active site and silicic acid or its deprotonated base silicate has shown that the rotation of the serine and histidine side chains, through the formation of hydrogen bonds, can bring two silicic acid molecules together, and that the formation of an $(OH)_3Si$-O-$Si(OH)_3$ dimer is an energetically favored process (Croce et al. 2004).

There is a debate over the interpretation of scientific results between supporters of the silicatein theory of biosilicification (Morse Group, Müller Group, Weaver Group, Zlotnikov

Group) and those researchers who assert the fundamental role of collagen in the same process (Ehrlich Group, Tabachnik Group, Ereskovsky Group, Pisera Group) based on data obtained using diverse X-ray- and electron diffraction-based techniques. As reported above, the first community supports with conviction the hypothesis that silicateins are the proteins which determine the crystallinity of proteinaceous axial filaments in both demosponges and glass sponges. However, the second community criticizes this view, given that the crystalline properties and X-ray patterns of collagen (Ramachandran and Kartha 1955; Rich and Crick 1955; Chanzy et al. 1976; Shoulders and Raines 2009) and chitin (Sikorski et al. 2009; Ogawa et al. 2010) have been studied in detail since the mid-20th century. It would be remiss to overlook or even to ignore this fact, given the numerous publications related to silicateins. Furthermore, the presence of collagen within spicules where silicateins have been isolated has been demonstrated (Müller et al. 2007) but not discussed as a possible alternative template for silicification in the same structure. For example, TEM images of spicules observed in the demosponge *Geodia cydonium* at higher resolution provide strong visual evidence that collagen fibrils are located deep within silica lumps (Müller et al. 2007) (Figure 22).

This fact was not taken into account in a recent paper (Schoeppler et al. 2017) where the crystalline protein documented using diverse modern X-ray methods in the spicules of the same sponge (*G. cidonium*) was accented as being solely silicatein. A similar situation exists in the case of a study of the proteinaceous axial filament of the world's longest biosilica, the up to 3-meter-long spicule of the glass sponge *Monorhaphis chuni* (Wang et al. 2009). Although the collagenous origin of the organic matrices within this spicule has been reported (Ehrlich et al. 2008), supporters of the silicatein theory again accepted the experimentally unconfirmed suggestion of the silicatein nature of this highly ordered paracrystalline structure (Zlotnikov et al. 2014, 2015; Werner et al. 2015).

The next paradox in the understanding of the chemistry and structural biology of glass sponges lies in the postulate that their siliceous skeletal structures are based only on amorphous silica (Masse et al. 2016), the so-called bio-opal. However, the hierarchically structured glass sponge *Caulophacus* species uses a silica and nanocalcite biocomposite to join together the spicules of its skeleton (Figure 23) (Ehrlich et al. 2011).

In the stalk and body skeleton of this poorly known deep-sea glass sponge, siliceous spicules are modified by the addition of conical calcite nanoseeds, which then form the basis for further silica secretion to create a spinose region. Spinose regions on adjacent spicules are subsequently joined by siliceous crosslinks, leading to unusually strong cross-spicule linkages. It has been proposed that, while the low concentrations of calcium in deep sea waters drove the evolution of silica skeletons, the brittleness of silica has led to retention of the more resilient calcite in very low concentrations at the skeletal joints. Nanocrystallites of calcite with diameters of 2 nm were found ubiquitously in the outermost layers of siliceous spicular formations in this hexactinellid (Ehrlich et al. 2011). The possibility of the presence of nanocrystalline calcium carbonate phases as minor components of axial filaments with paracrystalline properties in spicules of sponges, as mentioned above, has been never discussed or proposed.

Biosilica and multiphase biomineralization in sponges

The skeletons of sponges are natural examples of rigid silica-based or calcium carbonate-based composites. However, a revolutionary article published in 2010 (Ehrlich et al. 2010a) reported that sponges are organisms that are able to develop unique multiphase composites combining amorphous silica, chitin and crystalline $CaCO_3$ (aragonite). The presence of a silica–calcite composite in extant hexactinellids suggests that the mechanism of secretion is flexible in terms of the precise structures formed and that extant and early sponges share a common

30

biochemical basis for secreting both amorphous and crystalline mineral phases. Combining the benefits of three different phases—amorphous, organic and crystalline (silica, chitin, aragonite)—extends the biomimetic potential of marine sponges for chemists and material scientists. Some such naturally occurring complex multiphase biocomposites have been used for the bioinspired development of novel multiphase composite materials for biomedical applications *in vitro* (Niu et al. 2013). Recently, silica and calcium carbonates have been shown to be embedded within a chitinous matrix in the marine sponge *Suberea clavata* (Ehrlich et al. 2017).

PALEOBIOSILICA

Diatoms and sponges that form biogenic opal may be of considerable paleoenvironmental significance and be valuable for the reconstruction of evolution (Clarke 2003). Silicified fossils are fairly common and are found worldwide in rocks of all ages (Butts 2014). The exceptional preservation of organic molecules, biopolymers and skeletons of ancient pro- and eukaryotes within amorphous silica is a well-known phenomenon (Figure 24). Recently, Briggs' team presented evidence from the Ediacara Member of South Australia that Ediacara-style preservation was due to rapid, early-stage precipitation of silica, facilitated by the high silica saturation state of the oceans prior to the appearance of prolific silica biomineralizers (Tarhan et al. 2016). The Ediacaran Period spans 94 million years, from the end of the Cryogenian Period 635 million years ago (Mya) to the beginning of the Cambrian Period 541 Mya. Numerous independent lines of evidence indicate that the dissolved silica concentration of Precambrian and early Paleozoic oceans was much higher than it is today, possibly as high as 2.2 mM, close to amorphous silica saturation (Konhauser et al. 2001). Diffusion of silica-rich fluids from the water column to sediment generated a taphonomic window for the early silicification of soft-bodied unique ancient faunas. High dissolved silica concentrations can mediate rapid silicification of organic

matter, resulting in cellular-level preservation (Konhauser et al. 2001). The prevalence of early silicification confirms that Ediacara-style fossil assemblages can provide an accurate window into life on the Ediacaran seafloor, which can be used to reconstruct critical steps in the development and diversification of early animal ecosystems (Tarhan et al. 2016).

Silica precipitation and the formation of sinter is an important geochemical process in hot spring systems, and understanding how these structures form might be important for deciphering some of the earliest biological processes on Earth. Microbial fossils are well preserved in silica compared with $CaCO_3$ or iron precipitates, and silica sinters are excellent structures for studying ancient microbial life (Saw et al. 2008). Although entombment within silica has been shown to promote morphological preservation, the impact of early silicification on the molecular evolution of fossilized microorganisms during burial remains poorly understood (Alleon et al. 2016). Also, the preservation of DNA within silicofossils is of fundamental importance (Saw et al. 2008). Indeed, silica is a perfect environment to preserve nucleic acids for information storage (Vybornyi et al. 2017).

Currently, the most crucial methodological obstacle to the handling of silicofossils is the necessity of demineralizing them using aggressive chemical reagents to isolate organic matrices for further bioanalytical investigations. Such treatment leads to diverse artifacts, and would also explain the dramatic effects of protein extraction by chemical methods. Also, mostly unique fossils will be irretrievably lost. In the literature several reports describe "mild" (in comparison with HF and NaOH) treatments, conditions and chemical additives for the dissolution of problematic siliceous deposits in industrial water systems (Demadis et al. 2011a,b, 2012); these methods appear promising for the demineralization of silicofossils. Consequently, we believe that application of modern X-ray imaging techniques based on the "diffraction before destruction" principle is the best way forward as we take the next steps towards understanding the principles

governing the unique organization of organic matter on molecular and atomic levels within ancient and recent biomineralized constructs.

IMPLICATIONS. PORIFERAN BIOSILICA FOR TECHNOLOGY AND BIOMEDICINE

Ceramics and glasses, in their monolithic forms, typically exhibit low fracture toughness, but rigid natural marine biosilica has shown remarkable resistance to mechanical failure (Mayer 2017). Current artificial glass shaping technology requires treatment at high temperatures. By contrast, nature has mastered the fabrication of extremely complex glass structures at low temperatures—a capacity that is far beyond the reach of current human technology (Schoeppler et al. 2017). The remarkable mechanical properties of poriferan biosiliceous structures are a consequence of their hierarchical skeletal architecture (Aluma et al. 2011; Monn et al. 2015; Birkbak et al. 2016; Monn and Kesari 2017a, 2017b). Different forms of biosilica glass can have very different properties depending on their amorphous structure and organic incrustations (Zhang et al. 2015). Sponge biosilica has complex hierarchical mesoscale structures (Aizenberg et al. 2005; Weaver et al. 2007) combining hard, stiff components with soft, tough components to produce a composite that exhibits extraordinary fracture resistance (Figure 25). This leads to an unusual combination of fracture toughness and optical light propagation properties, due to the components' macro-, micro- and nanoscale hierarchical structure (Zhang et al. 2015). Thus, the structure–property connection in the skeletal elements of marine sponges should be extensively analyzed in the future (Weaver et al. 2010; Monn and Kesari 2017a). We believe that an interplay of flexibility, strength, and hierarchical microstructure with the unique optical properties of biosilica will be an exciting inspiration for future functional biomimicry and the next generation of high-performance composite materials (Weaver et al. 2007). In this context, the mechanism by which glass architectures are formed by living organisms remains a mystery, and its discovery is

of the highest importance in view of the unique combination of properties, such as toughness, stiffness, and resilience, characterizing the biosiliceous structures of sponge origin, which makes them attractive for technical and biomedical applications (Granito et al. 2017).

Chitin–silica skeletons isolated from *S. hawaiicus* (Figure 25 d,e,f) have recently been reported as the first natural material generated in laboratory conditions—a supercontinuum similar to those known from man-made photonic crystal fibers (Ehrlich et al. 2016). It is hypothesized that generation of the supercontinuum is favored by biocomposite spicules that incorporate isotopically pure biogenic silica ($\delta^{30}Si$ = −3.28) and 15.2 ± 1.3 μg N-acetyl-glucosamine (chitin) per mg of biosilica. The internal organization of these spicules is distinguished by a solid silica core with a 1 μm wide axial channel, as well as a highly-ordered silica–chitin composite. A promising feature of the spicules of *S. hawaiicus* is their minimal use of materials, that is, their high strength-to-weight ratio. While the fabrication of commercial glass fibers requires very high temperatures, hexactinellid sponges such as *S. hawaiicus* produce the spicules responsible for their anchorage at temperatures close to 4 °C. It is suggested that a better understanding of the dispersive and nonlinear properties of these natural optical fibers might facilitate the synthesis of new light-guiding materials (Donati 2016).

The biomimetic synthesis of silica–collagen (Ehrlich et al. 2008a; Niu et al. 2011; Weiher et al. 2013; Zhang et al. 2015; Hu et al. 2017; Sun et al. 2017) and silica–chitin (Ehrlich et al. 2008b; Madhumathi et al. 2009; Spinde et al. 2011; Bazhenov et al. 2015) nanocomposites, inspired by biomineralization, is a promising direction for modern biomedicine (Wang et al. 2012) and bone replacement (Heinemann et al. 2007a; Heinemann et al. 2007b). It has been proven that bioinspired, silicified collagen scaffolds possess the ability to enhance recruitment of progenitor cells and promote osteogenesis and angiogenesis by immunomodulation of

34

monocytes, and these are promising candidates for tissue engineering applications (Sun et al. 2017). Silica–collagen composites are suggested as an example of a preliminary phase in bone development, which has been conserved from the time when silica–collagen composites were necessary for the construction of the first metazoan skeletons, for instance in glass sponges (Ehrlich and Worch 2008). The role of silica–collagen composites in bone development is still enigmatic. However recent reports indicate that such composites induce the formation of calcium phosphates. This represents an important advance in the translation of biomineralization concepts into regimes for the *in situ* remineralization of bone and teeth (Sun et al. 2017).

ACKNOWLEDGMENTS

REFERENCES

Aitken, Z.H., Luo, S., Reynolds, S.N., Thaulow, C., and Greer, J.R. (2016) Microstructure provides insights into evolutionary design and resilience of *Coscinodiscus* sp. frustule. Proceedings of the National Academy of Sciences, 113, 2017–2022.

Aizenberg, J., Sundar, V.C., Yablon, A.D., Weaver, J.C., and Chen, G. (2004) Biological glass fibers: correlation between optical and structural properties. Proceedings of the National Academy of Sciences, 101, 3358–3363.

Aizenberg, J., Weaver, J.C., Thanawala, M.S., Sundar, V.C., Morse, D.E., and Fratzl, P. (2005) Skeleton of *Euplectella* sp.: Structural hierarchy from the nanoscale to the macroscale.

Science, 309, 275–278.

Albert, K., Huang, X.C., and Hsu, H.Y. (2017) Bio-templated silica composites for next-generation biomedical applications. Advances in Colloid and Interface Science, 10.1016/j.cis.2017.04.011.

Alleon, J., Bernard, S., Le Guillou, C., Daval, D., Skouri-Panet, F., Pont, S., Delbes, L., and Robert, F. (2016) Early entombment within silica minimizes the molecular degradation of microorganisms during advanced diagenesis. Chemical Geology, 437, 98–108.

Alonso, J.M., Górzny, M.L., and Bittner, A.M. (2013) The physics of tobacco mosaic virus and virus-based devices in biotechnology. Trends in Biotechnology, 31, 530–538.

Altintoprak, K., Seidenstücker, A., Welle, A., Eiben, S., Atanasova, P., Stitz, N., Plettl, A., Bill, J., Gliemann, H., Jeske, H., and others (2015) Peptide-equipped tobacco mosaic virus templates for selective and controllable biomineral deposition. Beilstein Journal of Nanotechnology, 6, 1399–1412.

Aluma, Y., Ilan, M., and Sherman, D. (2011) Comments on a skeleton design paradigm for a demosponge. Journal of Structural Biology, 175, 415–424.

Alvarez, G.S., Foglia, M.L., Copello, G.J., Desimone, M.F., and Diaz, L.E. (2009) Effect of various parameters on viability and growth of bacteria immobilized in sol-gel-derived silica matrices. Applied Microbiology and Biotechnology, 82, 639–646.

Amores, D.R., and Warren, L.A. (2007) Identifying when microbes biosilicify: The interconnected requirements of acidic pH, colloidal SiO_2 and exposed microbial surface. Chemical Geology, 240, 298–312.

——— (2009) Metabolic patterning of biosilicification. Chemical Geology, 268, 81–88.

Andre, R., Tahir, M.N., Natalio, F., and Tremel, W. (2012) Bioinspired synthesis of multifunctional inorganic and bio-organic hybrid materials. The FEBS Journal, 279, 1737–49.

Armbrust, E.V., Berges, J.A., Bowler, C., Green, B.R., Martinez, D., Putnam, N.H., Zhou, S., Allen, A.E., Apt, K.E., Bechner, M., and others (2004) The genome of the diatom *Thalassiosira pseudonana*: ecology, evolution, and metabolism. Science, 306, 79–86.

Austin, W., and Conway, K. (2007) Growth and morphology of a reef-forming glass sponge, *Aphrocallistes vastus* (Hexactinellida), and implications for recovery from widespread trawl damage. Porifera Research, 139–145.

Aw, M.S., Simovic, S., Addai-Mensah, J., and Losic, D. (2011) Silica microcapsules from diatoms as new carrier for delivery of therapeutics. Nanomedicine, 6, 1159–1173.

Bai, S., Naren, G., Noma, H., Etou, M., Ohashi, H., Fujino, Y., Doi, K., Okaue, Y., and Yokoyama, T. (2012) Silica deposition induced by isolated aluminum ions bound on chelate resin as a model compound of the surface of microbes. Colloids and Surfaces B: Biointerfaces, 95, 208–213.

Baines, S.B., Twining, B.S., Brzezinski, M.A., Krause, J.W., Vogt, S., Assael, D., and McDaniel, H. (2012) Significant silicon accumulation by marine picocyanobacteria. Nature Geoscience, 5, 886–891.

Bazhenov, V. V., Wysokowski, M., Petrenko, I., Stawski, D., Sapozhnikov, P., Born, R., Stelling, A.L., Kaiser, S., and Jesionowski, T. (2015) Preparation of monolithic silica–chitin composite under extreme biomimetic conditions. International Journal of Biological

Macromolecules, 76, 33–38.

Belkova, N.L., Zakharova, J.R., Tazaki, K., Okrugin, V.M., and Parfenova, V.V. (2004) Fe-Si biominerals in the Vilyuchinskie hot springs, Kamchatka Peninsula, Russia. Int. Microbiol., 7, 193–198.

Belton, D.J., Deschaume O., and Perry, C.C. (2012) An overview of the fundamentals of the chemistry of silica with relevance to biosilicification and technological advances. FEBS Journal, 279, 1710-1720.

Benning, L.G., Phoenix, V.R., Yee, N., and Konhauser, K.O. (2004) The dynamics of cyanobacterial silicification: An infrared micro-spectroscopic investigation. Geochimica et Cosmochimica Acta, 68, 743–757.

Birkbak, M.E., Guizar-Sicairos, M., Holler, M., and Birkedal, H. (2016) Internal structure of sponge glass fiber revealed by ptychographic nanotomography. Journal of Structural Biology, 194, 124–128.

Blank, C.E., Cady, S.L., and Pace, N.R. (2002) Microbial composition of near-boiling silica-depositing thermal springs throughout Yellowstone National Park. Applied & Environmental Microbiology, 68, 5123–5135.

Bonucci, E. (2014) Understanding nanocalcification: A role suggested for crystal ghosts. Marine Drugs, 12, 4231–4246.

Boury-Esnault, N., and Rutzler, K. (1997) Thesaurus of sponge morphology. Smithsonian Contributions to Zoology, 596, 1–55.

Bovee, E.C. (1981) Distribution and forms of siliceous structures among protozoa. In T.L.

Simpson and B.E. Volcani, Eds., Silicon and siliceous structures in biological systems. Springer, New York.

Bradbury, J. (2004) Nature's nanotechnologists: Unveiling the secrets of diatoms. PLoS Biology, 2, 1512–1515.

Brunner, E., Richthammer, P., Ehrlich, H., Paasch, S., Simon, P., Ueberlein, S., and van Pée, K.-H. (2009) Chitin-based organic networks: an integral part of cell wall biosilica in the diatom *Thalassiosira pseudonana*. Angewandte Chemie (International Edition), 48, 9724–9727.

Butts, S.H. (2014) Silicification. The Paleontological Society Papers, 20, 15–34.

Cha, J.N., Shimizu, K., Zhou, Y., Christiansen, S.C., Chmelka, B.F., Stucky, G.D., and Morse, D.E. (1999) Silicatein filaments and subunits from a marine sponge direct the polymerization of silica and silicones *in vitro*. Proceedings of the National Academy of Sciences, 96, 361–365.

Chanzy, H., Franc, J.M., and Herbage, D. (1976) High-angle electron diffraction of frozen hydrated collagen. The Biochemical Journal, 153, 139–140.

Checa, A.G., Bonarski, J.T., Willinger, M.G., Faryna, M., Berent, K., Kania, B., González-Segura, A., Pina, C.M., Pospiech, J., and Morawiec, A. (2013) Crystallographic orientation inhomogeneity and crystal splitting in biogenic calcite. Journal of the Royal Society Interface, 10, 20130425.

Cho, J.W., Partin, J.S., and Lennarz, W.J. (1996) A technique for detecting matrix proteins in the crystalline spicule of the sea urchin embryo. Proceedings of the National Academy of Sciences, 93, 1282–1286.

Cicco, S.R., Vona, D., De Giglio, E., Cometa, S., Mattioli-Belmonte, M., Palumbo, F., Ragni, R., and Farinola, G.M. (2015) Chemically modified diatoms biosilica for bone cell growth with combined drug-delivery and antioxidant properties. ChemPlusChem, 80, 1104–1112.

Clarke, J. (2003) The occurrence and significance of biogenic opal in the regolith. Earth-Science Reviews, 60, 175–194.

Cockerell, T.D.A. (1930) Siliceous shells of protozoa. Nature, 125, 975.

Croce, G., Frache, A., Milanesio, M., Viterbo, D., Bavestrello, G., Benatti, U., Giovine, M., and Amenitsch, H. (2003) Fiber diffraction study of spicules from marine sponges. Microscopy Research and Technique, 62, 378–381.

Croce, G., Frache, A., Milanesio, M., Marchese, L., Causà, M., Viterbo, D., Barbaglia, A., Bolis, V., Bavestrello, G., Cerrano, C., and others (2004) Structural characterization of siliceous spicules from marine sponges. Biophysical Journal, 86, 526–534.

Currie, H.A., and Perry, C.C. (2007) Silica in plants: Biological, biochemical and chemical studies. Annals of Botany, 100, 1383–1389.

De Yoreo, J.J., Gilbert, P.U.P.A., Sommerdijk, N.A.J.M., Penn, R.L., Whitelam, S., Joester, D., Zhang, H., Rimer, J.D., Navrotsky, A., Banfield, J.F., and others (2015) Crystallization by particle attachment in synthetic, biogenic, and geologic environments. Science, 349, aaa6760.

Denicola, D.M. (2000) A review of diatoms found in highly acidic environments. Hydrobiologia, 433, 111–122.

Demadis, K.D., Brückner, S.I., Brunner E., Paasch, S., Antonakaki I., and Casolaro M. (2015)

The intimate role of imidazole in the stabilization of silicic acid by a pH-responsive, histidine-grafted polyampholyte. Chemistry of Materials, 27, 6827-6836.

Demadis, K.D., Mavredaki, E., and Somara, M. (2011a) Additive-driven dissolution enhancement of colloidal silica. 1. Basic principles and relevance to water treatment. Industrial & Engineering Chemistry Research, 50, 12587-12595.

Demadis, K.D., Mavredaki, E., and Somara, M. (2011b) Additive-driven dissolution enhancement of colloidal silica. 2. Environmentally friendly additives and natural products. Industrial & Engineering Chemistry Research, 50,13866-13876.

Demadis, K.D., Somara, M., and Mavredaki, E. (2012) Additive-Driven Dissolution Enhancement of Colloidal Silica. 3. Fluorine-Containing Additives. Industrial & Engineering Chemistry Research, 51, 2952–2962.

Desikachary, T.V., and Dweltz, N.E. (1961) Chemical composition of the diatom frustule. Proceedings of the Indian Academy of Sciences – Section B, 53, 157–165.

Doi, K., Fujino, Y., Inagaki, F., Kawatsu, R., Tahara, M., Ohshima, T., Okaue, Y., Yokoyama, T., Iwai, S., and Ogata, S. (2009) Stimulation of expression of a silica-induced protein (Sip) in *Thermus thermophilus* by supersaturated silicic acid. Applied and Environmental Microbiology, 75, 2406–2413.

Donati, G. (2016) Bright sponges. Nature Photonics, 10, 625.

Douglas, S. (2005) Mineralogical footprints of microbial life. American Journal of Science, 305, 503–525.

Durak, G.M., Taylor, A.R., Walker, C.E., Probert, I., De Vargas, C., Audic, S., Schroeder, D.,

Brownlee, C., and Wheeler, G.L. (2016) A role for diatom-like silicon transporters in calcifying coccolithophores. Nature Communications, 7, 10543.

Durkin, C.A., Mock, T., and Armbrust, E.V. (2009) Chitin in diatoms and its association with the cell wall. Eukaryotic Cell, 8, 1038–1050.

Durkin, C.A., Koester, J.A., Bender, S.J., and Armbrust, E.V. (2016) The evolution of silicon transporters in diatoms. Journal of Phycology, 52, 716–731.

Eckert, C., Schröder, H.C., Brandt, D., Perovic-Ottstadt, and Muller, W.E.G. (2006) Histochemical and electron microscopic analysis of spiculogenesis in the demosponge *Suberites domuncula*. Zootaxa, 54, 1031–1040.

Ehrlich, H. (2010a) Biological materials of marine origin. Springer Science+Business Media B.V., Dordrecht.

Ehrlich, H. (2010b) Chitin and collagen as universal and alternative templates in biomineralization. International Geology Review, 52, 661–699.

——— (2011) Silica Biomineralization, Sponges. In V. Thiel and J. Reitner, Eds., Encyclopedia of geobiology pp. 796–808. Springer Netherlands, Amsterdam.

Ehrlich, H. (2013) Biomimetic potential of chitin-based composite biomaterials of poriferan origin. In A.J. Ruys, Ed., Biomimetic biomaterials: Structure and applications pp. 47–67. Woodhead Publishing Ltd.

Ehrlich, H. (2017) Extreme biomimetics. Springer International Publishing, Cham.

Ehrlich, H., and Witkowski, A. (2015) Biomineralization in diatoms: the organic templates. In C. Hamm, Ed., Evolution of lightweight structures Vol. 6, pp. 39–58. Springer Netherlands.

Ehrlich, H., and Worch, H. (2008) Collagen: a huge matrix in glass sponge flexible spicules of the meter-long *Hyalonema sieboldi*. Handbook of Biomineralization: Biological Aspects and Structure Formation, 1, 22–41.

Ehrlich, H., Maldonado, M., Spindler, K., Eckert, C., Hanke, T., Born, R., Simon, P., Heinemann, S., and Worch, H. (2007a) First evidence of chitin as a component of the skeletal fibers of marine sponges. Part I. Verongidae (Demospongia: Porifera). Journal of Experimental Zoology Part B, 356, 347–356.

Ehrlich, H., Krautter, M., Hanke, T., Simon, P., Knieb, C., Heinemann, S., and Worch, H. (2007b) First evidence of the presence of chitin in skeletons of marine sponges. Part II. Glass sponges (Hexactinellida: Porifera). Journal of Experimental Zoology Part B, 308B, 473–483.

Ehrlich, H., Heinemann, S., Heinemann, C., Simon, P., Bazhenov, V. V., Shapkin, N.P., Born, R., Tabachnick, K.R., Hanke, T., and Worch, H. (2008) Nanostructural organization of naturally occurring composites—part I: silica-collagen-based biocomposites. Journal of Nanomaterials, 2008, ID 623838.

Ehrlich, H., Simon, P., Carrillo-Cabrera, W., Bazhenov, V. V., Botting, J.P., Ilan, M., Ereskovsky, A. V., Muricy, G., Worch, H., Mensch, A., and others (2010a) Insights into chemistry of biological materials: newly discovered silica-aragonite-chitin biocomposites in Demosponges. Chemistry of Materials, 22, 1462–1471.

Ehrlich, H., Deutzmann, R., Brunner, E., Cappellini, E., Koon, H., Solazzo, C., Yang, Y., Ashford, D., Thomas-Oates, J., Lubeck, M., and others (2010b) Mineralization of the metre-long biosilica structures of glass sponges is templated on hydroxylated collagen. Nature

Chemistry, 2, 1084–1088.

Ehrlich, H., Demadis, K.D., Pokrovsky, O.S., and Koutsoukos, P.G. (2010c) Modern views on desilicification: biosilica and abiotic silica dissolution in natural and artificial environments. Chemical Reviews, 110, 4656–4689.

Ehrlich, H., Rigby, J.K., Botting, J.P., Tsurkan, M., Werner, C., Schwille, P., Petrasek, Z., Pisera, A., Simon, P., Sivkov, V., and others (2013) Discovery of 505-million-year old chitin in the basal demosponge *Vauxia gracilenta.* Scientific Reports, 3, 3497.

Ehrlich, H., Maldonado, M., Parker, A.R., Kulchin, Y.N., Schilling, J., Köhler, B., Skrzypczak, U., Simon, P., Reiswig, H.M., Tsurkan, M. V., and others (2016) Supercontinuum generation in naturally occurring glass sponges spicules. Advanced Optical Materials, 4, 1608–1613.

Ehrlich, H., Bazhenov, V.V., Debitus, C., de Voogd, N., Galli, R., Tsurkan, M.V., Wysokowski, M., Meissner, H., Bulut, E., Kaya, M., and others (2017) Isolation and identification of chitin from heavy mineralized skeleton of *Suberea clavata* (Verongida: Demospongiae: Porifera) marine demosponge. International Journal of Biological Macromolecules, 104, 1706-1712.

Exley, C. (2015) A possible mechanism of biological silicification in plants. Frontiers in Plant Science, 6, 853.

Ferrara, M.A., Dardano, P., De Stefano, L., Rea, I., Coppola, G., Rendina, I., Congestri, R., Antonucci, A., De Stefano, M., and De Tommasi, E. (2014) Optical properties of diatom nanostructured biosilica in Arachnoidiscus sp: Micro-optics from mother nature. PLoS ONE, 9, 3–10.

Ferris, F.G., Beveridge, T.J., and Fyfe, W.S. (1986) Iron-silica crystallite nucleation by bacteria in a geothermal sediment. Nature, 320, 609–611.

Finkel, Z. V (2016) Silicification in the microalgae. In M. Borowitzka, J. Beardall, and J. Raven, Eds., The physiology of microalgae. Developments in applied phycology, vol 6. Springer, Cham.

Florkin, M., Ed. (1968) Chemical Zoology V2: Porifera, Coelenterata, And Platyhelminthes. Academic Press, London.

Foissner, M., Weissenbacher, B., Krautgartner, W.-D., and Lutz-Meindl, U. (2009) A cover of glass: first report of biomineralized silicon in a ciliate, *Maryna umbrellata* (Ciliophora: Colpodea). Journal of Eukaryotic Microbiology, 56, 519–530.

Fuhrmann, T., Landwehr, S., El Rharbl-Kucki, M., and Sumper, M. (2004) Diatoms as living photonic crystals. Applied Physics B: Lasers and Optics, 78, 257–260.

Garrone, R. (1978) Phylogenesis of connective tissue: morphological aspects and biosynthesis of sponge intercellular matrix, Chapter II: 17-27 p. John Wiley & Sons.

Goessling, J.W. (2017) Biophotonics of diatoms linking frustule structure to photobiology. University of Copenhagen, PhD thesis.

Gold, D.A., Grabenstatter, J., de Mendoza, A., Riesgo, A., Ruiz-Trillo, I., and Summons, R.E. (2016) Sterol and genomic analyses validate the sponge biomarker hypothesis. Proceedings of the National Academy of Sciences, 113, 2684–2689.

Gordon, R., Losic, D., Tiffany, M.A., Nagy, S.S., and Sterrenburg, F.A.S. (2009) The glass menagerie: diatoms for novel applications in nanotechnology. Trends in Biotechnology, 27,

116–127.

Gower, L.B. (2008) Biomimetic model systems for investigating the amorphous precursor pathway and its role in biomineralization. Chemical Reviews, 108, 4551–4627.

Goto K., Effect of pH on polymerization of silicic acid. The Journal of Physical Chemistry, 60, 1007–1008.

Granito, R.N., Custódio, M.R., and Rennó, A.C.M. (2017) Natural marine sponges for bone tissue engineering: The state of art and future perspectives. Journal of Biomedical Materials Research – Part B Applied Biomaterials, 105, 1717–1727.

Gröger, P., Poulsen, N., Klemm, J., Kröger, N., and Schlierf, M. (2016) Establishing super-resolution imaging for proteins in diatom biosilica. Scientific Reports, 6, 36824.

Grzesik, M., Romanowska-Duda, Z., Piotrowski, K., and Janas, R. (2015) Diatoms (Bacillariophyceae) as an effective base of a new generation of organic fertilizers. Przemysł Chemiczny, 94, 391–396.

Guo, J., Li, C., Ling, S., Huang, W., Chen, Y., and Kaplan, D.L. (2017) Multiscale design and synthesis of biomimetic gradient protein/biosilica composites for interfacial tissue engineering. Biomaterials, 145, 44–55.

Haddad, F.S., and Kouyoumdjian, A. (1986) Silica stones in humans. Urologia Internationalis, 41, 70–76.

Hamm, C. (2015) Evolution of Lightweight Structures: Analyses and Technical Applications, Springer Science+Business Media.

Hamm, C.E. (2005) The evolution of advanced mechanical defenses and potential technological

applications of diatom shells. Journal of Nanoscience and Nanotechnology, 5, 108–119.

Hamm, C.E., Merkel, R., Springer, O., Jurkojc, P., Maier, C., Prechtel, K., and Smetacek, V. (2003) Architecture and material properties of diatom shells provide effective mechanical protection. Nature, 421, 841–843.

Heinemann, S., Heinemann, C., Ehrlich, H., Meyer, M., Baltzer, H., Worch, H., and Hanke, T. (2007) A novel biomimetic hybrid material made of silicified collagen: perspectives for bone replacement. Advanced Engineering Materials, 9, 1061–1068.

Heinemann, S., Ehrlich, H., Knieb, C., and Hanke, T. (2007) Biomimetically inspired hybrid materials based on silicified collagen. International Journal of Materials Research, 98, 603–608.

Hildebrand, M., and Lerch, S.J.L. (2015) Diatom silica biomineralization: parallel development of approaches and understanding. Seminars in Cell and Developmental Biology, 46, 27–35.

Hirota, R., Hata, Y., Ikeda, T., Ishida, T., and Kuroda, A. (2010) The silicon layer supports acid resistance of Bacillus cereus spores. Journal of Bacteriology, 192, 111–116.

Hu, C., Yu, L., and Wei, M. (2017) Biomimetic intrafibrillar silicification of collagen fibrils through a one-step collagen self-assembly/silicification approach. RSC Adv., 7, 34624–34632.

Hugo, R.C., Cady, S.L., and Smythe, W. (2011) The role of extracellular polymeric substances in the silicification of calothrix : evidence from microbial mat communities in hot springs at Yellowstone National Park, USA. Geomicrobiology Journal, 28, 667–675.

Iler, R.K. (1978) The chemistry of silica-solubility, polymerization, colloid and surface

properties, and biochemistry. John Wiley & Sons.

Illuminati, S., Annibaldi, A., Truzzi, C., and Scarponi, G. (2016) Heavy metal distribution in organic and siliceous marine sponge tissues measured by square wave anodic stripping voltammetry. Marine Pollution Bulletin, 111, 476–482.

Inagaki, F., Yokoyama, T., Doi, K., Izawa, E., and Ogata, S. (1998) Bio-deposition of amorphous silica by an extremely thermophilic bacterium *Thermus spp.* Bioscience, Biotechnology, and Biochemistry, 62, 1271–1272.

Inagaki, F., Motomura, Y., and Ogata, S. (2003) Microbial silica deposition in geothermal hot waters. Applied Microbiology and Biotechnology, 60, 605–611.

Ivanov, V.K., Fedorov, P.P., Baranchikov, A.Y., and Osiko, V. V. (2014) Oriented attachment of particles: 100 years of investigations of non-classical crystal growth. Russian Chemical Reviews, 83, 1204–1222.

Jones, L.H.P., Milne, A.A., and Sanders, J. V (1960) Tabashir: an opal of plant origin. Science, 151, 464–466.

Judd, J.W. (1887) The relation of tabasheer to mineral substances. Nature, 35, 488–491.

Kamińska, A., Sprynskyy, M., Winkler, K., and Szymborski, T. (2017) Ultrasensitive SERS immunoassay based on diatom biosilica for detection of interleukins in blood plasma. Analytical and Bioanalytical Chemistry, 409, 6337–6347.

Klinowski, J., Cheng, C.F., Sanz, J., Rojo, J., and Mackay, A.L. (1998) Structural studies of tabasheer, an opal of plant origin. Philosophical Magazine A, 77, 201–216.

Knecht, M.R., and Wright, D.W. (2004) Amine-terminated dendrimers as biomimetic templates

for silica nanosphere formation. Langmuir, 20, 4728–4732.

Konhauser, K.O., Phoenix, V.R., Bottrell, S.H., Adams, D.G., and Head, I.M. (2001) Microbial-silica interactions in Icelandic hot spring sinter: possible analogues for some Precambrian siliceous stromatolites. Sedimentology, 48, 415–433.

Konhauser, K.O., Jones, B., Phoenix, V.R., Ferris, G., and Renaut, R.W. (2004) The microbial role in hot spring silicification. Ambio, 33, 552–558.

Korhola, A., and Smol, J.P. (2001) Erbridians. In W.M. Last and J.P. Smol, Eds., Tracking environmental change using lake sediments pp. 225–234. Springer Science+Business Media B.V., Amsterdam.

Kotzsch, A., Pawolski, D., Milentyev, A., Shevchenko, A., Scheffel, A., Poulsen, N., Shevchenko, A., and Kröger, N. (2016) Biochemical composition and assembly of biosilica-associated insoluble organic matrices from the diatom *Thalassiosira pseudonana*. Journal of Biological Chemistry, 291, 4982–4997.

Kotzsch, A., Gröger, P., Pawolski, D., Bomans, P.H.H., Sommerdijk, N.A.J.M., Schlierf, M., and Kröger, N. (2017) Silicanin-1 is a conserved diatom membrane protein involved in silica biomineralization. BMC Biology, 15, 65.

Kölliker, A. (1864) Der feinere Bau der Protozoen. Wilhelm Engelmann, Leipzig.

Krajina, B.A., Proctor, A.C., Schoen, A.P., Spakowitz, A.J., and Heilshorn, S.C. (2018) Biotemplated synthesis of inorganic materials: An emerging paradigm for nanomaterial synthesis inspired by nature. Progress in Materials Science, 91, 1–23.

Kristiansen, J. (1986) Silica-scale bearing chrysophytes as environmental indicators. British

Phycological Journal, 21, 425–436.

Kröger, N., and Poulsen, N. (2008) Diatoms—From Cell Wall Biogenesis to Nanotechnology.
Annual Review of Genetics, 42, 83–107.

Kuhlman, A.M.J. (1963) The second most abundant element in the Earth's crust. The Journal of
The Minerals, Metals & Materials Society, 15, 502–505.

Kumar, S., Milstein, Y., Brami, Y., Elbaum, M., and Elbaum, R. (2017a) Mechanism of silica
deposition in sorghum silica cells. New Phytologist, 213, 791–798.

Kumar, S., Soukup, M., and Elbaum, R. (2017b) Silicification in grasses: variation between
different cell types. Frontiers in Plant Science, 8, 438.

Laidler, J.R., and Stedman, K.M. (2010) Virus silicification under simulated hot spring
conditions. Astrobiology, 10, 569–576.

Laidler, J.R., Shugart, J.A., Cady, S.L., Bahjat, K.S., and Stedman, K.M. (2013) Reversible
inactivation and desiccation tolerance of silicified viruses. Journal of Virology, 87, 13927–
13929.

Lalonde, S. V., Konhauser, K.O., Reysenbach, A.L., and Ferris, F.G. (2005) The experimental
silicification of Aquificales and their role in hot spring sinter formation. Geobiology, 3, 41–
52.

Lau, C.Y., Aitchison, J.C., and Pointing, S.B. (2008) Early colonization of thermal niches in a
silica-depositing hot spring in central Tibet. Geobiology, 6, 136–146.

LeDuff, P., Roesijadi, G., and Rorrer, G.L. (2016) Micro-photoluminescence of single living
diatom cells. Luminescence, 31, 1379–1383.

Leonardo, S., Prieto-Simón, B., and Campas, M. (2016) Past, present and future of diatoms in biosensing. TrAC – Trends in Analytical Chemistry, 79, 276–285.

Levi, C. (1963) Slcéroblastes et spiculogenese chez une éponge siliceuse. C. R. Acad. Sc., 256, 497–498.

Li, D., Nielsen, M.H., Lee, J.R.I., Frandsen, C., Banfield, J.F., and De Yoreo, J.J. (2012) Direction-Specific Interactions Control Crystal Growth by Oriented Attachment. Science, 336, 1014–1018.

Losic, D., Ed. (2018) Diatom nanotechnology: progress and emerging applications. The Royal Society of Chemistry, Croydon, UK.

Losic, D., Mitchell, J.G., and Voelcker, N.H. (2009) Diatomaceous lessons in nanotechnology and advanced materials. Advanced Materials, 21, 2947–2958.

Madhumathi, K., Sudheesh Kumar, P.T., Kavya, K.C., Furuike, T., Tamura, H., Nair, S. V., and Jayakumar, R. (2009) Novel chitin/nanosilica composite scaffolds for bone tissue engineering applications. International Journal of Biological Macromolecules, 45, 289–292.

Maldonado, M., Carmona, M.C., Uriz, M.J., and Cruzado, A. (1999) Decline in mesozoic reef-building sponges explained by silicon limitation. Nature, 401, 785–788.

Maldonado, M., Navarro, L., Grasa, A., Gonzalez, A., and Vaquerizo, I. (2011) Silicon uptake by sponges: a twist to understanding nutrient cycling on continental margins. Scientific Reports, 1, 2011.

Mann, S., and Williams, R.J.P. (1982) High resolution electron microscopy studies of the silica lorica in the choanoflagellate *Stephanoeca diplocostata* Ellis. Proceedings of the Royal

51

Society B: Biological Sciences, 216, 137–146.

Marron, A.O., Alston, M.J., Heavens, D., Akam, M., Caccamo, M., Holland, P.W.H., and Walker, G. (2013) A family of diatom-like silicon transporters in the siliceous loricate choanoflagellates. Proceedings of the Royal Society B: Biological Sciences, 280, 20122543–20122543.

Masse, S., Pisera, A., Laurent, G., and Coradin, T. (2016) A solid state NMR investigation of recent marine siliceous sponge spicules. Minerals, 6, 21.

Mastropietro, F., Godard, P., Burghammer, M., Chevallard, C., Daillant, J., Duboisset, J., Allain, M., Guenoun, P., Nouet, J., and Chamard, V. (2017) Revealing crystalline domains in a mollusc shell single-crystalline prism. Nature Materials, 16, 946–952.

Mateu, M.G. (2011) Virus engineering: functionalization and stabilization. Protein Engineering, Design and Selection, 24, 53–63.

Mayer, G. (2017) Mechanical energy dissipation in natural ceramic composites. Journal of the Mechanical Behavior of Biomedical Materials, 76, 21–29.

McCartney, K., Witkowski, J., Jordan, R.W., Daugbjerg, N., Malinverno, E., van Wezel, R., Kano, H., Abe, K., Scott, F., Schweizer, M., and others (2014) Fine structure of silicoflagellate double skeletons. Marine Micropaleontology, 113, 10–19.

Medarevic, D., Losic, D., and Ibric, S. (2016) Diatoms – nature materials with great potential for bioapplications. Hemijska Industrija, 70, 613–627.

Medlin, L.K. (2016) Evolution of the diatoms: major steps in their evolution and a review of the supporting molecular and morphological evidence. Phycologia, 55, 79–103.

Merola, F., Memmolo, P., Miccio, L., Bianco, V., and Paturzo, M. (2015) Diagnostic tools for lab-on-chip applications based on coherent imaging microscopy. Proceedings of the IEEE, 103, 192–204.

Michels, J., Vogt, J., and Gorb, S.N. (2012) Tools for crushing diatoms – opal teeth in copepods feature a rubber-like bearing composed of resilin. Scientific Reports, 2, 465.

Michels, J., Vogt, J., Simon, P., and Gorb, S.N. (2015) New insights into the complex architecture of siliceous copepod teeth. Zoology, 118, 141–146.

Millington, W.F., and Gawlik, S.R. (1967) Silica in the wall of pediastrum. Nature.

Mishra, M., Arukha, A.P., Bashir, T., Yadav, D., and Prasad, G.B.K.S. (2017) All new faces of diatoms: Potential source of nanomaterials and beyond. Frontiers in Microbiology, 8, 1239.

Monn, M.A., and Kesari, H. (2017a) A new structure-property connection in the skeletal elements of the marine sponge *Tethya aurantia* that guards against buckling instability. Scientific Reports, 7, 39547.

——— (2017b) Enhanced bending failure strain in biological glass fibers due to internal lamellar architecture. Journal of the Mechanical Behavior of Biomedical Materials, 76, 69–75.

Monn, M.A., Weaver, J.C., Zhang, T., Aizenberg, J., and Kesari, H. (2015) New functional insights into the internal architecture of the laminated anchor spicules of *Euplectella aspergillum*. Proceedings of the National Academy of Sciences, 112, 4976–4981.

Monniot, F., Martoja, R., and Monniot, C. (1992) Silica distribution in ascidian ovaries, a tool for systematics. Biochemical Systematics and Ecology, 20, 541–552.

Moreno, M.D., Ma, K., Schoenung, J., and Dávila, L.P. (2015) An integrated approach for

probing the structure and mechanical properties of diatoms: Toward engineered nanotemplates. Acta Biomaterialia, 25, 313–324.

Morrow, C., and Cardenas, P. (2015) Proposal for a revised classification of the Demospongiae (Porifera). Frontiers in Zoology, 12, 7.

Mugnaioli, E., Natalio, F., Schloßmacher, U., Wang, X., Müller, W.E.G., and Kolb, U. (2009) Crystalline nanorods as possible templates for the synthesis of amorphous biosilica during spicule formation in demospongiae. ChemBioChem, 10, 683–689.

Müller, W.E.G., Schloßmacher, U., Eckert, C., Krasko, A., Boreiko, A., Ushijima, H., Wolf, S.E., Tremel, W., Müller, I.M., and Schröder, H.C. (2007) Analysis of the axial filament in spicules of the demosponge *Geodia cydonium*: Different silicatein composition in microscleres (asters) and megascleres (oxeas and triaenes). European Journal of Cell Biology, 86, 473–487.

Müller, W.E.G., Boreiko, A., Schlossmacher, U., Wang, X., Eckert, C., Kropf, K., Li, J., and Schroder, H.C. (2008a) Identification of a silicatein(-related) protease in the giant spicules of the deep-sea hexactinellid *Monorhaphis chuni*. Journal of Experimental Biology, 211, 300–309.

Müller, W.E.G., Wang, X., Kropf, K., Boreiko, A., Schloßmacher, U., Brandt, D., Schröder, H.C., and Wiens, M. (2008b) Silicatein expression in the hexactinellid *Crateromorpha meyeri:* The lead marker gene restricted to siliceous sponges. Cell and Tissue Research, 333, 339–351.

Müller, W.E.G., Mugnaioli, E., Schröder, H.C., Schloßmacher, U., Giovine, M., Kolb, U., and Wang, X. (2013) Hierarchical composition of the axial filament from spicules of the

siliceous sponge *Suberites domuncula*: From biosilica-synthesizing nanofibrils to structure- and morphology-guiding triangular stems. Cell and Tissue Research, 351, 49–58.

Naik, R.R., Brott, L.L., Clarson, S.J., and Stone, M.O. (2002) Silica-precipitating peptides isolated from a combinatorial phage display peptide library. Journal of Nanoscience and Nanotechnology, 2, 95–100.

Nassif, N., and Livage, J. (2011) From diatoms to silica-based biohybrids. Chem. Soc. Rev., 40, 849–859.

Natalio, F., Corrales, T.P., Panthöfer, M., Schollmeyer, D., Lieberwirth, I., Müller, W.E.G., Kappl, M., Butt, H.-J., and Tremel, W. (2013) Flexible minerals: self-assembled calcite spicules with extreme bending strength. Science, 339, 1298–302.

Neethirajan, S., Gordon, R., and Wang, L. (2009) Potential of silica bodies (phytoliths) for nanotechnology. Trends in Biotechnology, 27, 461–467.

Nichols, S., and Wörheide, G. (2005) Sponges: New Views of Old Animals. Integrative and Comparative Biology, 45, 333–334.

Nishizono, T., Eta, S., Enokida, H., and Nishiyama, K. (2004) Case report renal silica calculi in an infant. International Journal of Urology, 11, 119–121.

Niu, L., Jiao, K., Qi, Y., Yiu, C.K.Y., Ryou, H., Arola, D.D., Chen, J., Breschi, L., Pashley, D.H., and Tay, F.R. (2011) Infiltration of silica inside fibrillar collagen. Angewandte Chemie (International Edition), 50, 11688–11691.

Niu, L., Jiao, K., Ryou, H., Yiu, C.K.Y., Chen, J., Breschi, L., Arola, D.D., Pashley, D.H., and Tay, F.R. (2013) Multiphase intrafibrillar mineralization of collagen. Angewandte Chemie

(International Edition), 52, 5762–5766.

Nomura, M., and Ishida, K.I. (2016) Fine-structural observations on siliceous scale production and shell assembly in the testate amoeba *Paulinella chromatophora*. Protist, 167, 303–318.

Nowak, A.P., Lisowska-Oleksiak, A., Wicikowska, B., and Gazda, M. (2017) Biosilica from sea water diatoms algae—electrochemical impedance spectroscopy study. Journal of Solid State Electrochemistry, 21, 2251–2258.

Ogawa, Y., Kimura, S., Wada, M., and Kuga, S. (2010) Crystal analysis and high-resolution imaging of microfibrillar α-chitin from Phaeocystis. Journal of Structural Biology, 171, 111–116.

Ogden, C.G. (1991) The ultrastructure of Heleopera petricola an agglutinate soil amoeba; with comments on feeding and silica deposition. European Journal of Protistology, 27, 238–248.

Ogden, C.G. (1991) Ultrastructure of the vegetative organisation and initial stages of silica plate deposition in the soil testate amoeba *Corythion dubium*. Protoplasma, 163, 136–144.

Orange, F., Disnar, J.R., Westall, F., Prieur, D., and Baillif, P. (2011) Metal cation binding by the hyperthermophilic microorganism, Archaea *Methanocaldococcus jannaschii*, and its effects on silicification. Palaeontology, 54, 953–964.

Orange, F., Lalonde, S. V, and Konhauser, K.O. (2013) Experimental simulation of evaporation-driven silica sinter formation and microbial silicification in hot spring systems. Astrobiology, 13, 163–176.

Papanthasiou, K.E., Turhanen, P., Brückner, S.I., Brunner, E., and Demadis K.D. (2017) Smart, programmable and responsive injectable hydrogels for controlled release of cargo

osteoporosis drugs. Scientific Reports, 7, 4743.

Parker, A.R., and Townley, H.E. (2007) Biomimetics of photonic nanostructures. Nature Nanotechnology, 2, 347–353.

Peng, X., Xu, H., Jones, B., Chen, S., and Zhou, H. (2013) Silicified virus-like nanoparticles in an extreme thermal environment: implications for the preservation of viruses in the geological record. Geobiology, 11, 511–526.

Pfister, L., Wetzel, C.E., Klaus, J., Martínez-Carreras, N., Antonelli, M., Teuling, A.J., and McDonnell, J.J. (2017) Terrestrial diatoms as tracers in catchment hydrology: a review. Wiley Interdisciplinary Reviews: Water, 4, e1241.

Pohnert, G. (2002) Biomineralization in diatoms mediated through peptide- and polyamine-assisted condensation of silica. Angewandte Chemie (International Edition) 41, 3167–3169.

Pokroy, B., Quintana, J.P., Caspi, E.N., Berner, A., and Zolotoyabko, E. (2004) Anisotropic lattice distortions in biogenic aragonite. Nature Materials, 3, 900–902.

Pouget, E.M., Bomans, P.H.H., Goos, J.A.C.M., Frederik, P.M., de With, G., and Sommerdijk, N.A.J.M. (2009) The initial stages of template-controlled CaCO3 formation revealed by cryo-TEM. Science, 323, 1455–1458.

Prado Figueroa, M. (2012) The growth of chalcedony (nanocrystalline silica) in electric organs from living marine fish. In Y. Mastai, Ed., Advances in crystallization processes. InTech.

Prado Figueroa, M., Flores, L., Sanchez, J., and Cesaretti, N. (2008a) Biosilicification (chalcedony) in human cerebral cortex, hippocampus and cerebellum from aged patients. Micron, 39, 859–867.

Prado Figueroa, M., Barrera, F., and Cesaretti, N.N. (2008b) Chalcedony (a crystalline variety of silica): Biogenic origin in electric organs from living *Psammobatis extenta (*family Rajidae). Micron, 39, 1027–1035.

Preari, M., Spinde, K., Lazic, J., Brunner, E., and Demadis, K.D. (2014) Bioinspired Insights into Silicic Acid Stabilization Mechanisms: The Dominant Role of Polyethylene Glycol-Induced Hydrogen Bonding. Journal of American Chemical Society, 136, 4236-4244.

Qi, Y., Wang, J., Wang, X., Cheng, J.J., and Wen, Z. (2017) Selective adsorption of Pb(II) from aqueous solution using porous biosilica extracted from marine diatom biomass: Properties and mechanism, Applied Surface Science, 396, 965-977.

Ramachandran, G.N., and Kartha, G. (1955) Strucutre of collagen. Nature, 176, 593–595.

Reitner, J., and Thiel, V. (2011) Encyclopedia of geobiology. Springer Science+Business Media B.V., Amsterdam.

Ren, F., Campbell, J., Wang, X., Rorrer, G.L., and Wang, A.X. (2013) Enhancing surface plasmon resonances of metallic nanoparticles by diatom biosilica. Optics Express, 21, 15308.

Renaudie, J., and Lazarus, D.B. (2013) On the accuracy of paleodiversity reconstructions: a case study in Antarctic Neogene radiolarians. Paleobiology, 39, 491–509.

Rich, A., and Crick, F.H.C. (1955) The structure of collagen. Nature, 175, 863–864.

Romann, J., Valmalette, J.-C., Chauton, M.S., Tranell, G., Einarsrud, M.-A., and Vadstein, O. (2015) Wavelength and orientation dependent capture of light by diatom frustule nanostructures. Scientific Reports, 5, 17403.

Royston, E.S., Brown, A.D., Harris, M.T., and Culver, J.N. (2009) Preparation of silica stabilized tobacco mosaic virus templates for the production of metal and layered nanoparticles. Journal of Colloid and Interface Science, 332, 402–407.

Sahebi, M., Hanafi, M.M., Siti Nor Akmar, A., Rafii, M.Y., Azizi, P., Tengoua, F.F., Nurul Mayzaitul Azwa, J., and Shabanimofrad, M. (2015) Importance of silicon and mechanisms of biosilica formation in plants. BioMed Research International, 2015, ID: 396010.

Sandford, F. (2003) Physical and chemical analysis of the siliceous skeletons in six sponges of two groups (demospongiae and hexactinellida). Microscopy Research and Technique, 62, 336–355.

Sarikaya, M., Fong, H., Sunderland, N., Flinn, B.D., Mayer, G., Mescher, A., and Gaino, E. (2001) Biomimetic model of a sponge-spicular optical fiber—mechanical properties and structure. Journal of Materials Research, 16, 1420–1428.

Sato, K., Ozaki, N., Nakanishi, K., Sugahara, Y., Oaki, Y., Salinas, C., Herrera, S., Kisailus, D., Imai, H., Collins, M.J., and others (2017) Effects of nanostructured biosilica on rice plant mechanics. RSC Adv., 7, 13065–13071.

Saw, J.H., Mountain, B.W., Feng, L., Omelchenko, M. V, Hou, S., Saito, J. a, Stott, M.B., Li, D., Zhao, G., Wu, J., and others (2008) Encapsulated in silica: genome, proteome and physiology of the thermophilic bacterium *Anoxybacillus flavithermus* WK1. Genome biology, 9, R161.

Schenk, A.S., Eiben, S., Goll, M., Reith, L., Kulak, A.N., Meldrum, F.C., Jeske, H., Wege, C., and Ludwigs, S. (2017) Virus-directed formation of electrocatalytically active nanoparticle-based Co_3O_4 tubes. Nanoscale, 9, 6334–6345.

Schoeppler, V., Reich, E., Vacelet, J., Rosenthal, M., Pacureanu, A., Rack, A., Zaslansky, P., Zolotoyabko, E., and Zlotnikov, I. (2017) Shaping highly regular glass architectures: A lesson from nature. Science Advances, 3, eaao2047.

Shimizu, K., Cha, J., Stucky, G.D., and Morse, D.E. (1998) Silicatein α: Cathepsin L-like protein in sponge biosilica. Proceedings of the National Academy of Sciences, 95, 6234–6238.

Shimizu, K., Amano, T., Bari, M.R., Weaver, J.C., Arima, J., and Mori, N. (2015) Glassin, a histidine-rich protein from the siliceous skeletal system of the marine sponge *Euplectella*, directs silica polycondensation. Proceedings of the National Academy of Sciences, 112, 11449–11454.

Shoulders, M.D., and Raines, R.T. (2009) Collagen structure and stability. Annual Review of Biochemistry, 78, 929–958.

Sikorski, P., Hori, R., and Wada, M. (2009) Revisit of α-chitin crystal structure using high resolution X-ray diffraction data. Biomacromolecules, 10, 1100–1105.

Škaloud, P., Kristiansen, J., and Škaloudová, M. (2013) Developments in the taxonomy of silica-scaled chrysophytes – From morphological and ultrastructural to molecular approaches. Nordic Journal of Botany, 31, 385–402.

Skinner, H.C.W., and Ehrlich, H. (2013) Biomineralization. In K.K. Turekian and H.D. Holland, Eds., Treatise on geochemistry, biogeochemistry pp. 105–162. Elsevier Science.

Sommer, M., Kaczorek, D., Kuzyakov, Y., and Breuer, J. (2006) Silicon pools and fluxes in soils and landscapes – A review. Journal of Plant Nutrition and Soil Science, 169, 310–329.

Song, Z.Q., Wang, F.P., Zhi, X.Y., Chen, J.Q., Zhou, E.M., Liang, F., Xiao, X., Tang, S.K.,

Jiang, H.C., Zhang, C.L., and others (2013) Bacterial and archaeal diversities in Yunnan and Tibetan hot springs, China. Environmental Microbiology, 15, 1160–1175.

Spinde, K., Kammer, M., Freyer, K., Ehrlich, H., Vournakis, J.N., and Brunner, E. (2011) Biomimetic silicification of fibrous chitin from diatoms. Chemistry of Materials, 23, 2973–2978.

Spinde, K., Pachis, K., Antonakaki, I., Brunner, E., and Demadis, K.D. (2011) Influence of Polyamines and Related Macromolecules on Silicic Acid Polycondensation: Relevance to "Soluble Silicon Pools"? Chemistry of Materials, 23, 4676–4687

Spinthaki, A., Skordalou, G., Stathoulopoulou, A., and Demadis, K.D. (2016) Modified macromolecules in the prevention of silica scale. Pure and Applied Chemistry, 88, 1037–1047.

Spinthaki, A., Zerfass, C., Paulsen, H., Hobe, S., and Demadis, K.D. (2017) Pleiotropic role of recombinant silaffin-like cationic polypeptide P5S3: Peptide-induced silicic acid stabilization, silica formation and inhibition of silica dissolution. ChemistrySelect, 2, 6–17.

Sprynskyy, M., Pomastowski, P., Hornowska, M., Król, A., Rafińska, K., and Buszewski, B. (2017) Naturally organic functionalized 3D biosilica from diatom microalgae. Materials and Design, 132, 22–29.

Steinmetz, N.F., Shah, S.N., Barclay, J.E., Rallapalli, G., Lomonossoff, G.P., and Evans, D.J. (2009) Virus-templated silica nanoparticles. Small, 5, 813–816.

Su, Y., Lundholm, N., Friis, S.M.M., and Ellegaard, M. (2015) Implications for photonic applications of diatom growth and frustule nanostructure changes in response to different light wavelengths. Nano Research, 8, 2363–2372.

Sumper, M., and Brunner, E. (2006) Learning from diatoms: Nature's tools for the production of nanostructured silica. Advanced Functional Materials, 16, 17–26.

Sun, J.-L., Jiao, K., Niu, L. na, Jiao, Y., Song, Q., Shen, L. juan, Tay, F.R., and Chen, J. hua (2017) Intrafibrillar silicified collagen scaffold modulates monocyte to promote cell homing, angiogenesis and bone regeneration. Biomaterials, 113, 203–216.

Sun, X.W., Zhang, Y.X., and Losic, D. (2017) Diatom silica, an emerging biomaterial for energy conversion and storage. J. Mater. Chem. A, 5, 8847–8859.

Swift, D.M., and Wheeler, A.P. (1992) Evidence of an organic matrix from diatom biosilica. Journal of Phycology, 28, 202–209.

Tabachnick, K., Janussen, D., and Menschenina, L. (2017) Cold biosilicification in Metazoan: psychrophilic glass sponges. In H. Ehrlich, Ed., Extreme Biomimetics pp. 53–80. Springer International Publishing, Cham, Switzerland.

Tabatabaei Dakhili, S.Y., Caslin, S.A., Faponle, A.S., Quayle, P., de Visser, S.P., and Wong, L.S. (2017) Recombinant silicateins as model biocatalysts in organosiloxane chemistry. Proceedings of the National Academy of Sciences, 114, 5285–5291.

Tarhan, L.G., Hood, A.V.S., Droser, M.L., Gehling, J.G., and Briggs, D.E.G. (2016) Exceptional preservation of soft-bodied Ediacara Biota promoted by silica-rich oceans. Geology, 44, 951–954.

Tesson, B., and Hildebrand, M. (2010) Extensive and intimate association of the cytoskeleton with forming silica in diatoms: Control over patterning on the meso- and micro-scale. PLoS ONE, 5, e14300.

Thomson, T. (1836) Chemische analyse des tabashir. J. Prakt. Chem., 8, 21–25.

Townley, H.E., Parker, A.R., and White-Cooper, H. (2008) Exploitation of diatom frustules for nanotechnology: Tethering active biomolecules. Advanced Functional Materials, 18, 369–374.

Treguer, P., Nelson, D.M., Van Bennekom, A.J., DeMaster, D.J., Leynaert, A., and Queguiner, B. (1995) The silica balance in the world ocean: A reestimate. Science, 268, 375–379.

Tréguer, P.J., and De La Rocha, C.L. (2013) The world ocean silica cycle. Annual Review of Marine Science, 5, 477–501.

Uriz, M.J. (2006) Mineral skeletogenesis in sponges. Canadian Journal of Zoology, 84, 322–356.

Uriz, M.J., Turon, X., Becerro, M.A., and Agell, G. (2003) Siliceous spicules and skeleton frameworks in sponges: Origin, diversity, ultrastructural patterns, and biological functions. Microscopy Research and Technique, 62, 279–299.

van Soest, R.W.M., Boury-Esnault, N., Vacelet, J., Dohrmann, M., Erpenbeck, D., de Voogd, N.J., Santodomingo, N., Vanhoorne, B., Kelly, M., and Hooper, J.N.A. (2012) Global diversity of sponges (Porifera). PLoS ONE, 7, e35105.

Vybornyi, M., Vyborna, Y., and Häner, R. (2017) Silica Mineralization of DNA-inspired 1D and 2d supramolecular polymers. Chemistry Open, 6, 488–491.

Wagner, D., and Kelley, C.D. (2017) The largest sponge in the world? Marine Biodiversity, 47, 367–368.

Wallace, A.F., DeYoreo, J.J., and Dove, P.M. (2009) Kinetics of silica nucleation on carboxyl- and amine-terminated surfaces: insights for biomineralization. Journal of the American

Chemical Society, 131, 5244–50.

Walsh, P.J., Clarke, S.A., Julius, M., and Messersmith, P.B. (2017) Exploratory testing of diatom silica to map the role of material attributes on cell fate. Scientific Reports, 7, 14138.

Wang, G., Wang, H., Zhou, H., Nian, Q., Song, Z., and Al, W.E.T. (2015) Hydrated silica exterior produced by biomimetic silicification confers viral vaccine heat resistance. ACS Nano, 9, 799–808.

Wang, G., Zhou, H., Nian, Q.-G., Yang, Y., Qin, C.-F., and Tang, R. (2016) Robust vaccine formulation produced by assembling a hybrid coating of polyethyleneimine–silica. Chem. Sci., 7, 1753–1759.

Wang, X., Schröder, H.C., Wiens, M., Ushijima, H., and Müller, W.E.G. (2012) Bio-silica and bio-polyphosphate: applications in biomedicine (bone formation). Current Opinion in Biotechnology, 23, 570–578.

Wang, X., Deng, Y., Li, S., Wang, G., Qin, E., Xu, X., Tang, R., and Qin, C. (2012) Biomineralization-based virus shell-engineering: Towards neutralization escape and tropism expansion. Advanced Healthcare Materials, 1, 443–449.

Wang, X.H., Zhang, X.H., Schröder, H.C., and Müller, W.E.G. (2009) Giant basal spicule from the deep-sea glass sponge *Monorhaphis chuni*: synthesis of the largest bio-silica structure on Earth by silicatein. Frontiers of Materials Science in China, 3, 226–240.

Weaver, J.C., and Morse, D.E. (2003) Molecular biology of demosponge axial filaments and their roles in biosilicification. Microscopy Research and Technique, 62, 356–367.

Weaver, J.C., Aizenberg, J., Fantner, G.E., Kisailus, D., Woesz, A., Allen, P., Fields, K., Porter,

M.J., Zok, F.W., Hansma, P.K., and others (2007) Hierarchical assembly of the siliceous skeletal lattice of the hexactinellid sponge *Euplectella aspergillum*. Journal of Structural Biology, 158, 93–106.

Weaver, J.C., Milliron, G.W., Allen, P., Miserez, A., Rawal, A., Garay, J., Thurner, P.J., Seto, J., Mayzel, B., Friesen, L.J., and others (2010) Unifying design strategies in demosponge and hexactinellid skeletal systems. Journal of Adhesion, 86, 72–95.

Weiher, F., Schatz, M., Steinem, C., and Geyer, A. (2013) Silica precipitation by synthetic minicollagens. Biomacromolecules, 14, 683–7.

Weiner, S., and Addadi, L. (2011) Crystallization pathways in biomineralization. Annual Review of Materials Research, 41, 21–40.

Wen, A.M., and Steinmetz, N.F. (2016) Design of virus-based nanomaterials for medicine, biotechnology, and energy. Chem. Soc. Rev., 45, 4074–4126.

Werner, P., Blumtritt, H., Zlotnikov, I., Graff, A., Dauphin, Y., and Fratzl, P. (2015) Electron microscope analyses of the bio-silica basal spicule from the *Monorhaphis chuni* sponge. Journal of Structural Biology, 191, 165–174.

Werner, P., Blumtritt, H., and Natalio, F. (2017) Organic crystal lattices in the axial filament of silica spicules of Demospongiae. Journal of Structural Biology, 198, 186–195.

Wilhelm, S., and Kind, M. (2015) Influence of pH, Temperature and Sample Size on Natural and Enforced Syneresis of Precipitated Silica. Polymers, 7, 2504-2521.

Wujek, D.E., Adesalu, T.A., and Nwankwo, D.I. (2005) Silica-scaled chrysophyceae and synurophyceae (chrysophyta) from Nigeria. II. Lake Lekki. Tropical Freshwater Biology,

12/13, 99–103.

Wujek, D.E., Kadiri, M.O., and Dziedzic, R.M. (2010) Silica-scaled chrysophyceae and synurophyceae from Nigeria. III. Chrysophytes from rivers of Edo state. Fottea, 10, 93–98.

Wysokowski, M., Petrenko, I., Stelling, A., Stawski, D., Jesionowski, T., and Ehrlich, H. (2015) Poriferan chitin as a versatile template for extreme biomimetics. Polymers, 7, 235–265.

Wysokowski, M., Bartczak, P., Zółtowska-Aksamitowska, S., Chudzińska, A., Piasecki, A., Langer, E., Bazhenov, V. V., Petrenko, I., Noga, T., Stelling, A.L., and others (2017) Adhesive Stalks of Diatom *Didymosphenia geminata* as a Novel Biological Adsorbent for Hazardous Metals Removal. Clean Soil, Air, Water, 45, 1600678.

Xiong, W., Yang, Z., Zhai, H., Wang, G., Xu, X., Ma, W., and Tang, R. (2013) Alleviation of high light-induced photoinhibition in cyanobacteria by artificially conferred biosilica shells. Chemical Communications,49, 7525–7527.

Yamanaka, S., Yano, R., Usami, H., Hayashida, N., Ohguchi, M., Takeda, H., and Yoshino, K. (2008) Optical properties of diatom silica frustule with special reference to blue light. Journal of Applied Physics, 103, 74701.

Yang, W., Lopez, P.J., and Rosengarten, G. (2011) Diatoms: self assembled silicananostructures, and templates for bio/chemical sensors and biomimetic membranes. The Analyst, 136, 42–53.

Yee, N., Phoenix, V.R., Konhauser, K.O., Benning, L.G., and Ferris, F.G. (2003) The effect of cyanobacteria on silica precipitation at neutral pH: Implications for bacterial silicification in geothermal hot springs. Chemical Geology, 199, 83–90.

Yoneda, S., Ito, F., Yamanaka, S., and Usami, H. (2016) Optical properties of nanoporous silica frustules of a diatom determined using a 10 um microfiber probe. Japanese Journal of Applied Physics, 55, 72001.

Zhang, W., Luo, X., Niu, L., Yang, H., Yiu, C.K., Wang, T., Zhou, L., Mao, J., Huang, C., Pashley, D.H., and others (2015) Biomimetic intrafibrillar mineralization of type I collagen with intermediate precursors-loaded mesoporous carriers. Scientific Reports, 5, 11199.

Zhang, Y., Reed, B.W., Chung, F.R., and Koski, K.J. (2015) Mesoscale elastic properties of marine sponge spicules. Journal of Structural Biology, 193, 67–74.

Zlotnikov, I., Werner, P., Blumtritt, H., Graff, A., Dauphin, Y., Zolotoyabko, E., and Fratzl, P. (2014) A perfectly periodic three-dimensional protein/silica mesoporous structure produced by an organism. Advanced Materials, 26, 1682–1687.

Zlotnikov, I., Werner, P., Fratzl, P., and Zolotoyabko, E. (2015) Eshelby twist as a possible source of lattice rotation in a perfectly ordered protein/silica structure grown by a simple organism. Small, 11, 5636–5641.

Zolotoyabko, E. (2017) Anisotropic lattice distortions in biogenic minerals originated from strong atomic interactions at organic/inorganic interfaces. Advanced Materials Interfaces, 4, 1600189.

FIGURE CAPTIONS

FIGURE 1. Structural features and the levels of structural organization in biosilica.

FIGURE 2. Overview of structurally defined biosilica produced at micro- and nanoscale: sombrero-like gemmoscleres of the freshwater sponge *Drulia* sp. (a), diatom frustules (b) and thermophilic bacteria (c) (reprinted from Belkova et al. 2004, Creative Commons License).

FIGURE 3. Diversity in shape and form of biosilica microstructures to be found in glass sponges and termed as amphidiscs, aspidoplumicomes, codonhexactins, clavules, diactines, dictyonalias, discohexasters, drepanocomes, etc. (for review see Boury-Esnault and Rutzler 1997). The central SEM image represents the 3D skeleton of the glass sponge *Tretochone duplicata.*

FIGURE 4. Light (a) and fluorescence (b) microscopy images of tabasheer microparticles.

FIGURE 5. SEM images of the freshwater diatom *Didymosphenia geminata* cells (a,b,c) under different magnifications.

FIGURE 6. TEM image of the demineralized frustule of *T. pseudonana.* The isolated organic microscaffold excellently resembles the nanoarchitecture of the living diatom cell.

FIGURE 7. SEM image: the cell of *T. rotula* prior to (a,c,e) and after 48 h of demineralization using 2.5 M NaOH at 37 °C (b,d,f). Both chitinous threads (arrows) and nanofibrils from the dissolved frustule are well visible.

FIGURE 8. Skeletal siliceous networks in Hexactinellida. The repeating structural motifs (a) are to be found within hierarchically organized skeletal networks such as that from *Aspidoscopulia* sp. (light microscopy – b; fluorescence microscopy – c). In some glass sponges (d,e – *Poliopogon* sp.) they are visible even at macroscale.

FIGURE 9. Light microscopy images. The proteinaceous axial filament is located within the axial channel of the *Lubomirskya baicalensis* demosponge spicules and become visible after Coumassie Blue staining (a). Such axial filaments can even be observed in exceptionally well preserved 2 MYA spicules of the same sponge species (b). (Images courtesy Dr. Serguei Belikov)

FIGURE 10. First electron microscopy visualization of the scleroblast and a "proteic rodlet" of *Mycale contarenii*. Magnification x 47,000 (adapted from Levi 1963).

FIGURE 11. SEM view through the collagenous tissue of *S. domuncula* demosponge. Numerous spicules were mechanically disrupted due to sample preparation (a,b). The axial filament (arrow) represents the thread made of interconnected non-mineralized individual nanofibrils (c) which morphologically resemble the structure of typical collagen fibrils (see also Figure 12).

FIGURE 12. SEM images of diverse spicules with mineralized axial filaments (a,c,e) to be found within the same *S. domuncula* body fragment as represented in Figure 11. Nanoparticles of some mineral phase are well visible on the surface of (b,d) and within (f) corresponding axial filaments. We strongly suggest that only the use of the HR-TEM method with electron diffraction device will shed light on the origin and nature of these nanoparticles.

FIGURE 13. Monitoring spicule growth in sponges using SEM. First, the unique, collagen-producing cells are seen to line up along the surface of the spicule (a), which forms a characteristic nanofibrillar structure (b). The line of cells can move from left to right along the spicule (c and d), depositing a rough, collagenous nanofibrillar layer in their wake (e and f). See also Eckert et al. (2006).

FIGURE 14. A hypothetical mechanism for spicule formation in *S. domuncula*. A bundle of collagen-producing cells forms into an "embryonal" axial filament, growing by fission of the

cells along a linear axis (I). Next, a silica layer is deposited around the cellular filament (II). The cells fission again and emerge from the new silica tube onto its surface (III), where the axial growth is then continued (IV) and repeated so that layers are formed (V). (Image courtesy Vasily V. Bazhenov)

FIGURE 15. The honeycomb architecture of the glass sponge *Aphrocalystes beatrix* is well visible using stereo (a,b) and scanning electron microscopy (c–f). The axial channel (g) and axial filaments (h) are also present.

FIGURE 16. It is hard to believe that this glassy rod represents the up to 3 cm thick fragment of the up to 3-meter-long individual spicule of the deep-sea glass sponge *Monorhaphis*. (Image courtesy W.E.G. Müller)

FIGURE 17. HF-based demineralization of glass sponge spicules (a) and skeletal frameworks (b) leads to isolation of both organic matrices with axial filaments (c) (*Corynonema populiferum* sponge) or only axial filaments (d) (*Farrea* sp.).

FIGURE 18. Diversity in size and geometry of axial channels in diverse glass sponges: (a,b) *Sarostegia oculata*; (c) *Aspidoscopulia* sp., (d) *Sericolophus havaiicus*, (e) *Farrea* sp. The unusual axial channel system in *Tretopleura styloformis* (f) suggests the presence of numerous polygonal forms of the axial filament.

FIGURE 19. An attempt to dissolve native *Verongula gigantea* demosponge fibers (a) with HCl solution resulted only in dissolution of the acid-soluble calcium carbonate-based mineral component. This yielded a perforated fiber surface (b,c). These structures are visible in a light microscope (d) as well as in SEM (e). The siliceous nature of these acid-resistant skeletal layers was confirmed using EDX analysis (f).

FIGURE 20. Siliceous acid-resistant layers isolated from *V. gigantea* fibers using TEM (a) and HR-TEM (b) have a nanofibrillar structure (arrows).

FIGURE 21. Schematic view: the role of special hydroxylated collagen in silica condensation in the *Hyalonema sieboldi* glass sponge anchoring spicules. For details see Ehrlich et al. 2010b.

FIGURE 22. TEM image**:** Collagen fibrils (arrows) protrude into the silica lumps of the *Geodia cydonium* spicule (adapted from Müller et al. 2007).

FIGURE 23. Skeletal stalks of the psychrophilic deep-sea *Caulophacus* sp. glass sponge (a) contain hundreds of club-like spicules (b). HR-TEM observations show with strong evidence the location of a nanostructured crystalline phase (c,d) identified as calcite.

FIGURE 24. Silicofossils. Light microscopy image of the fossilized (37 MYA) sponge *Neopelta* sp. (a) represents typical structures of lithistid desmas (b). However, a fluorescence microscopy image (c) of the same structure shows the presence of organic material with characteristic autofluorescence (arrows). (Images courtesy Dr. Andrzej Pisera)

FIGURE 25. The glass sponge anchoring spicules have exceptional mechanical properties, combining mechanical stability with strength and stiffness. Highly flexible spicules of *Hyalonema* sp (a,b,c) contain collagen as the organic matrix. However, the very flexible *S. hawaiicus* glass sponge spicules (d,e) are made of nanostructured chitin (SEM image, f).

Figure 1

Chalcedony in human cerebral cortex

Chalcedony in fish electric organs

Macro-level

Micro-level

Nano-level

Microcrystalline Amorphous

BIOSILICA
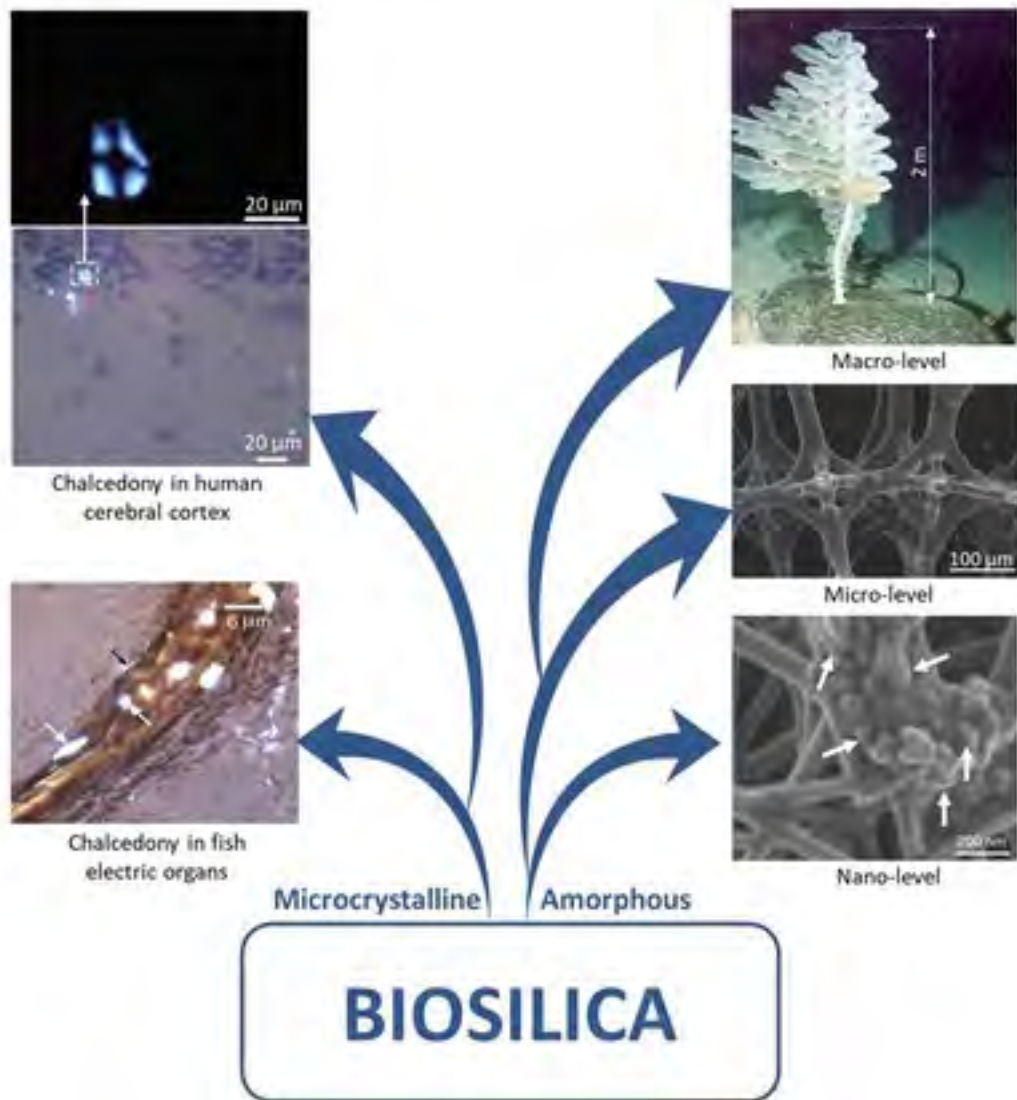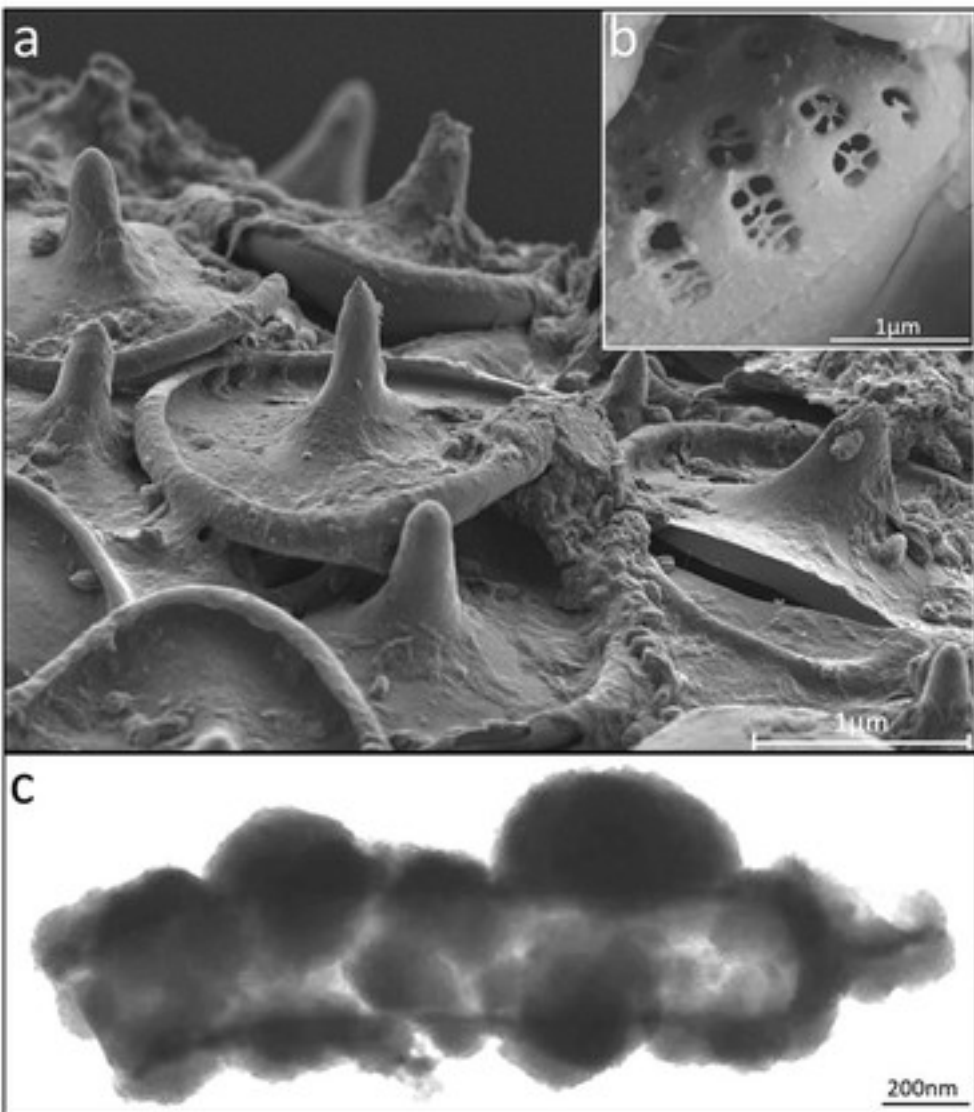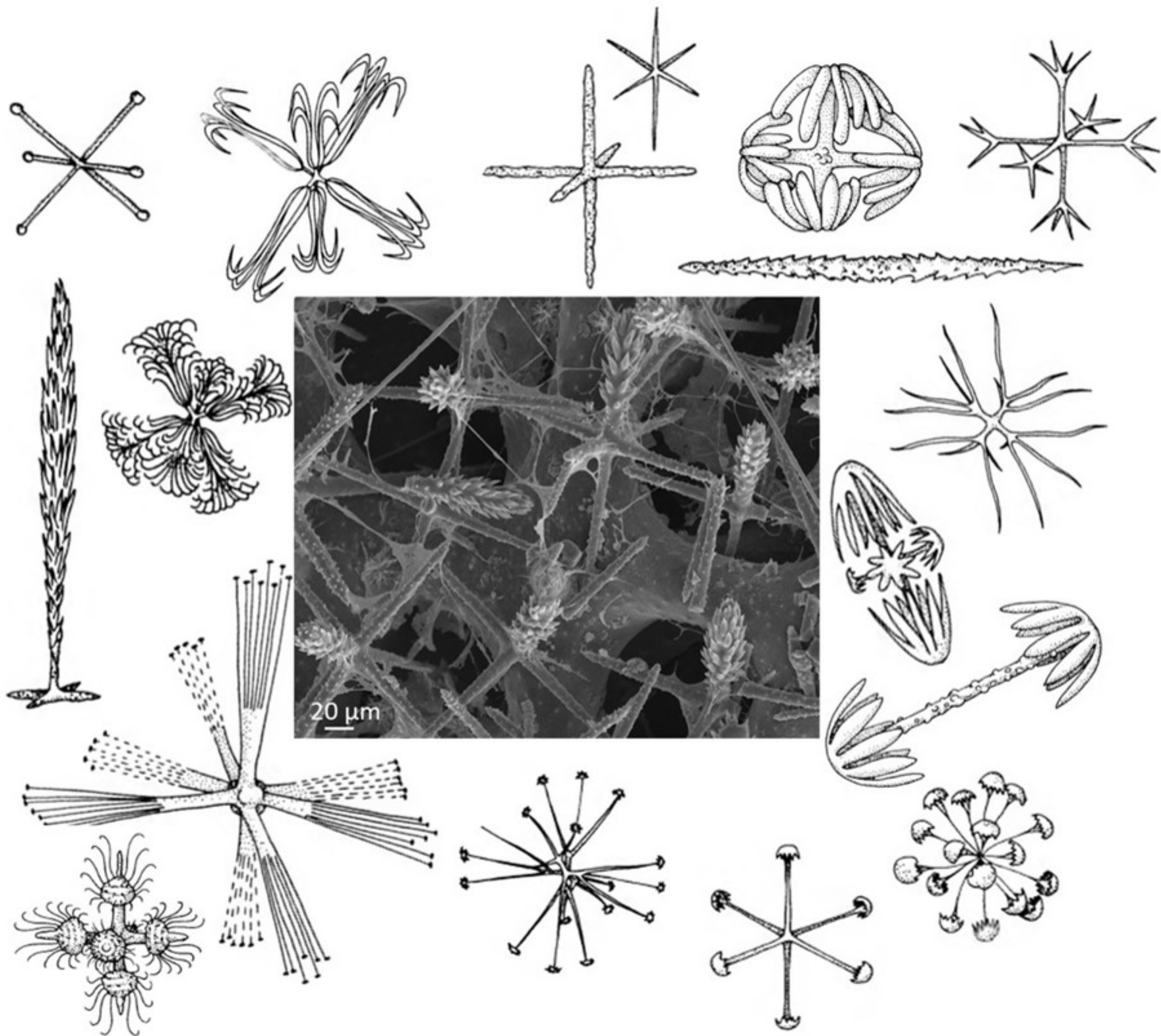
Figure 2

Figure 3

Figure 4

Figure 5

Figure 6

200 nm

Figure 7
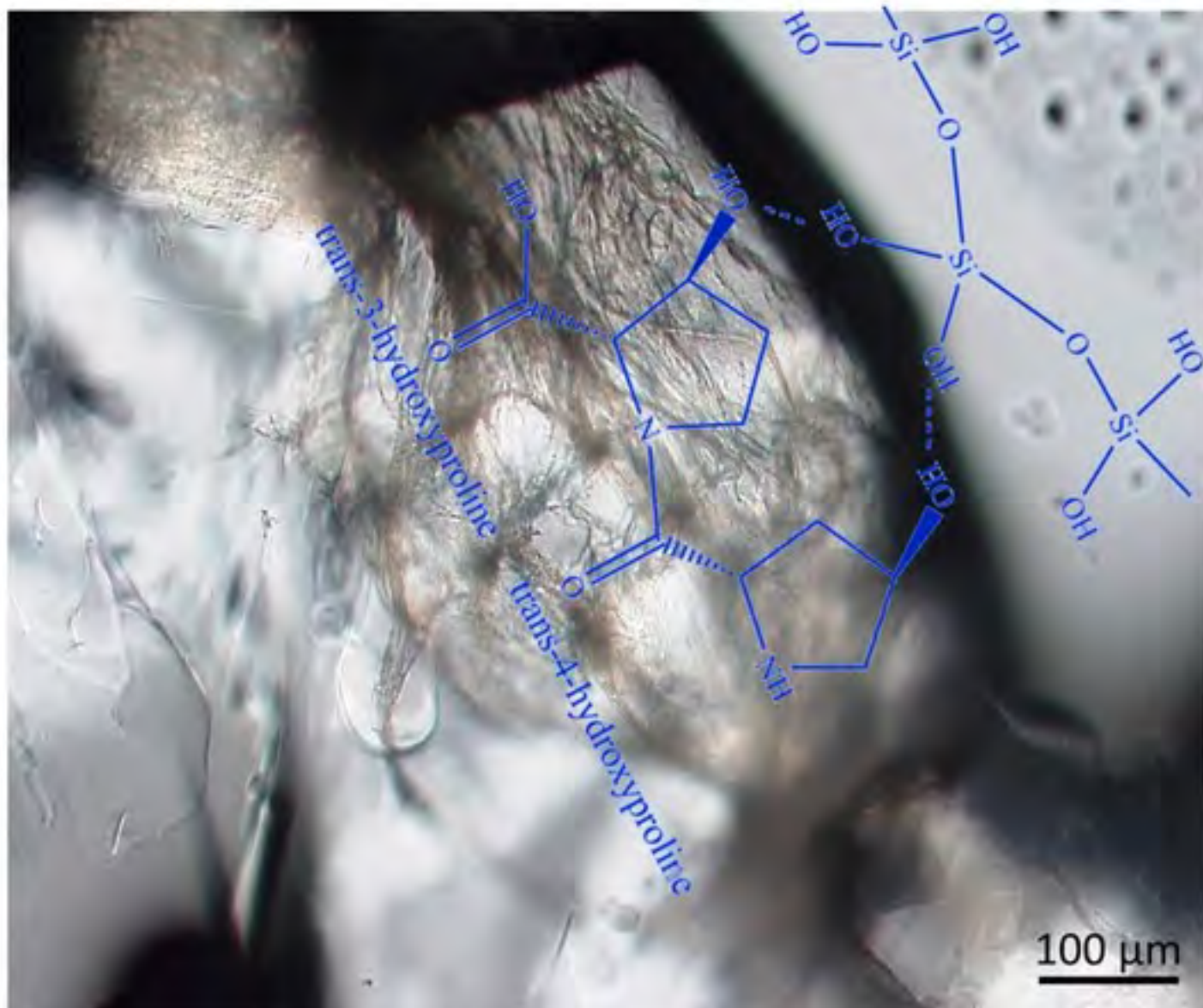
Figure 8

a

b

c

100 μm

100 μm

d

e

1 cm

1 cm
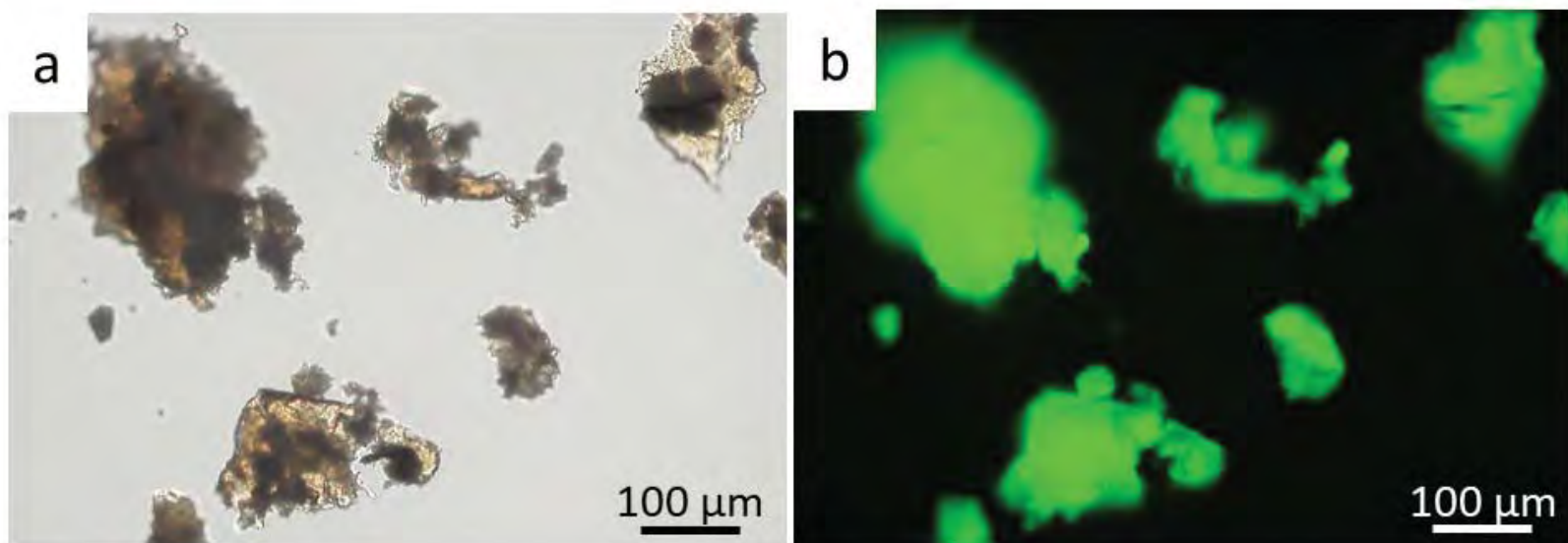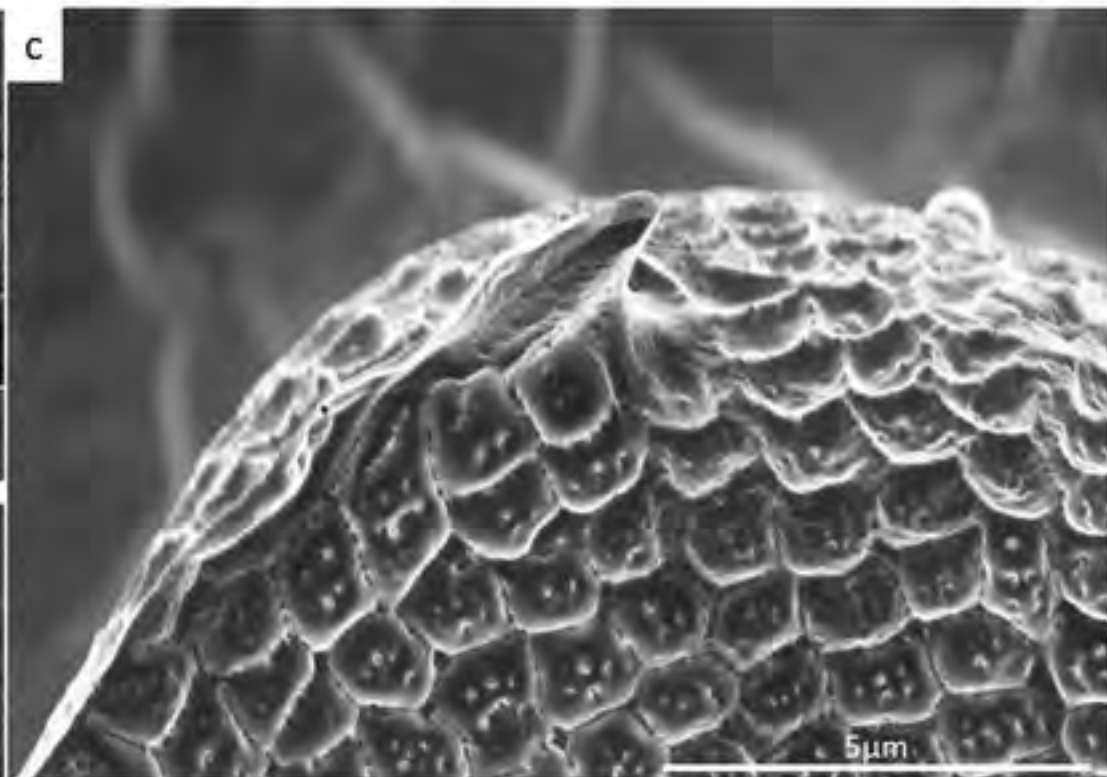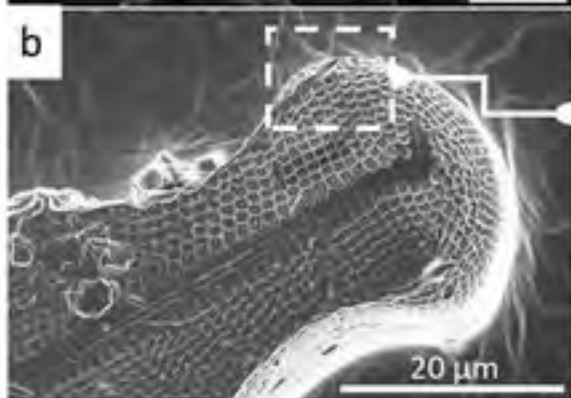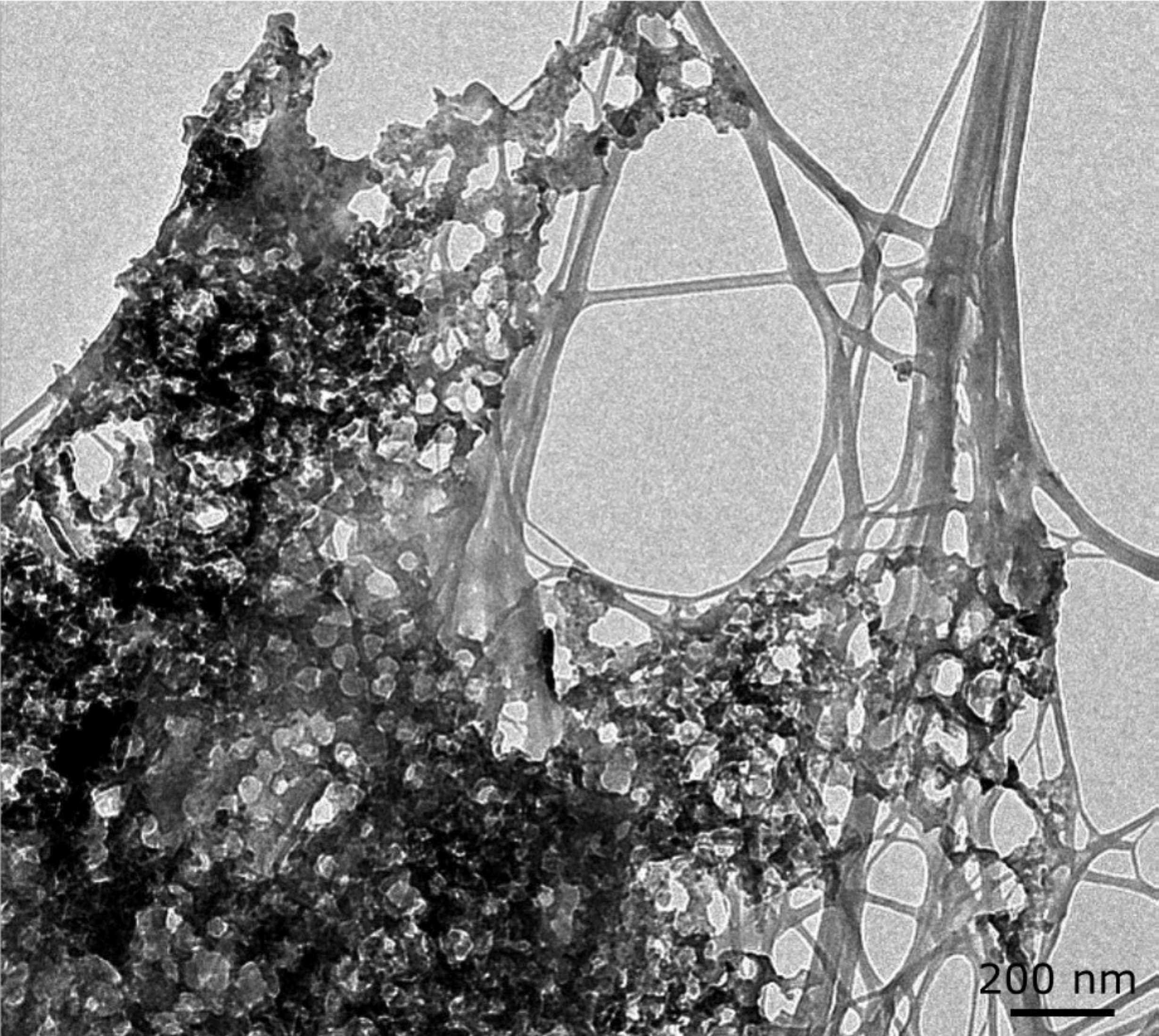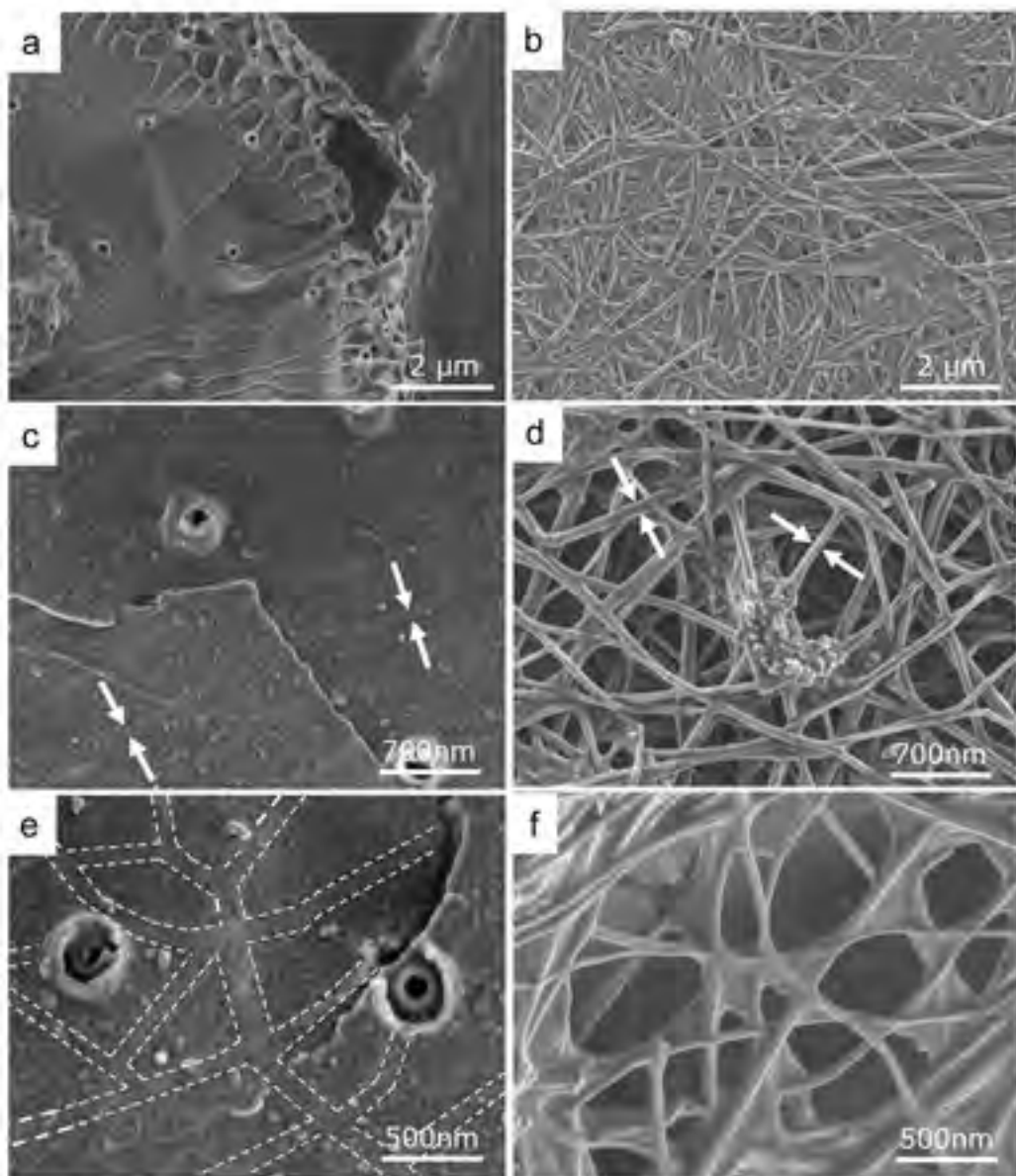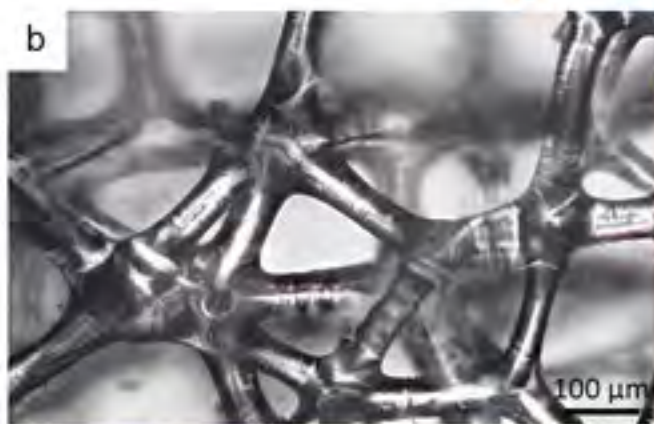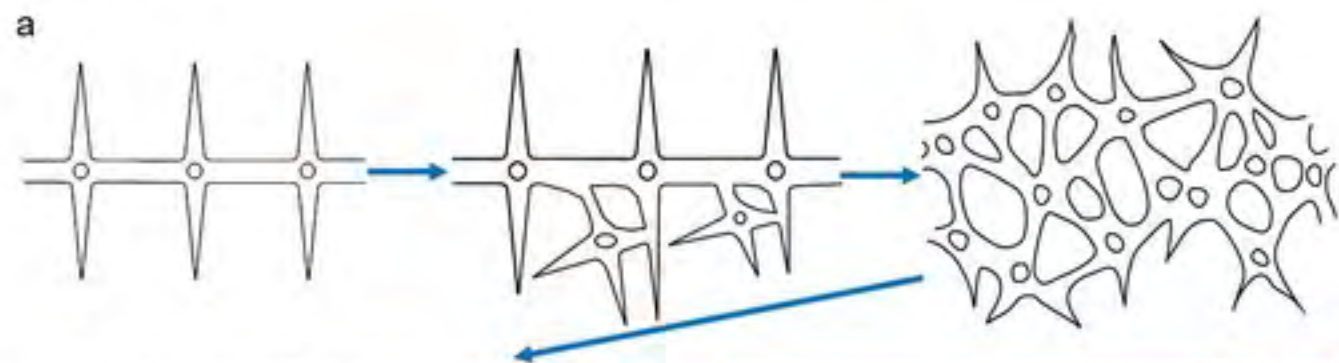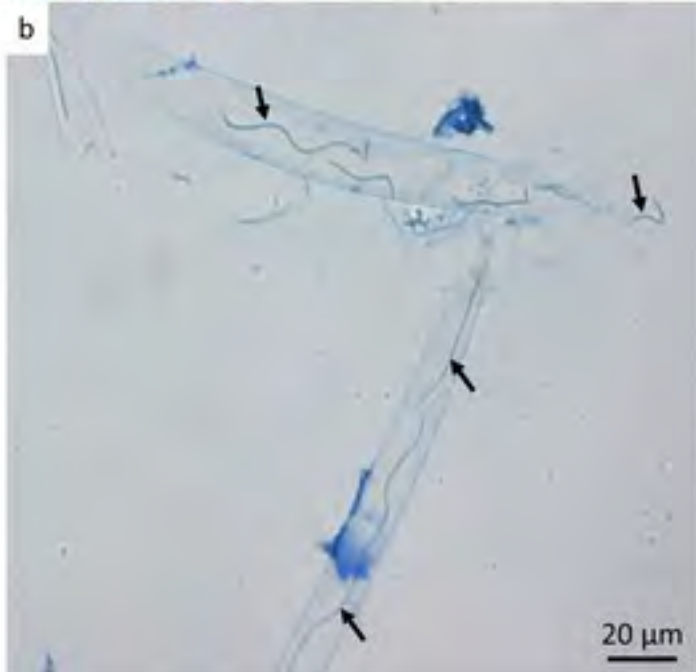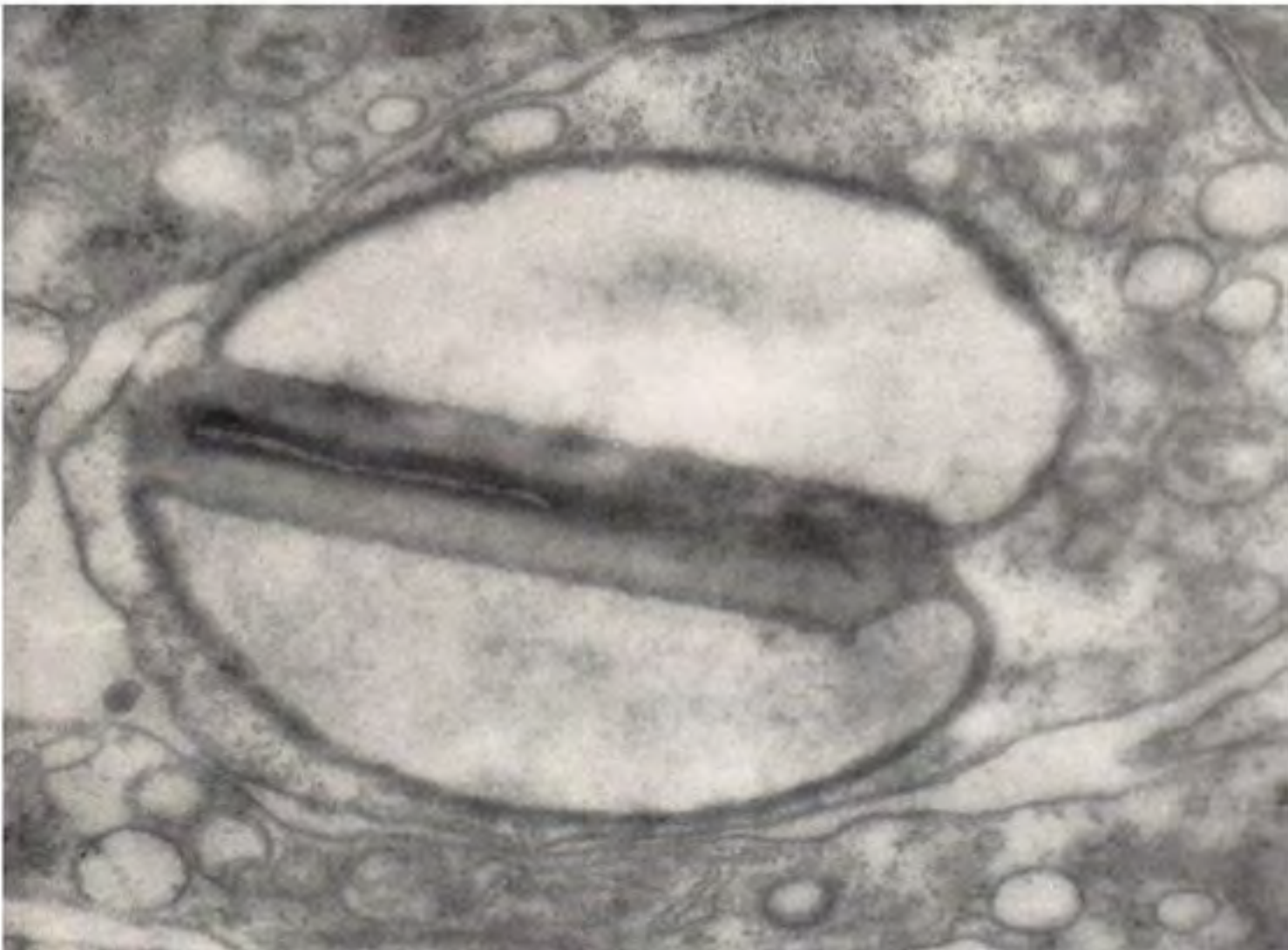
Figure 9

Figure 10

Figure 11
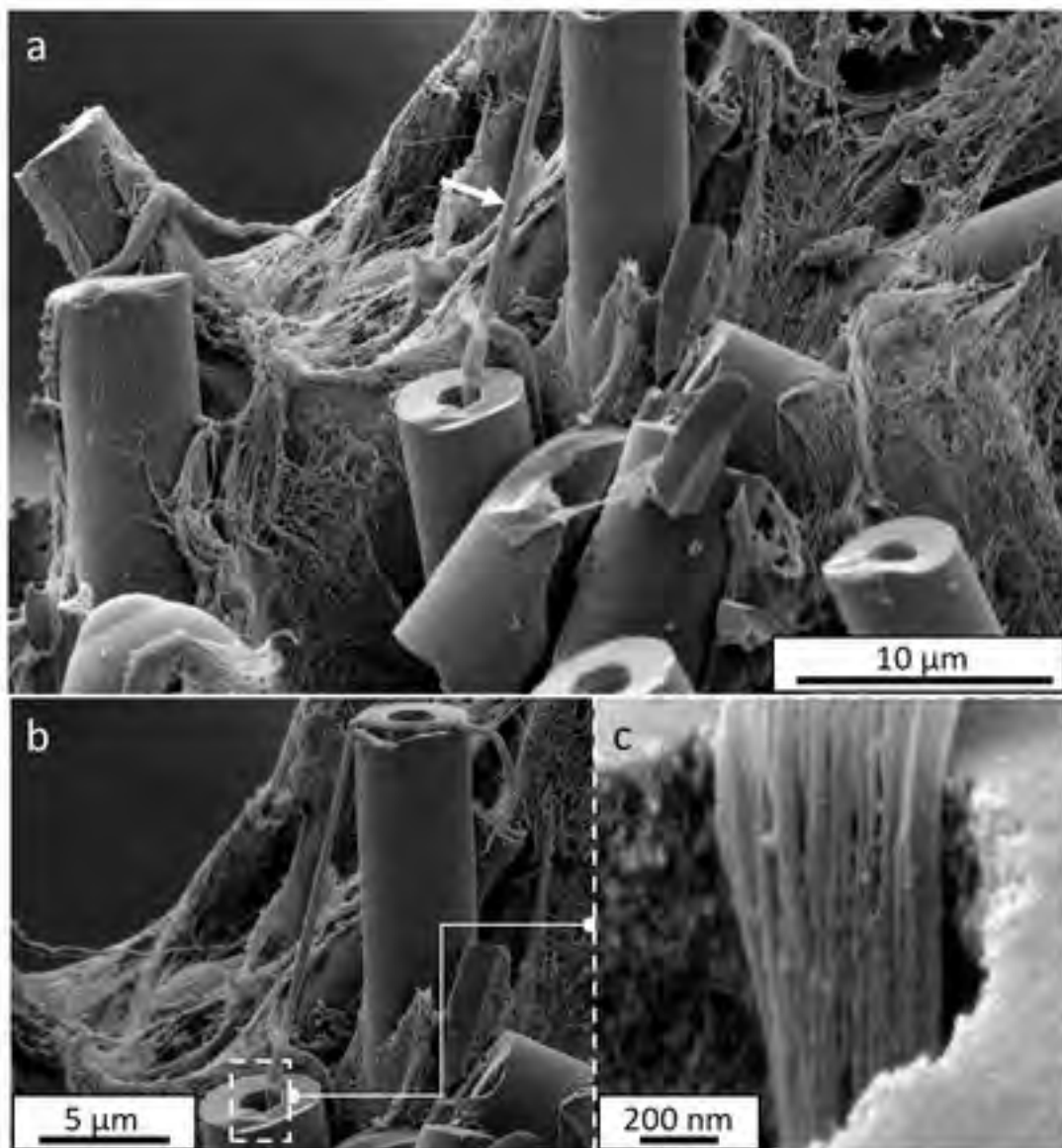
Figure 12
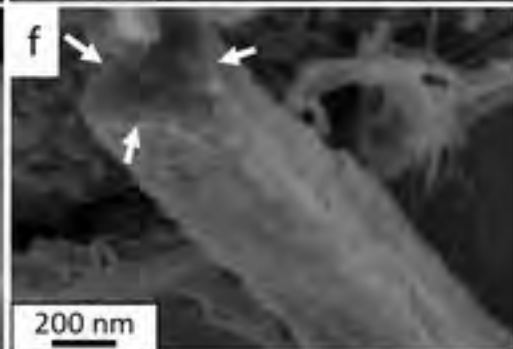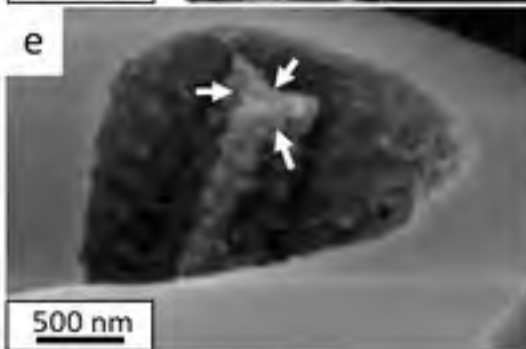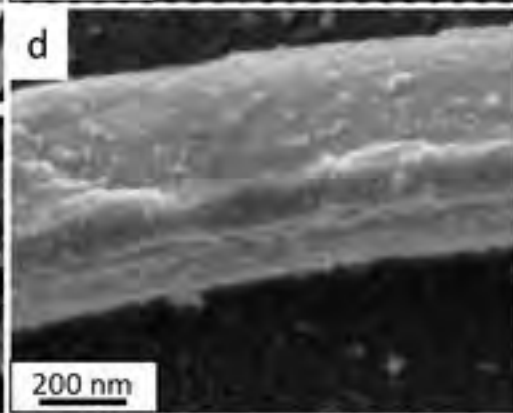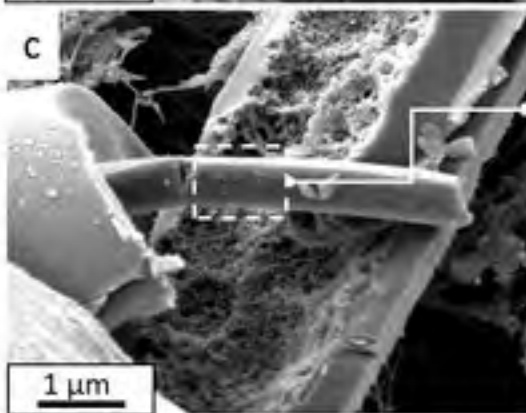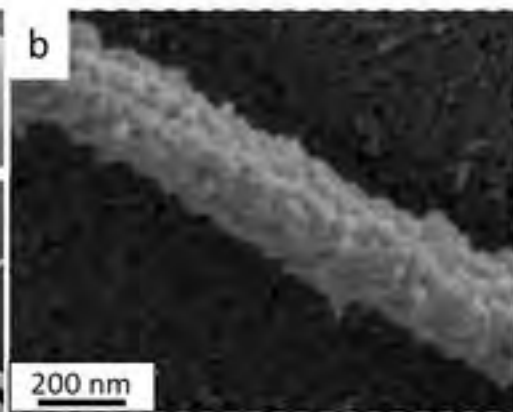
Figure 13

Figure 14

I

II

III

IV

V
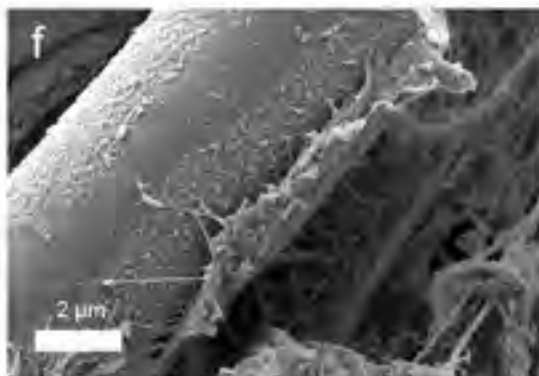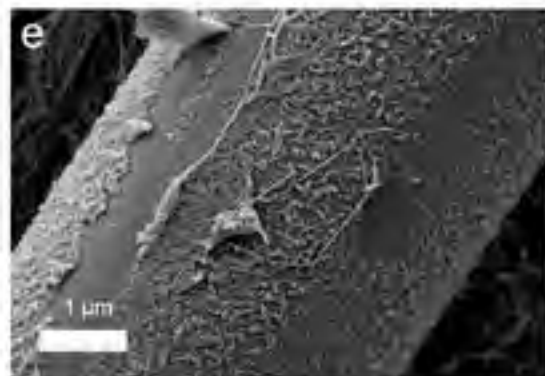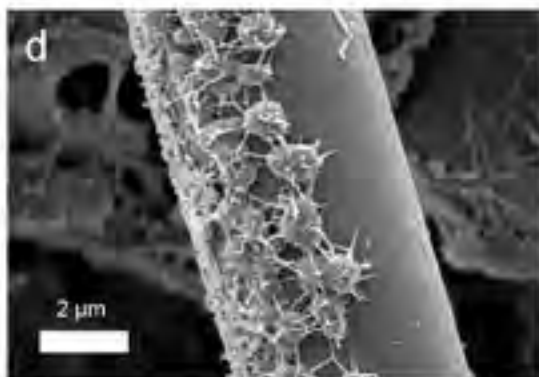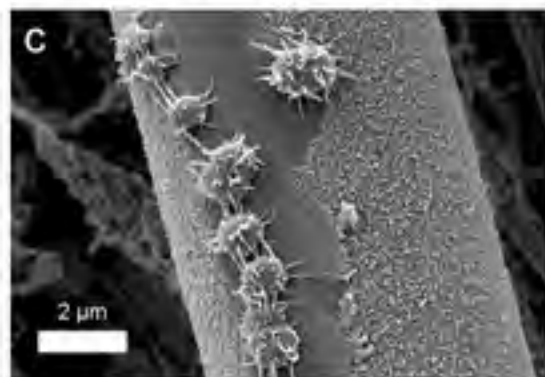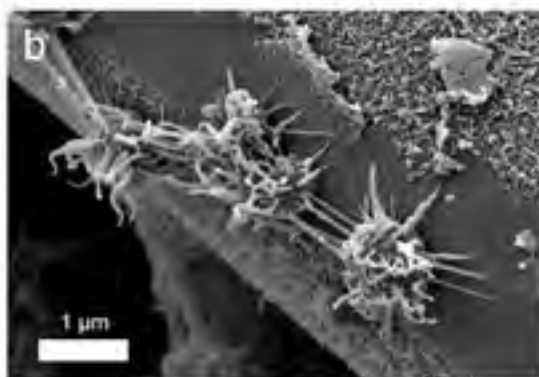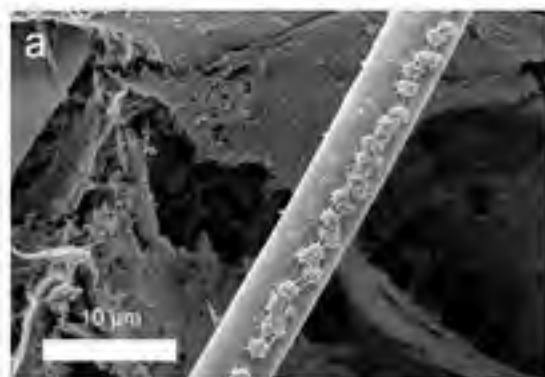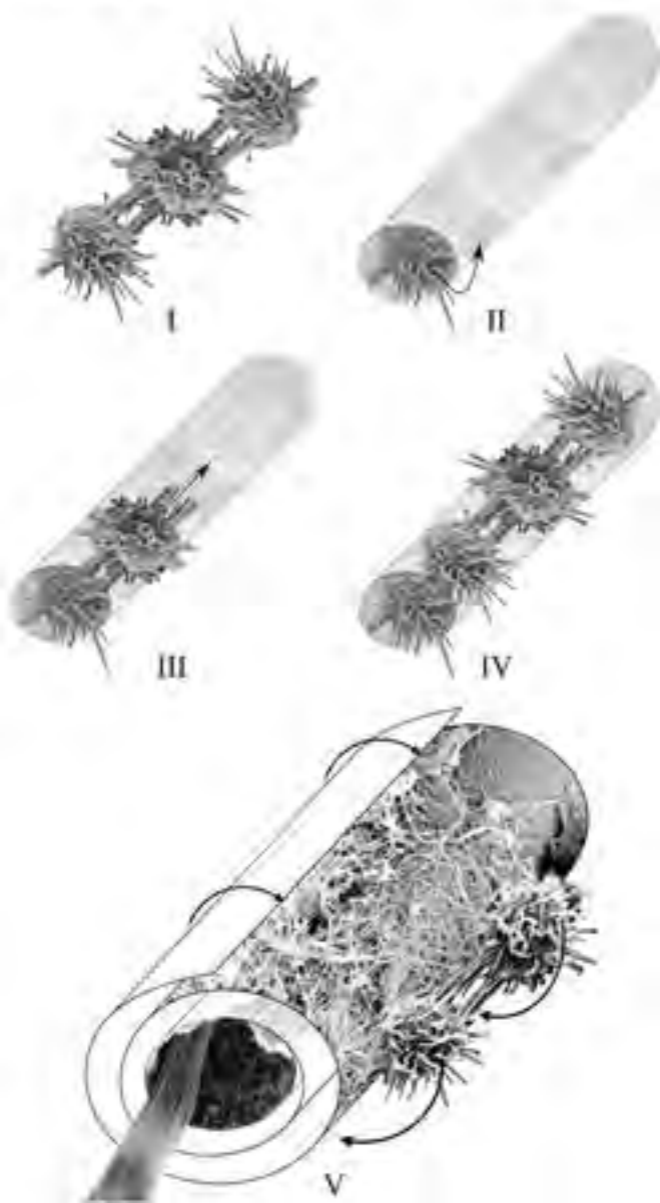
Figure 15

Figure 16

Figure 17

a. organic matrix / spicule — 1 mm
b. axial filament — 100 μm
c. 100 μm
d. 10 μm
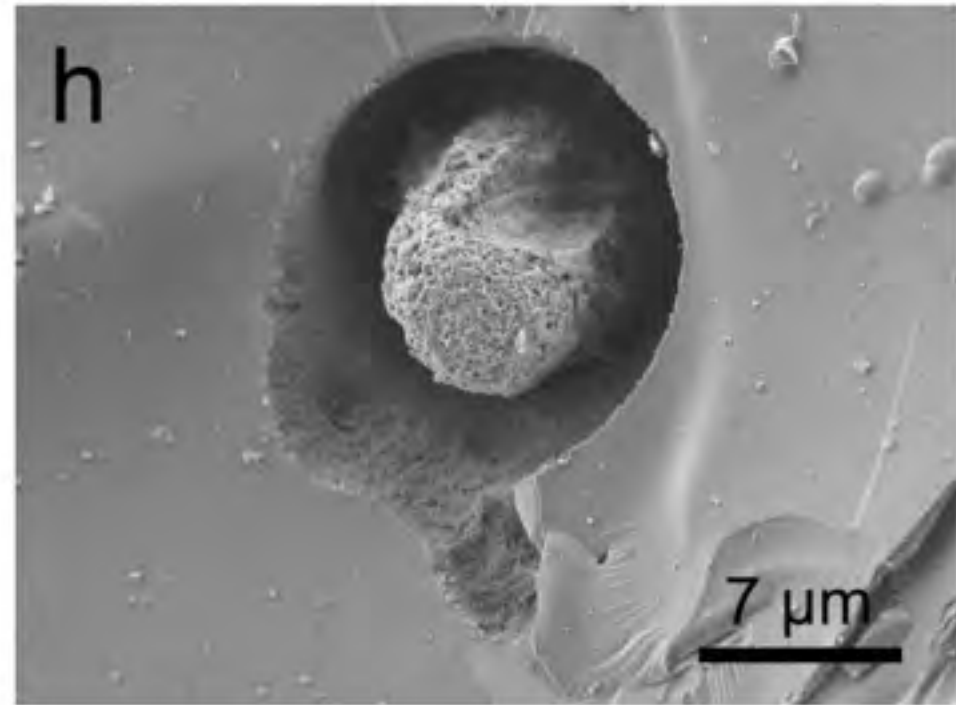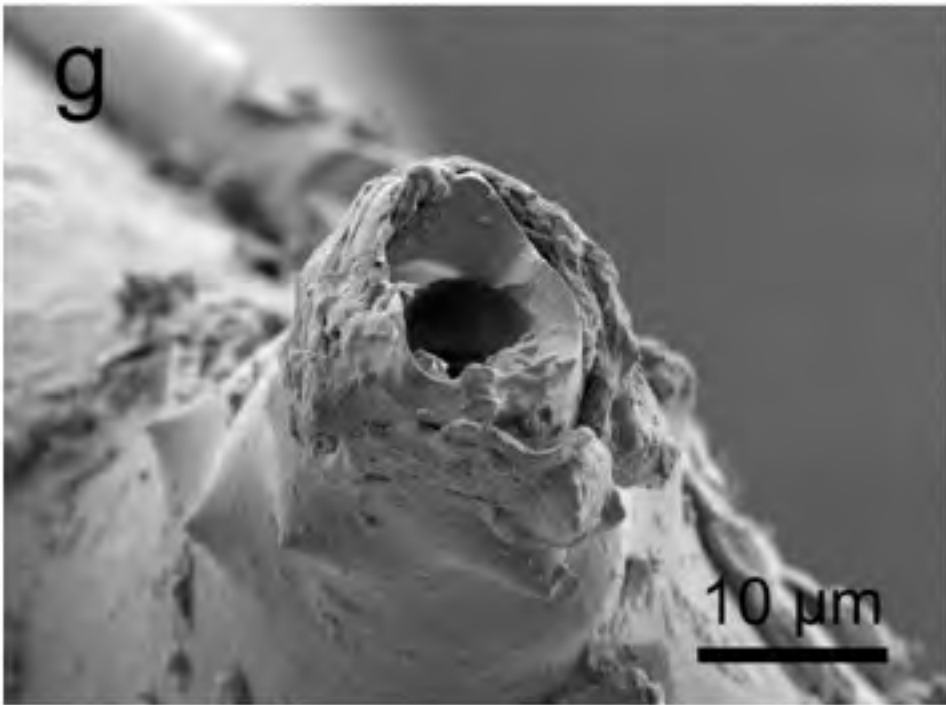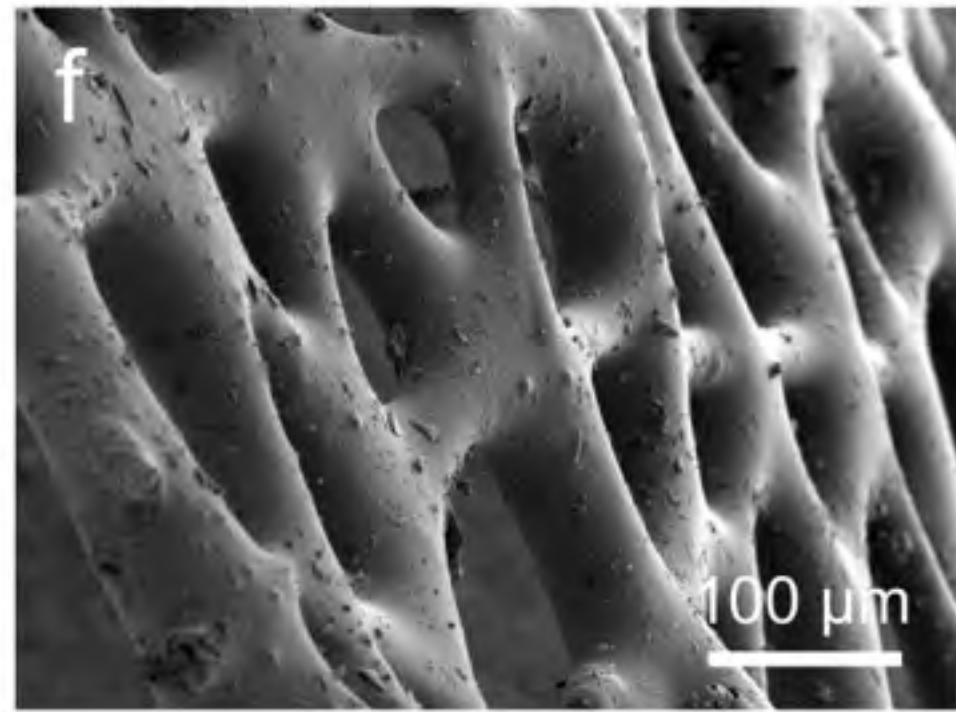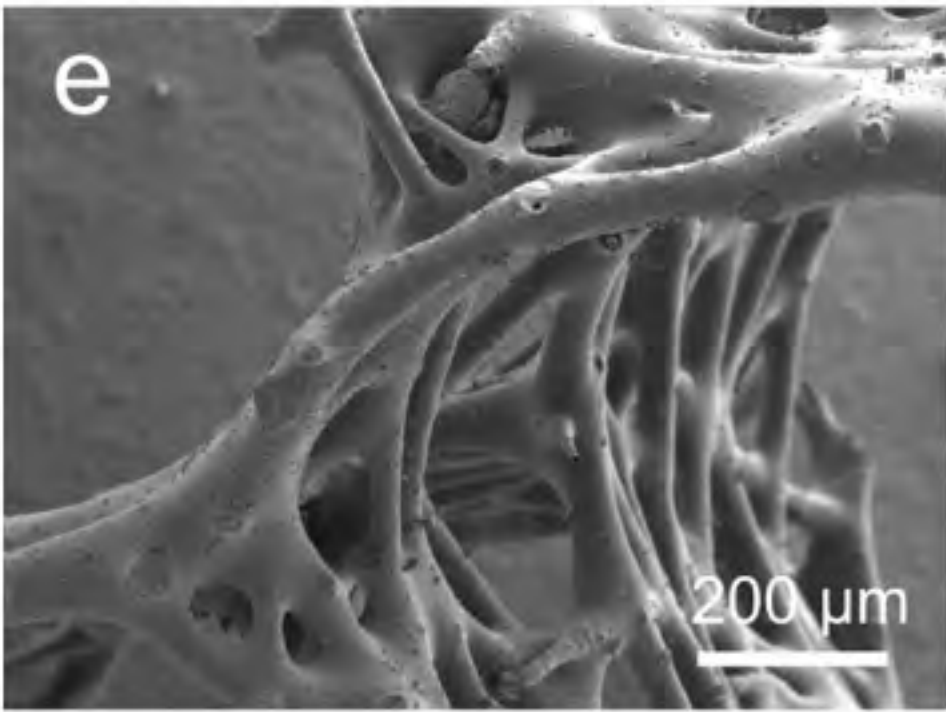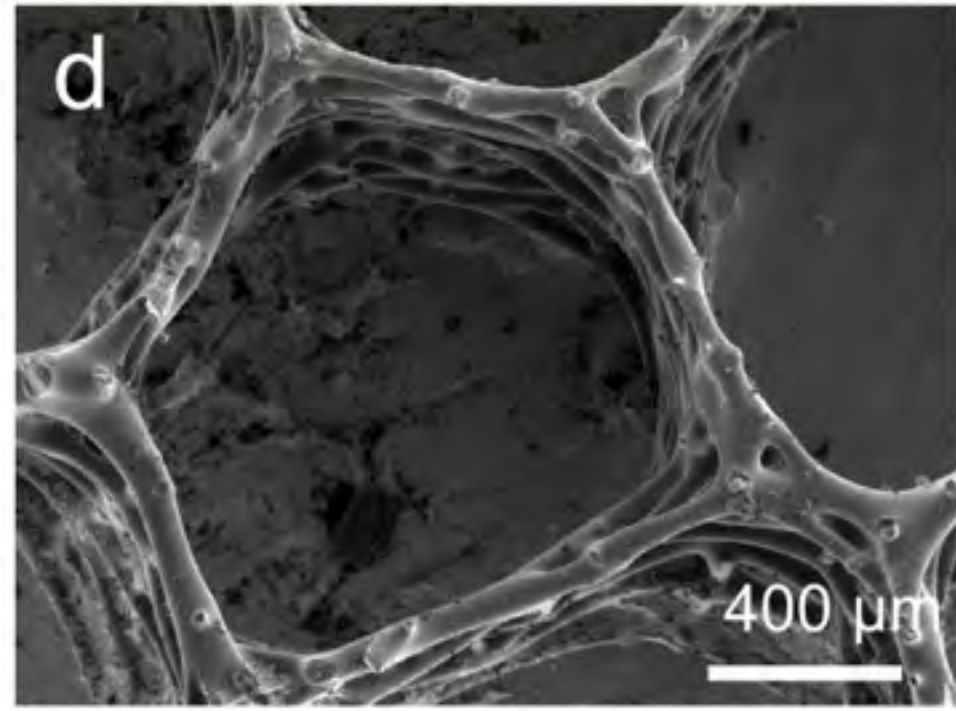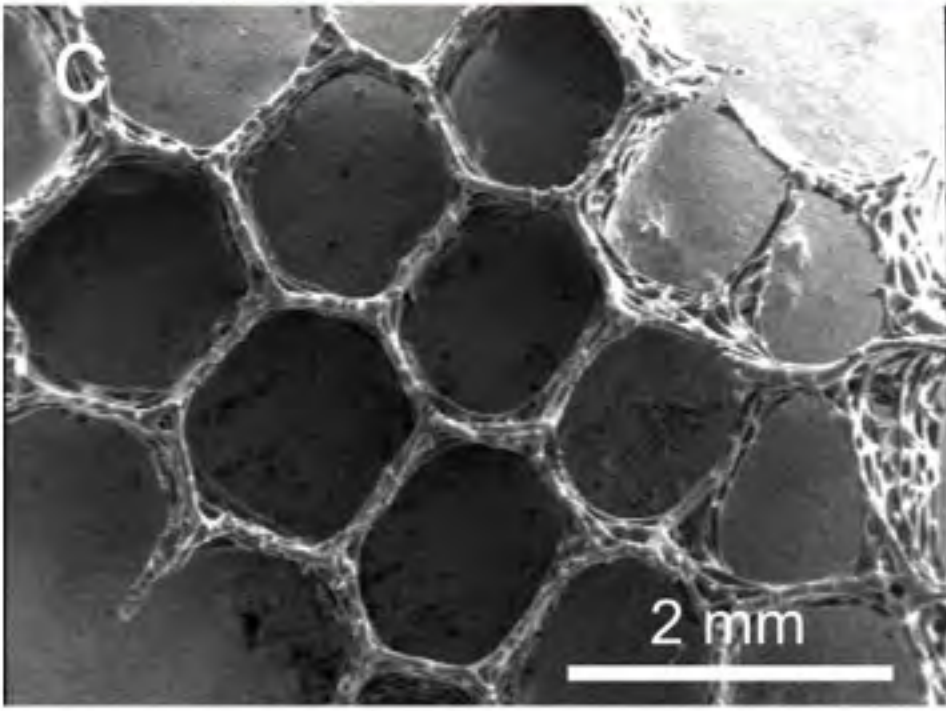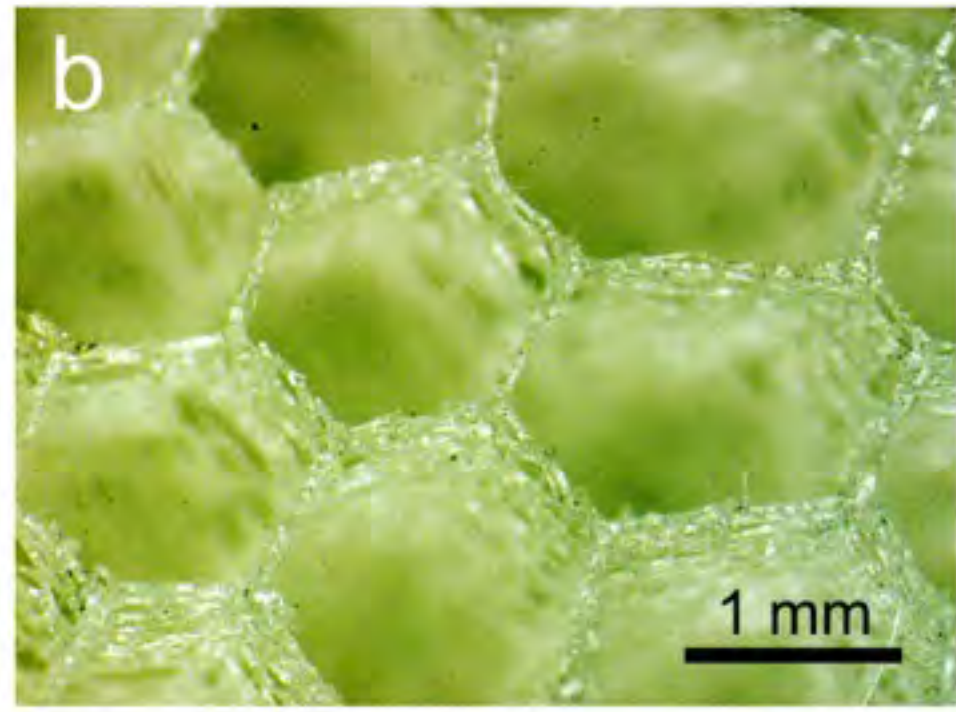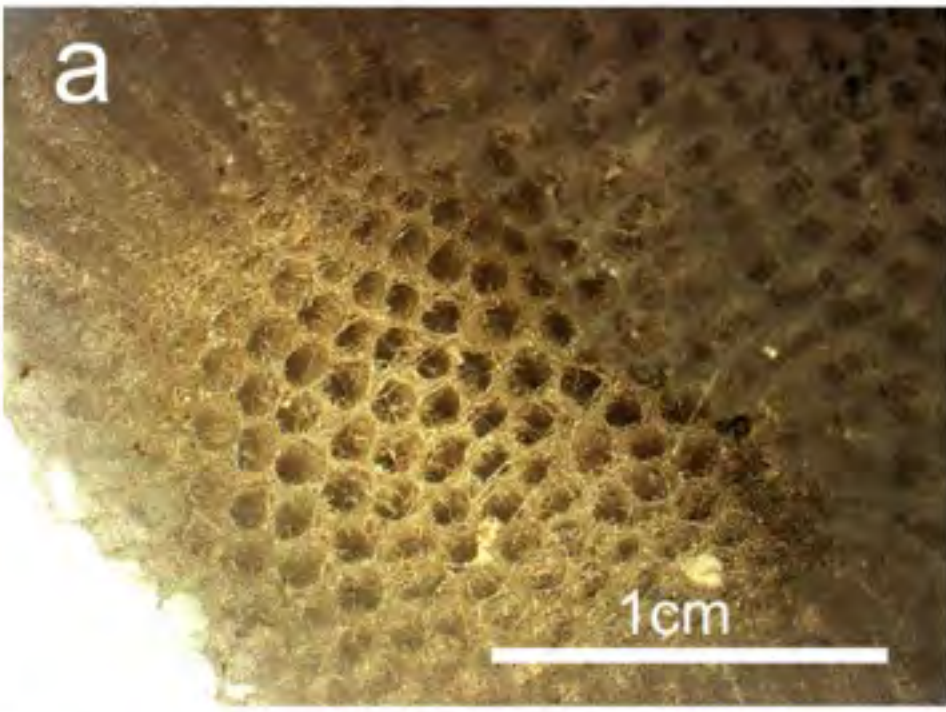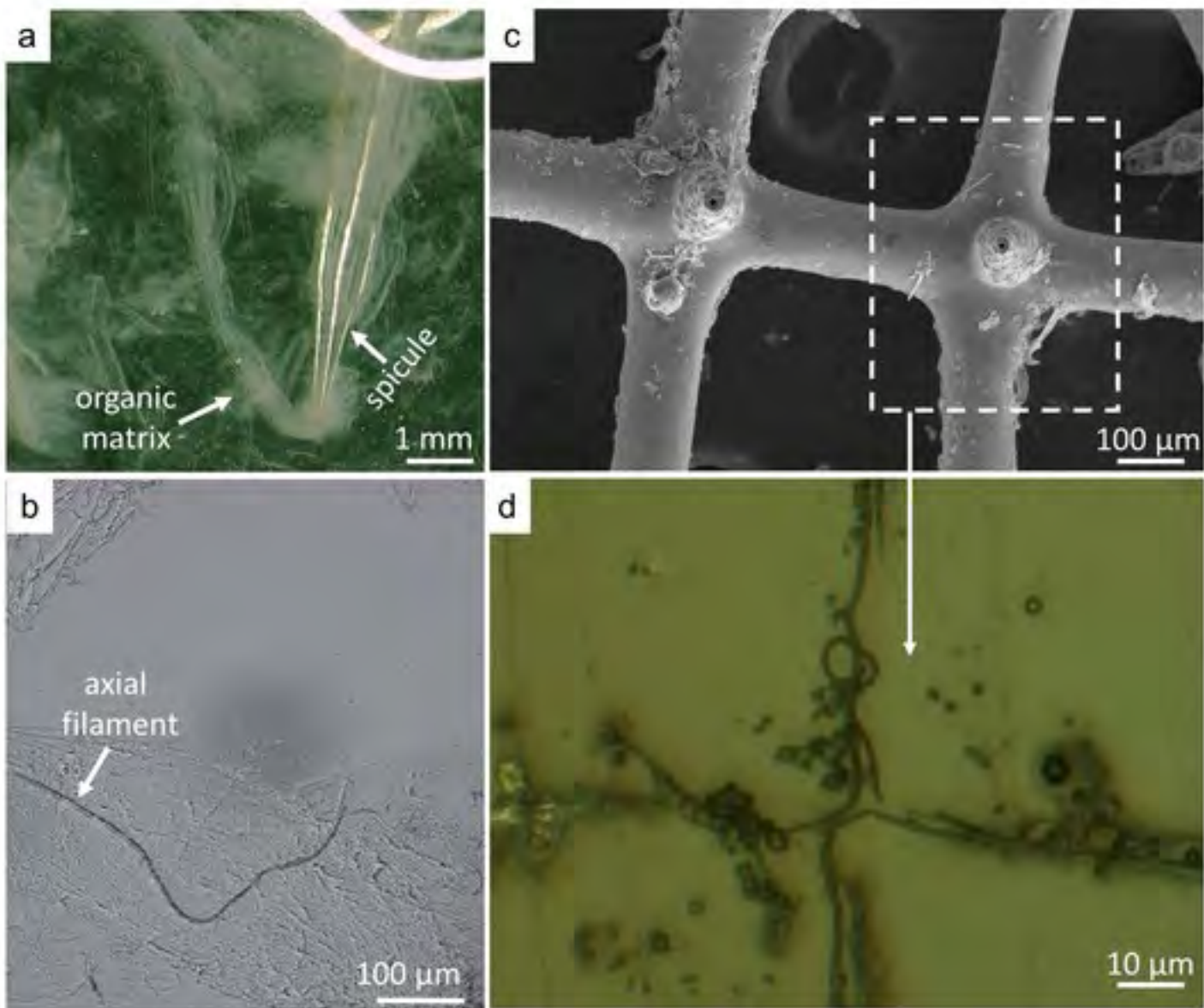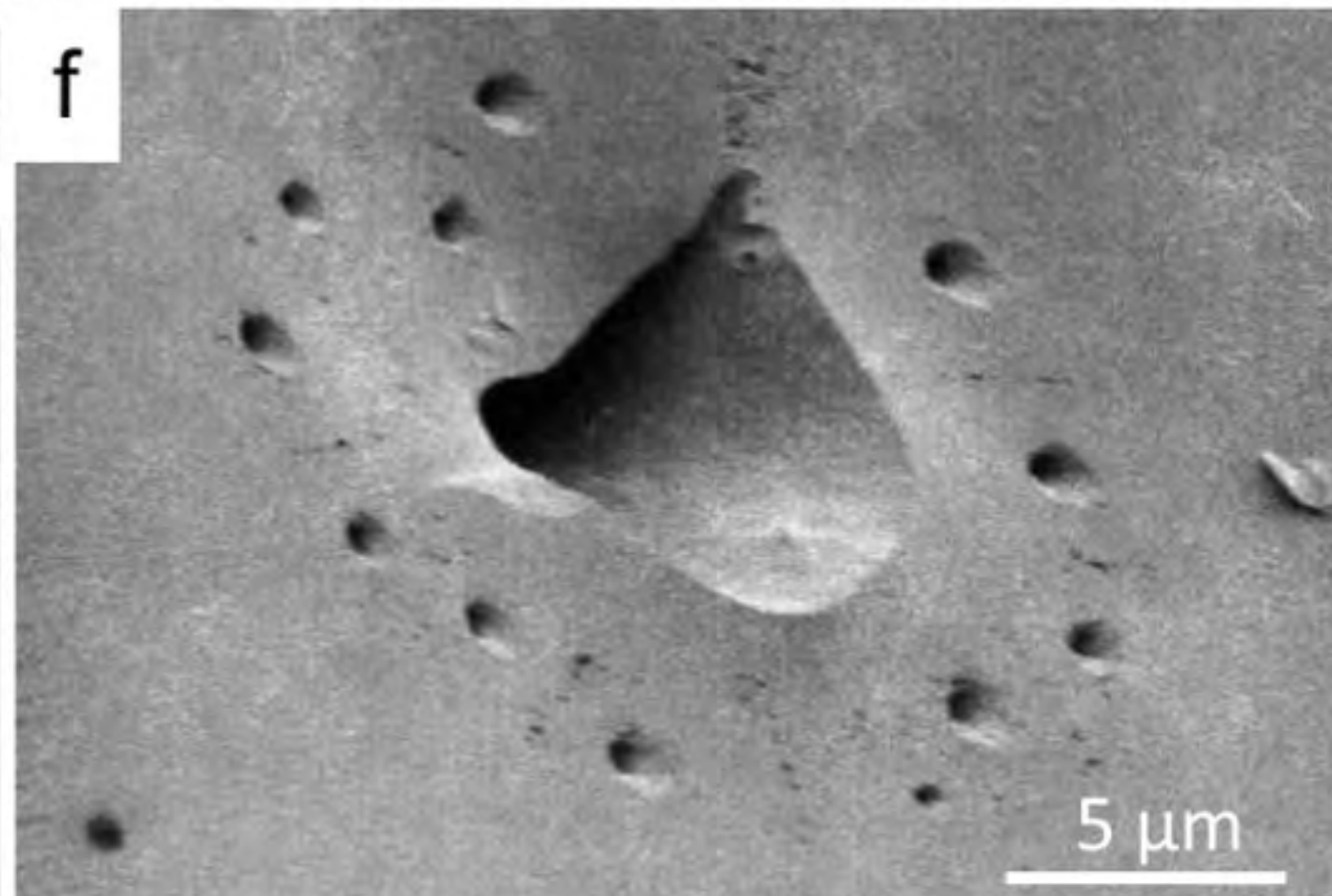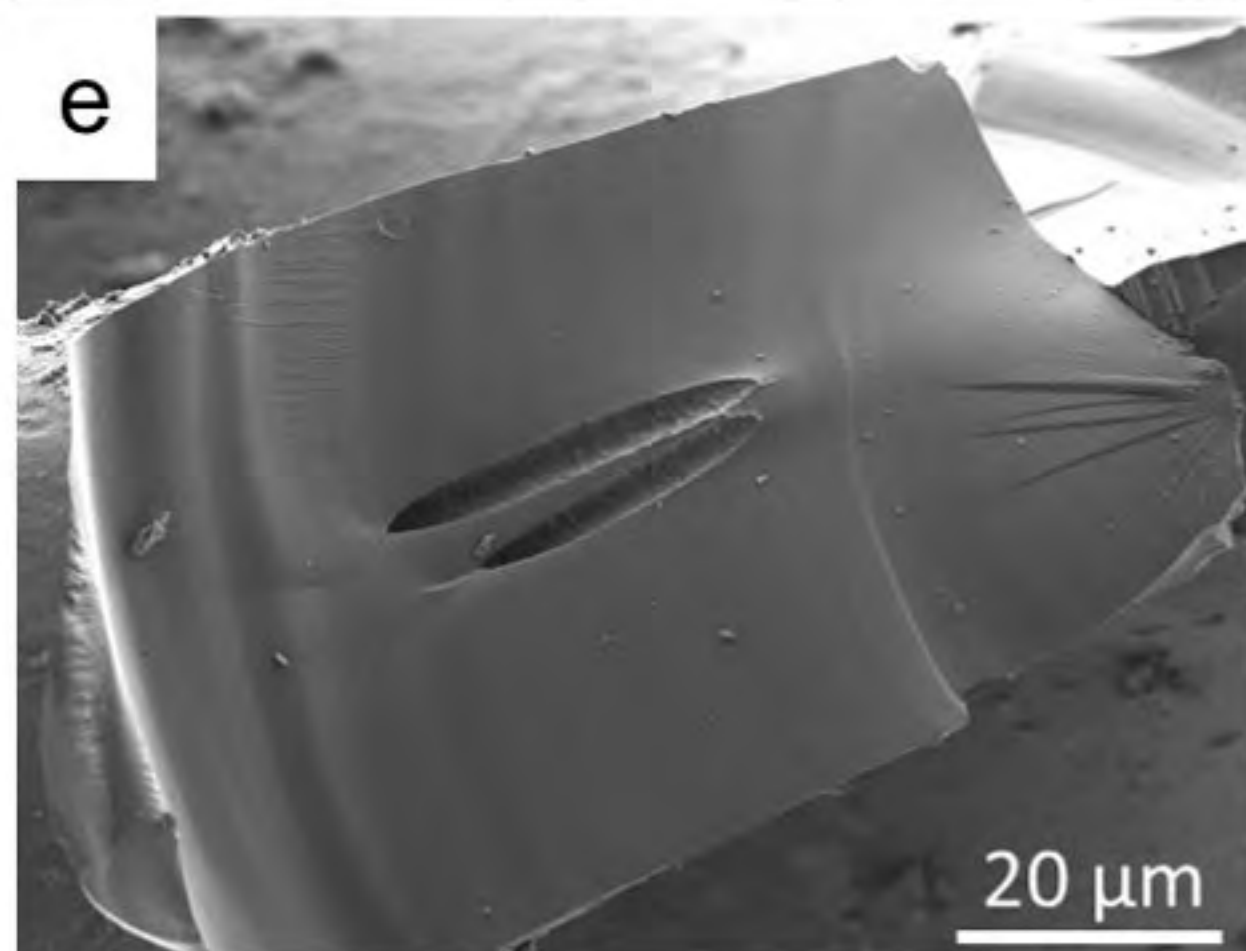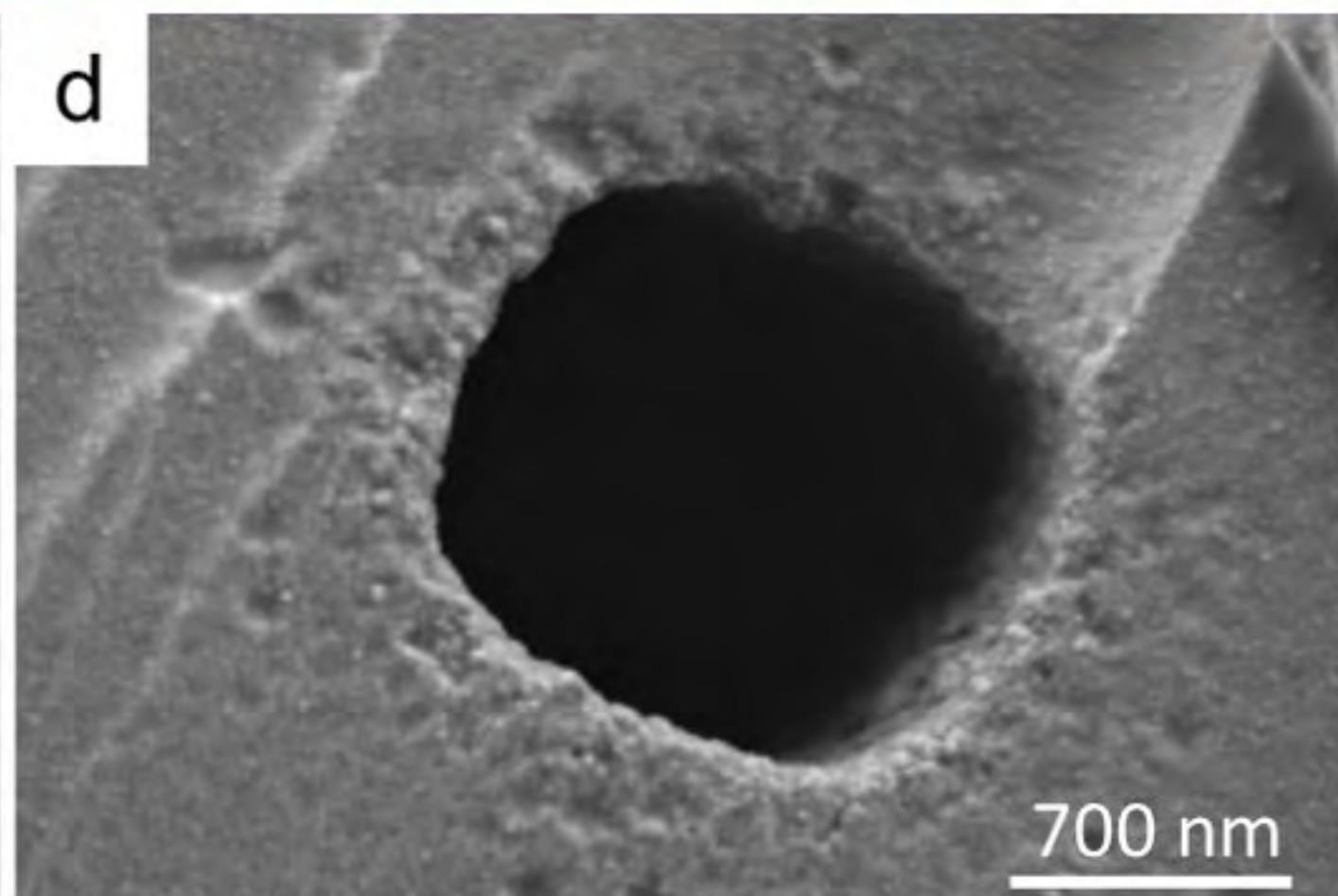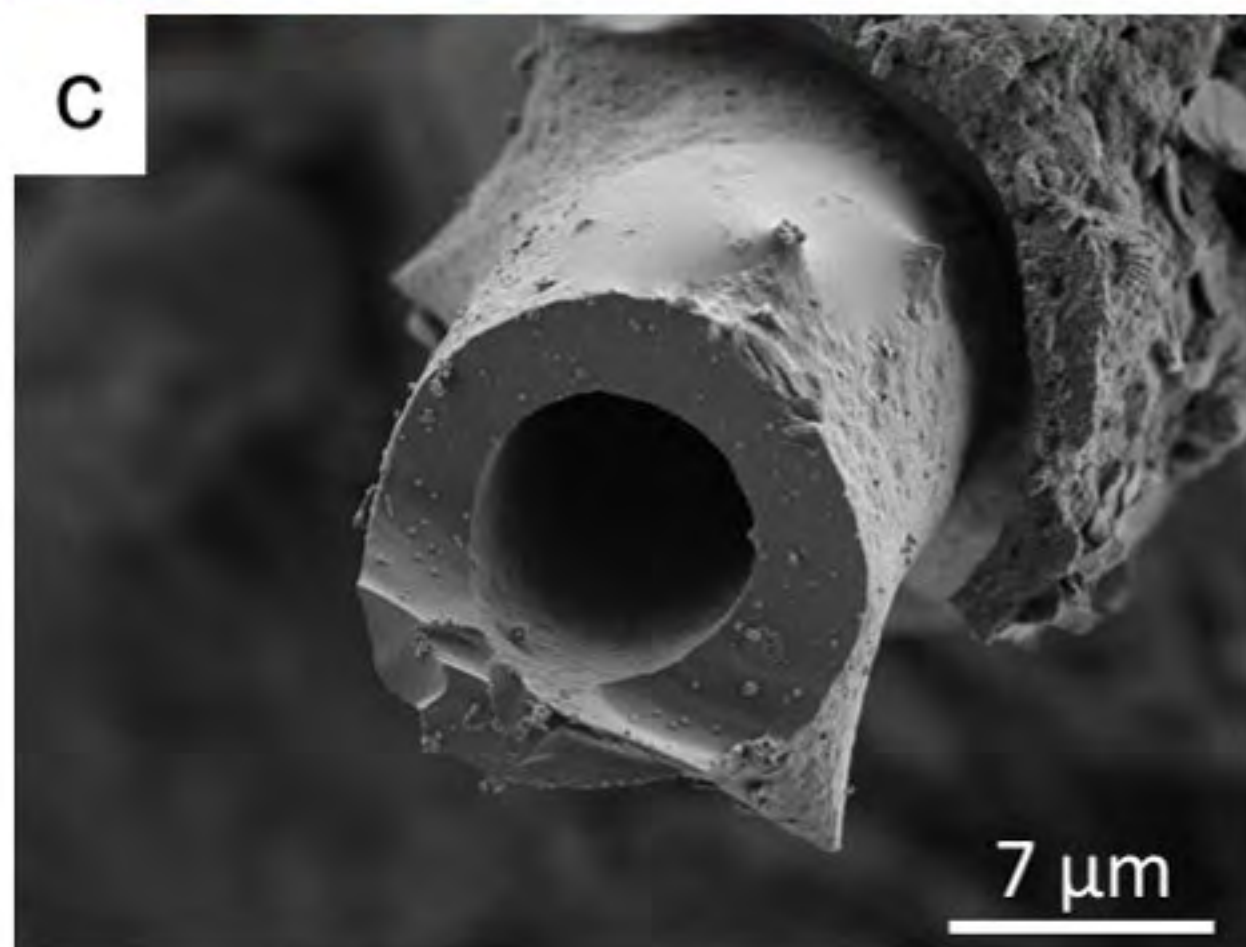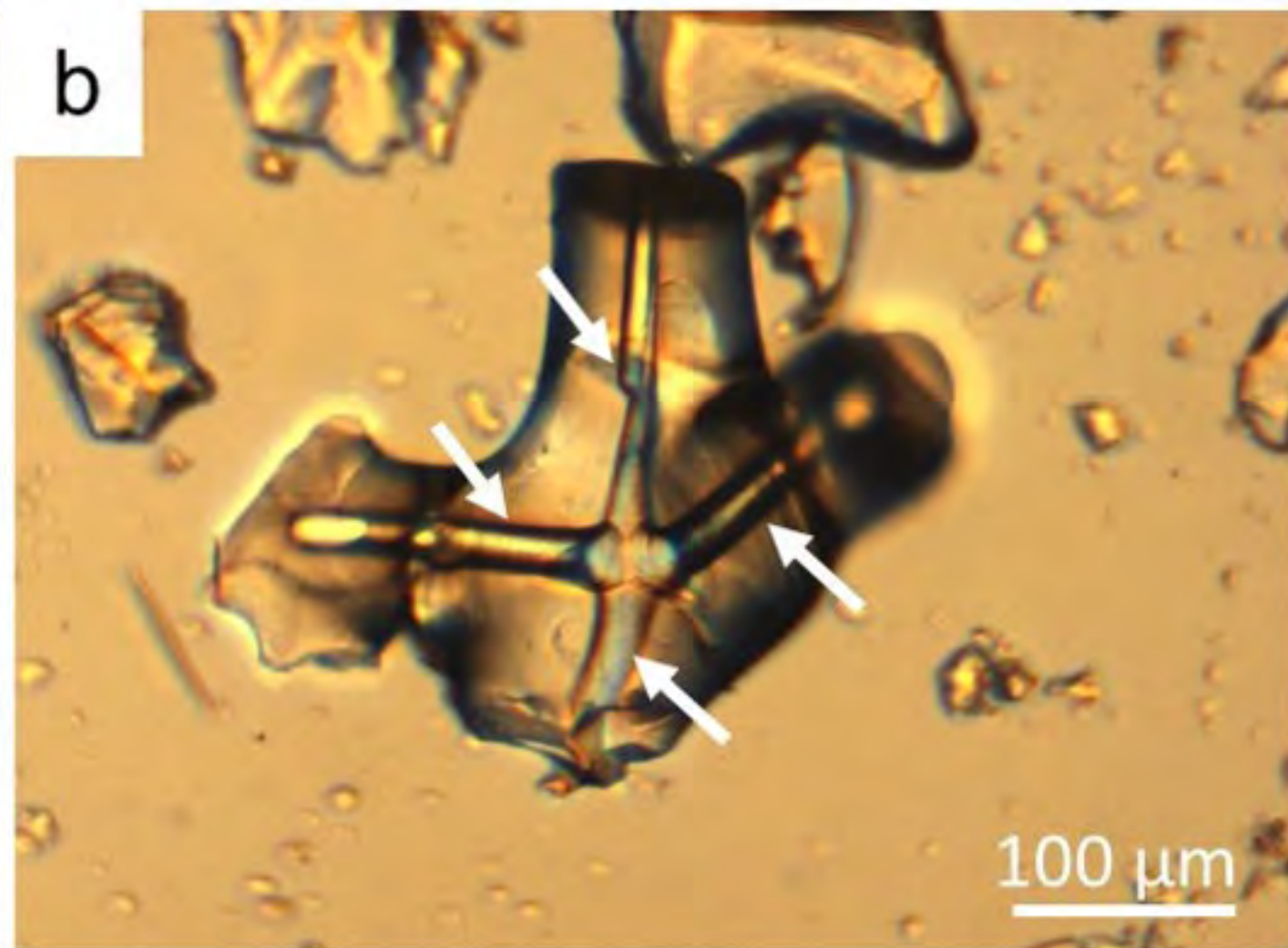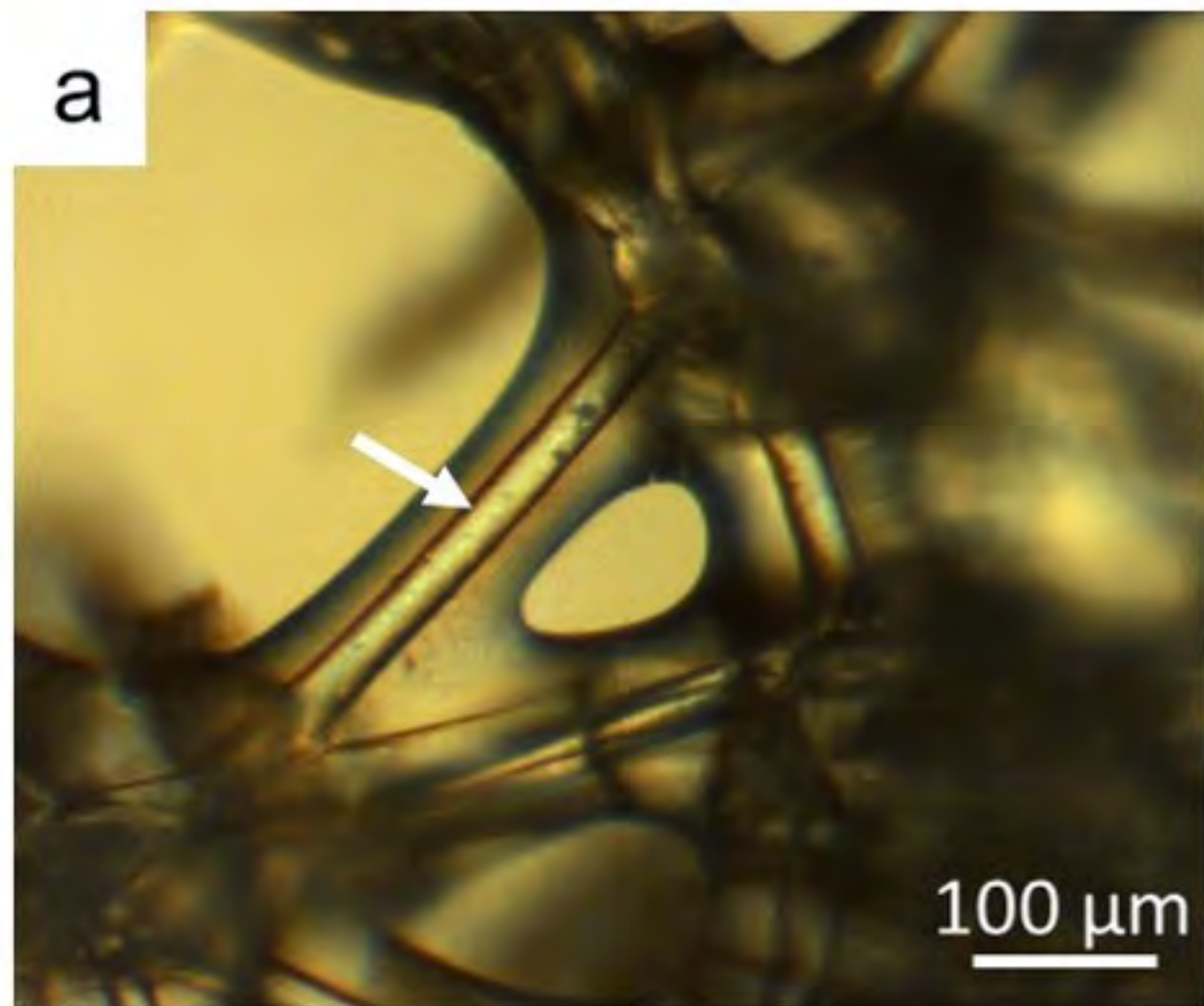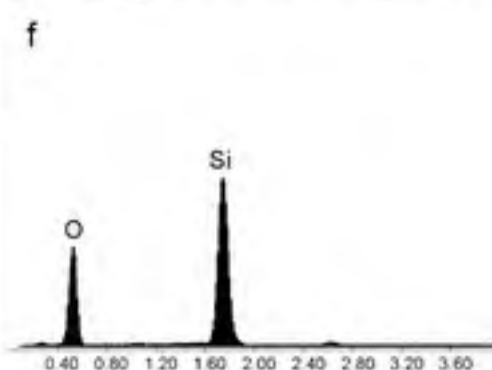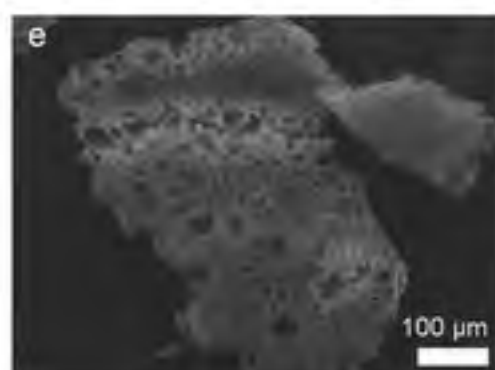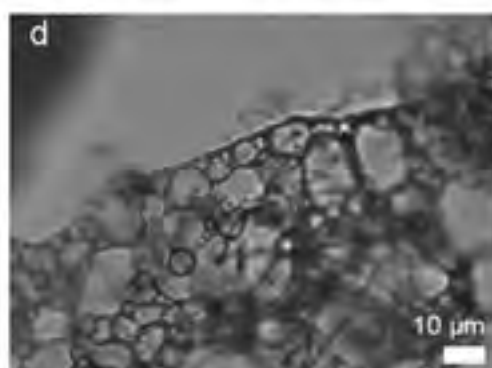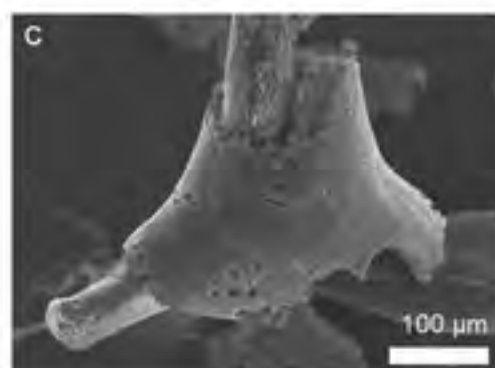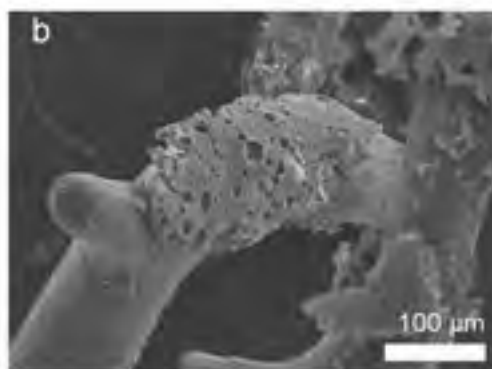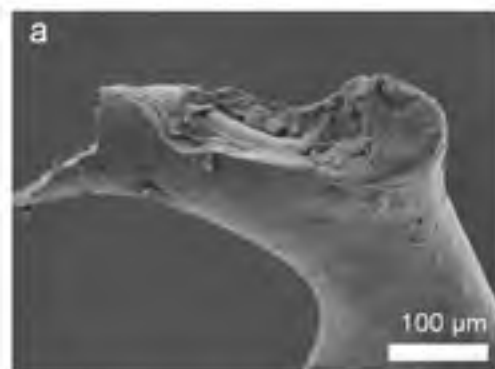
Figure 18

Figure 19

Figure 20
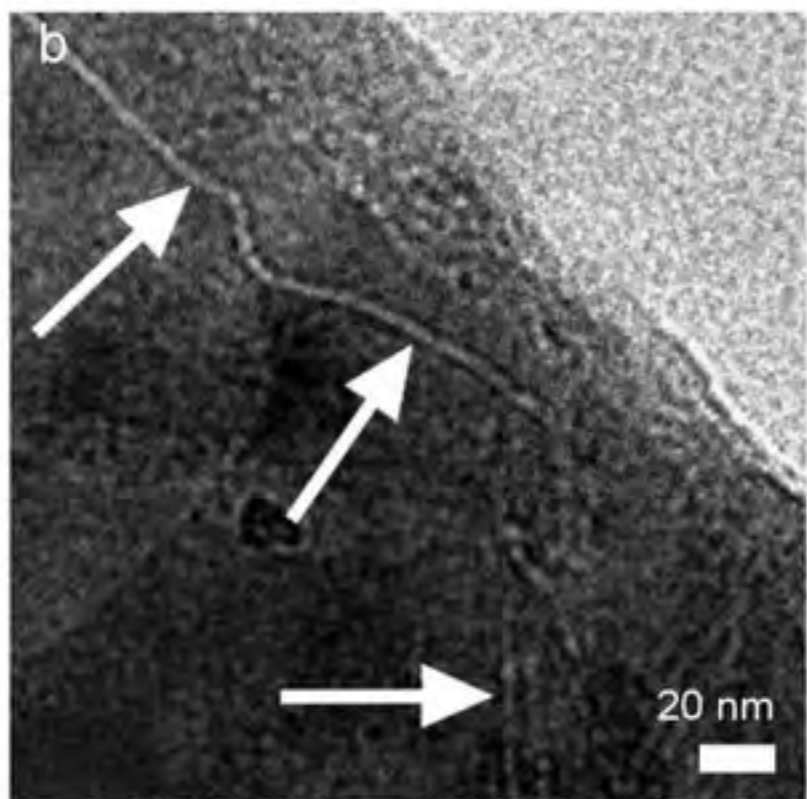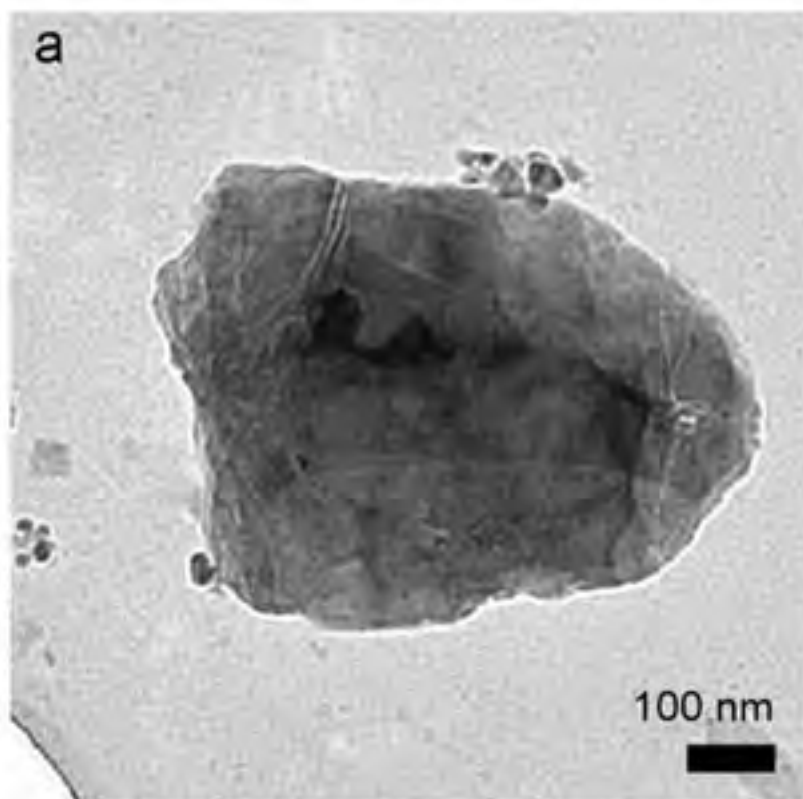
Figure 21

Figure 22

col

1 µm
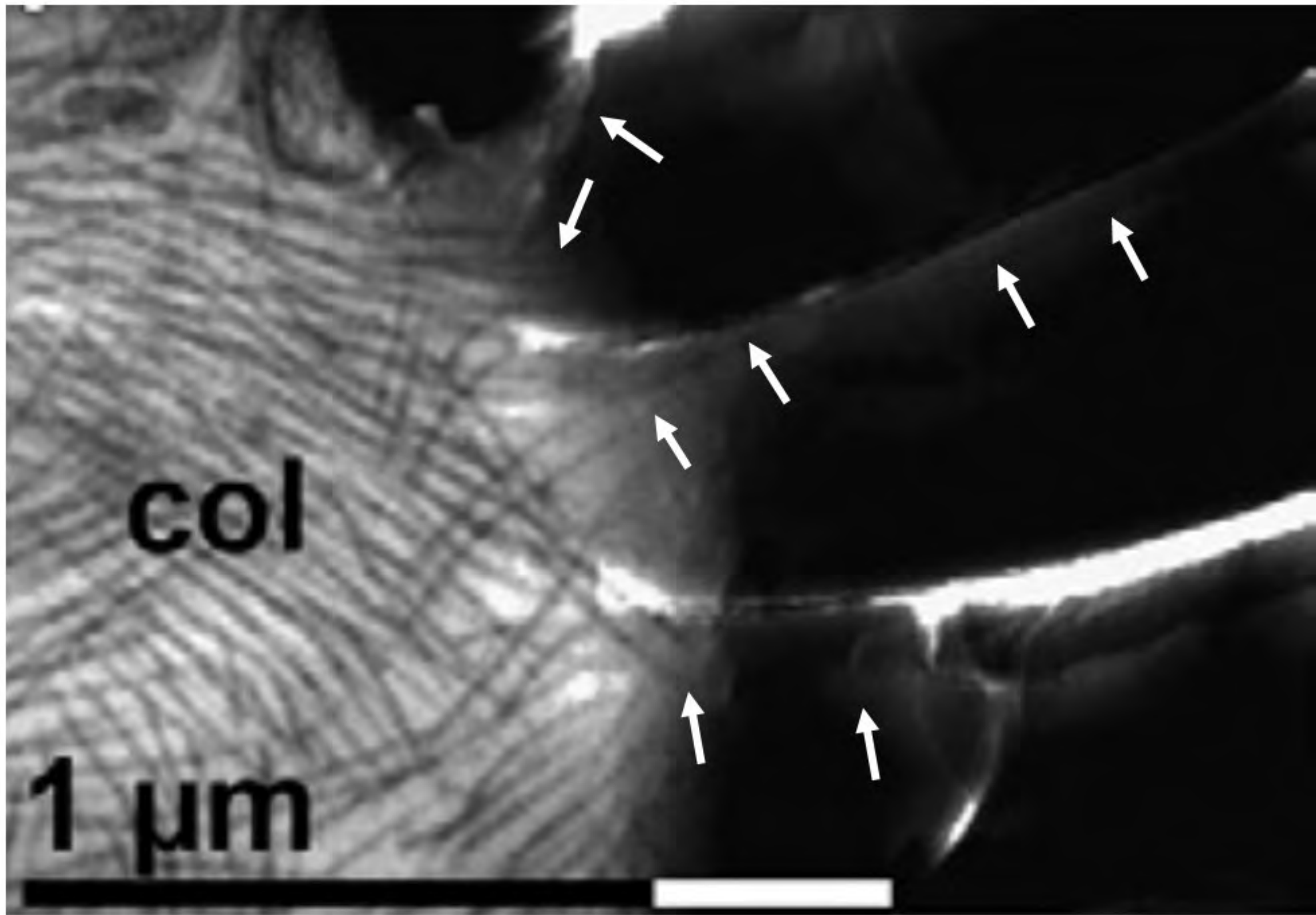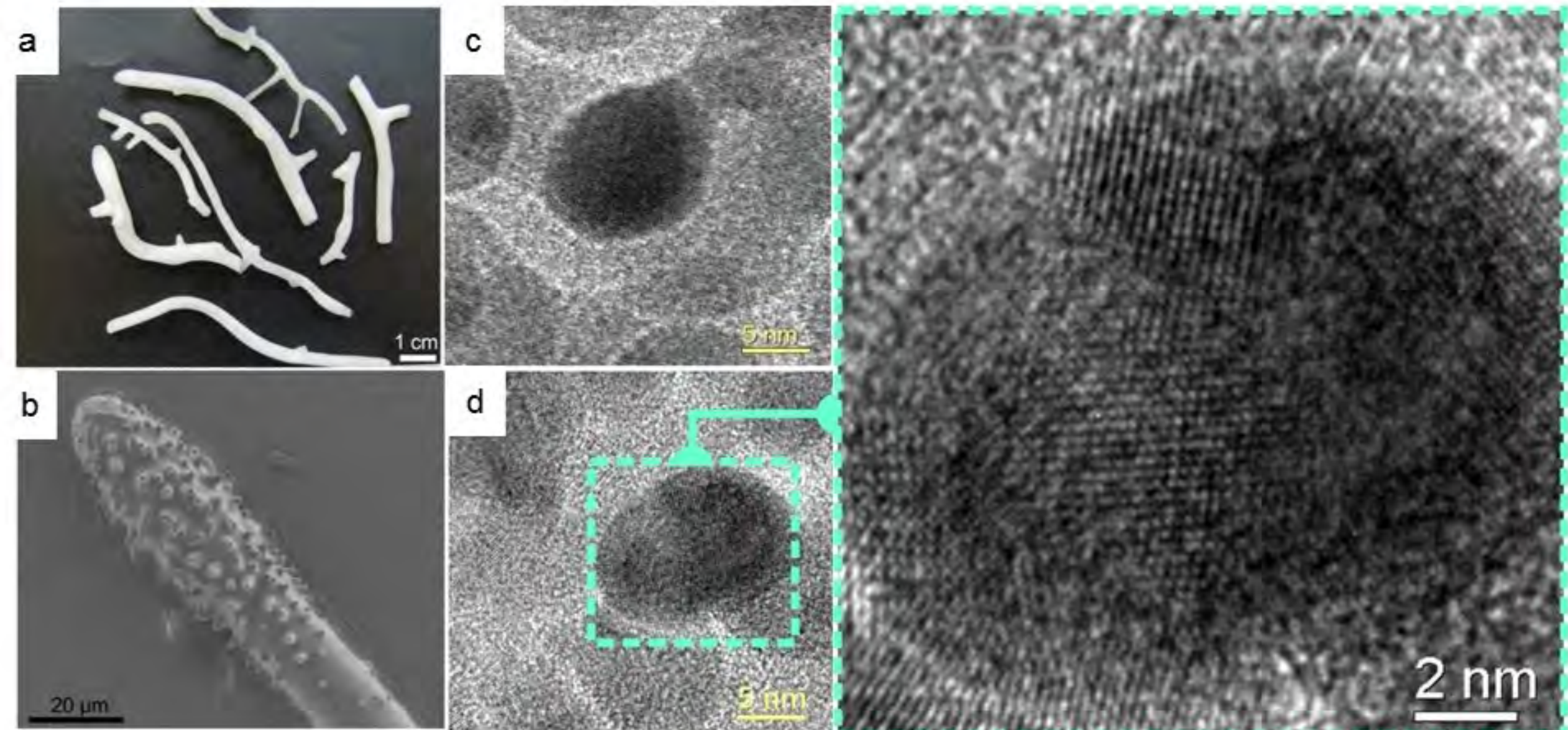
Figure 23
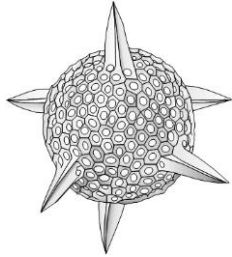
Figure 24
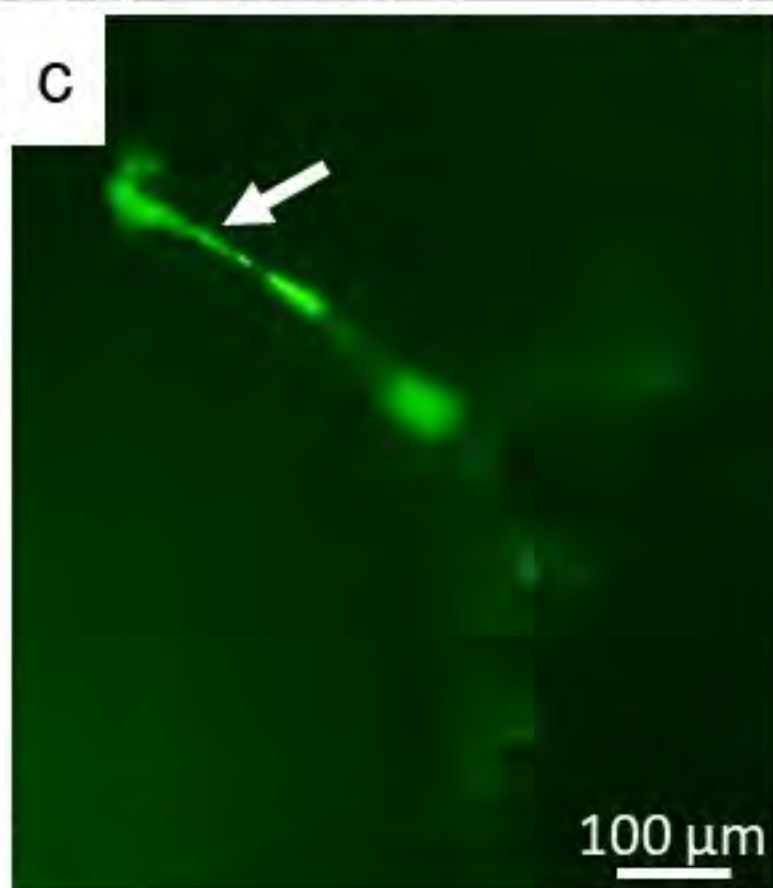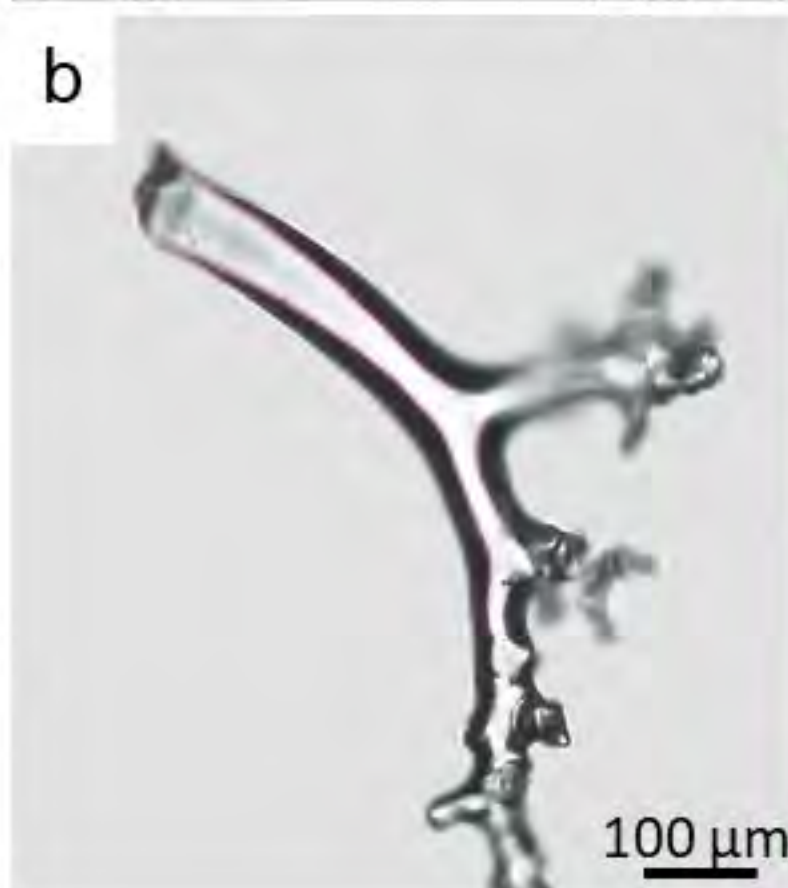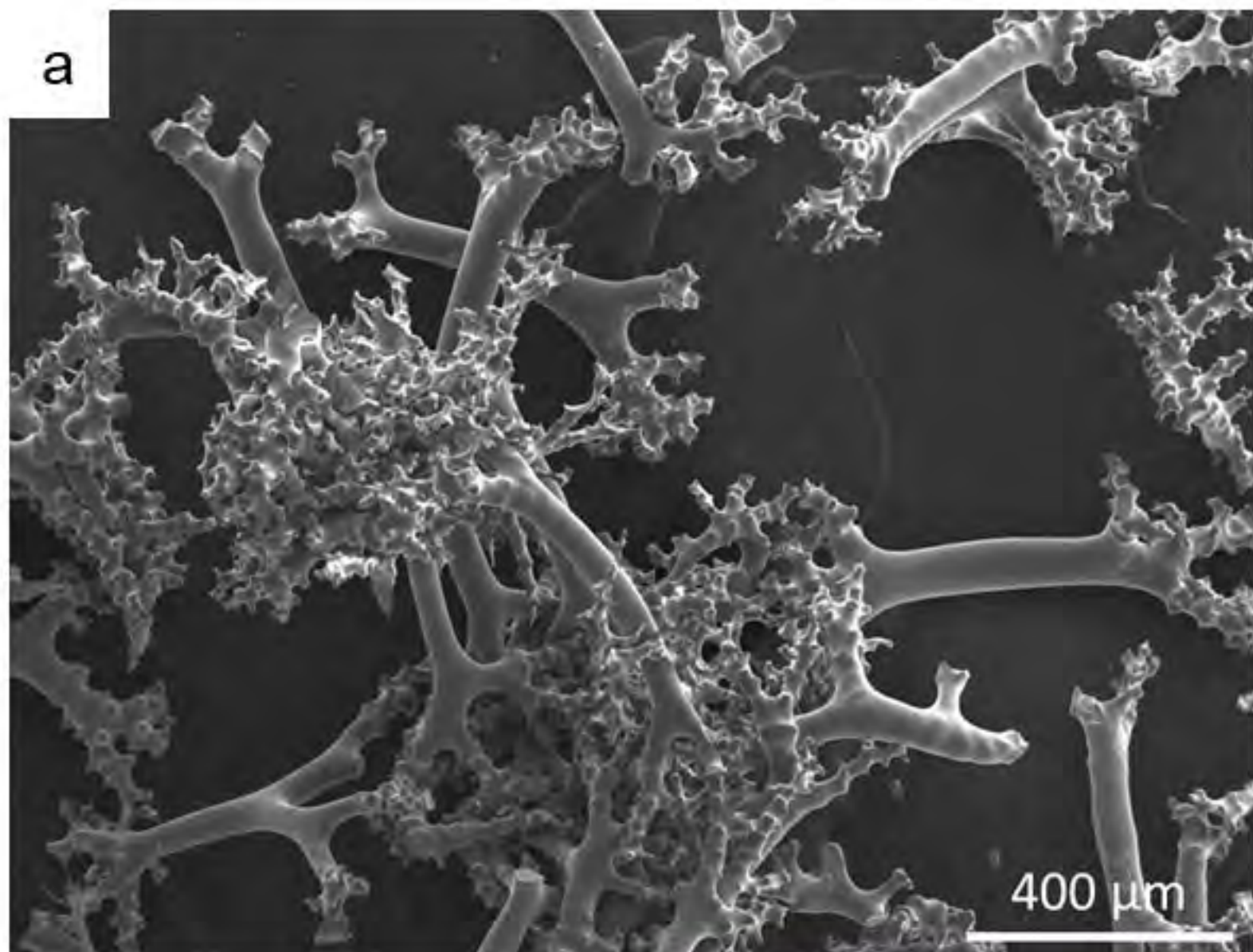
Figure 25
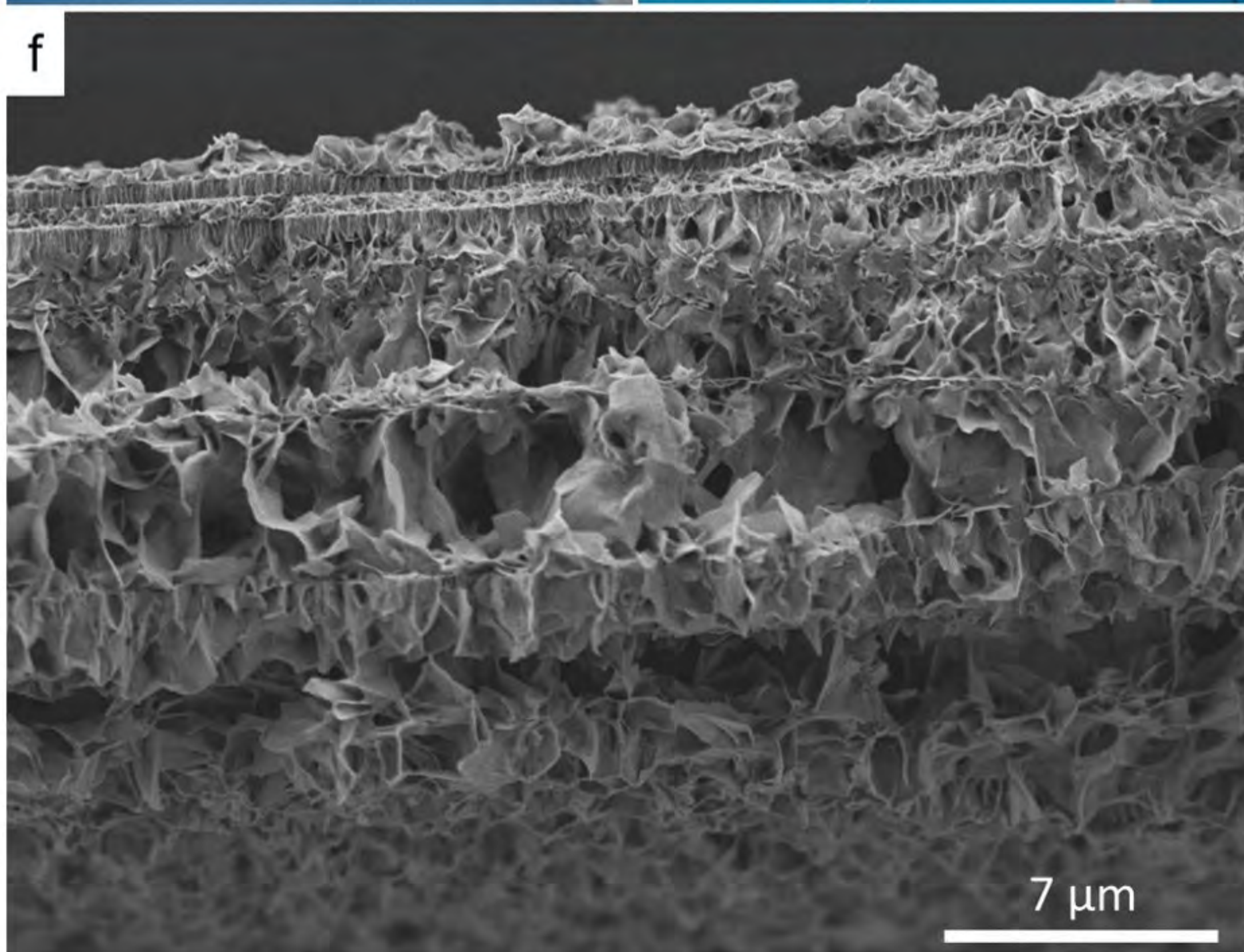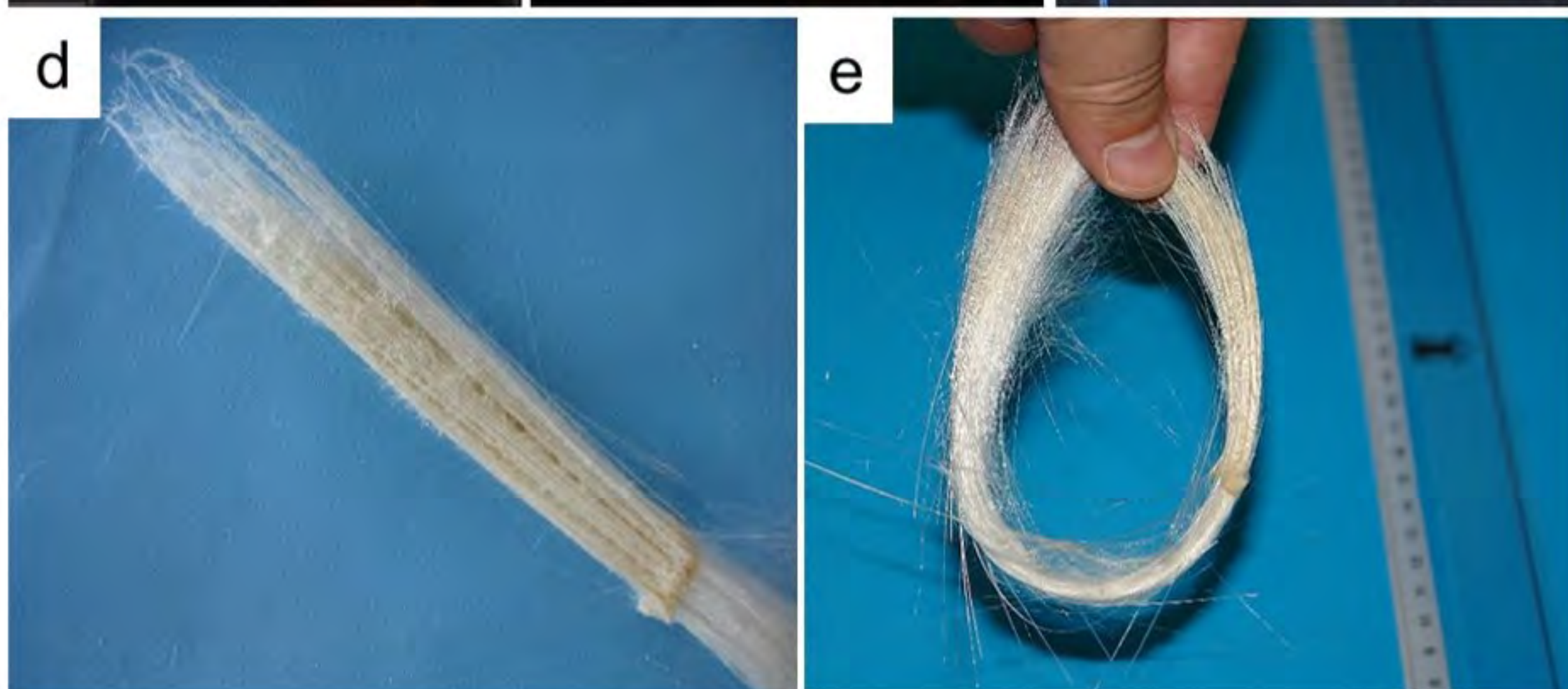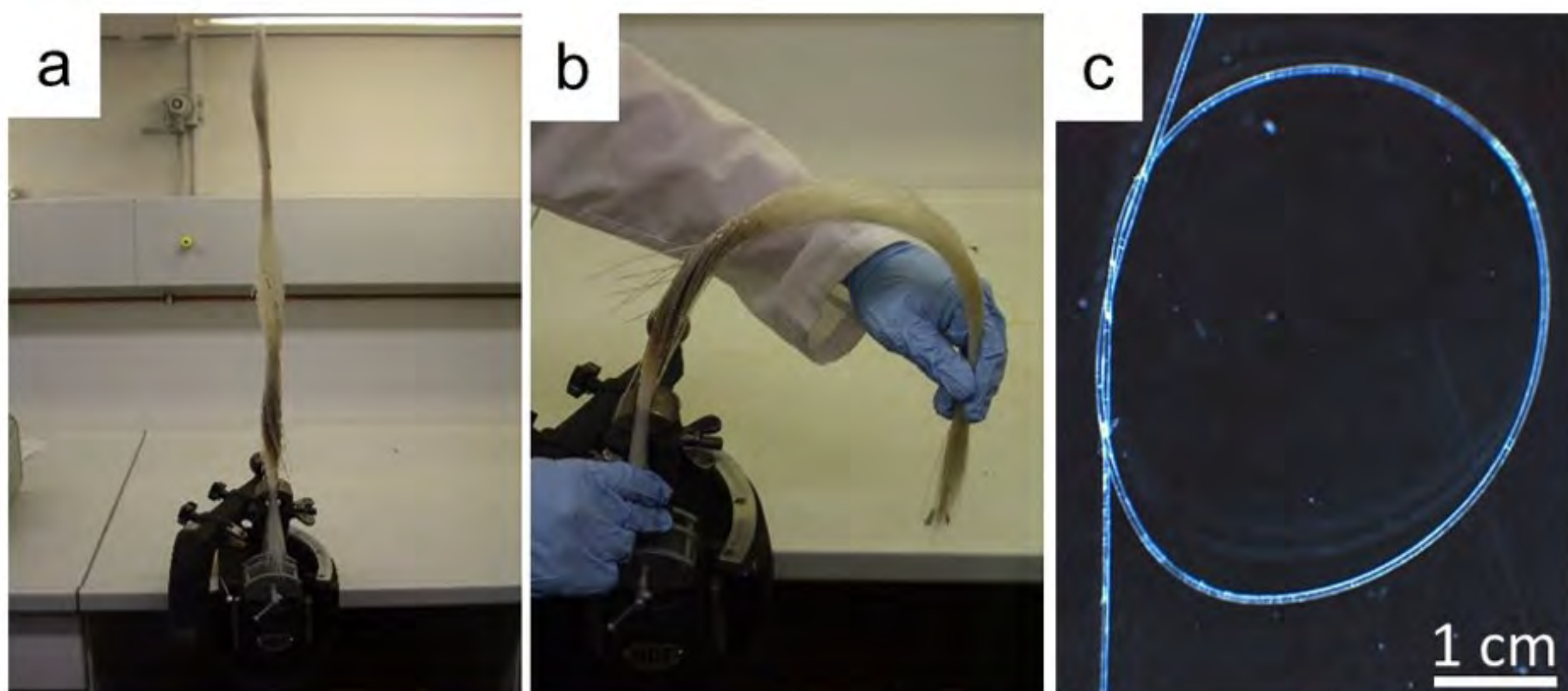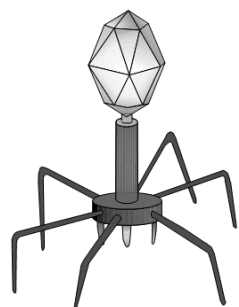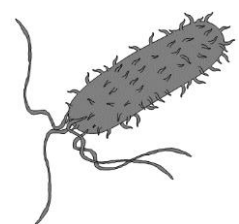
TABLE 1: DIVERSITY OF BIOSILICA STRUCTURES IN NATURE

Organism	Structures of biosilica	Reference
Viruses	40–200 nm nanoparticles in diameter	(Peng et al. 2013)
Bacteria	siliceous "geyser eggs"; siliceous shrubs; siliceous sinters; siliceous microstromatolite laminae silica; scale from geothermal power plant lilypad stromatolites (up to 3 m long and 1.5 m wide) siliceous spicules (up to 3 cm high and up to 5 mm in diameter) granular silica spherules silica layer of spores	(Inagaki et al. 1998, 2003; Yee et al. 2003; Belkova et al. 2004; Benning et al. 2004; Konhauser et al. 2004; Hirota et al. 2010; Orange et al. 2013; Song et al. 2013)
Ciliate	"sparkling granules"	(Foissner et al. 2009)
Picocyanobacteria	dense amorphous mineral within the cell wall	(Baines et al. 2012)
Choanoflagellates	amorphous silica structures within costal strips	(Mann and Williams 1982; Marron et al. 2013)
Silicoflagellates	silica-based skeletons in the form of a network of bars	(McCartney et al. 2014)

1
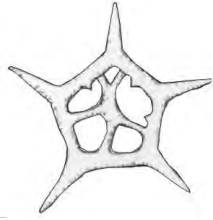
Radiolarians	sophisticated 3D skeletons	(Renaudie and Lazarus 2013)
Ascidian	granular inclusions	(Monniot et al. 1992)
Foraminifera	siliceous test	(Cockerell 1930)
Erbridians	Internal skeleton of rugose or spiny rods	(Korhola and Smol 2001; Finkel 2016)
Amoeba	siliceous shell plates	(Bovee 1981; Ogden 1991)
Testate amoeba	shell composed of many small siliceous scales	(Ogden 1991; Nomura and Ishida 2016)
Chrysophyta	scales	(Kristiansen 1986; Wujek et al. 2005, 2010; Škaloud et al. 2013)
Green algae	network of interconnected spheres	(Millington and Gawlik 1967)
Diatoms	frustules spines heavily silicified resting spores nanogranules in mitochondria	(Ehrlich et al. 2010c)

Plants

siliceous setae silica fiber inflorescence bristles silica cells silica bodies (phytoliths) tabasheer

(Nishizono et al. 2004; Currie and Perry 2007; Neethirajan et al. 2009; Exley 2015)
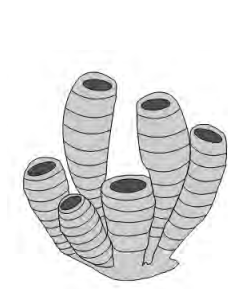
Coccolithophores

silica scales

(Durak et al. 2016)

Crustaceans

opal and willemite-based teeth

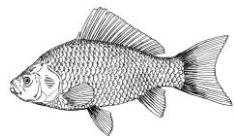(H Ehrlich 2010; Michels et al. 2012, 2015)

Sponges

skeletal frameworks and spicule (macrosclerae), microsclerae

(Maldonado et al. 1999, 2011; Uriz et al. 2003; Ehrlich 2010)

Fishes

chalcedony in electrocytes and cholinergic nerves

(Prado Figueroa et al. 2008b; Prado Figueroa 2012)

Mammals

Chalcedony in brain silica calculi and stones

(Haddad and Kouyoumdjian

dental calculi
silica nanogranules

1986; Prado
Figueroa et al.
2008a; Skinner and
Ehrlich 2013)